Macro-scale avian migration, foraging, and dispersal: environmental and geopolitical perspectives

Christopher Michael Hensz

Submitted to the graduate degree program in Ecology and Evolutionary Biology and the Graduate Faculty of the University of Kansas in partial fulfillment of the requirements for the degree of Doctor of Philosophy

Chairperson Jorge Soberón

A. Townsend Peterson

Mark Robbins

Maria Orive

David Nualart

Date Defended: April 11th, 2018

The dissertation committee for Christopher Michael Hensz certifies that this is the approved version of the following dissertation:

Macro-scale avian migration, foraging, and dispersal: environmental and geopolitical perspectives

Chair Jorge Soberón

Date Approved: April 11th, 2018

ABSTRACT

Animal movements are complex behaviors shaped by internal and external processes at multiple spatial and temporal scales. Until recently, investigations of animal movements across landscapes often favored description over analyses or hypothesis testing. The field of movement ecology arose to address two major obstructions facing quantitative analyses of animal movements: limited data and the need for well-defined methods to test movement hypotheses. Early efforts to systematically collect movement data required marking individual animals with physical tags and recapturing them at a later date. Modern tracking technology can now yield records of location, altitude, and speed at the resolution of minutes, opening up a host of new research questions. Increased availability of high-quality tracking data led to the development of numerous analysis tools that often lead to conflicting interpretations of identical datasets.

Here I present novel movement ecology methods and models to characterize movements of migrating and invasive bird species, and address international policy dimensions of migratory species conservation. The first chapter delivers novel applications of circular-linear regression and generalized linear models to relate remotely sensed oceanographic environments to tracking data (global location sensors, GLS) of 11 arctic terns (*Sterna paradisaea*). The second chapter extends applications of these movement models, testing for environmental drivers of turning angles and path tortuosity of 6 pelagic seabird species in order Procellariiformes. The third chapter describes a series of natal dispersal simulations of the invasion of Eurasian collared dove (*Streptopelia decaocto*) across North America from 1997 – 2016, incorporating Allee effects, and identifying changes in dispersal behavior on an inter-annual basis. In the final chapter, I investigate participation patterns and species composition of the Convention on Migratory Species (CMS), suggesting pathways to improved species coverage under the convention.

ACKNOWLEDGEMENTS

I would like to acknowledge the guidance and support I received from my advisor, Jorge Soberón. His advice and our discussions helped me to succeed at my doctoral pursuits. In addition, I would like to thank the rest of my committee: Town Peterson, Mark Robbins, Maria Orive, and David Nualart for answering all of my many questions with patience. I am grateful to my many academic collaborators throughout my graduate career, especially those in the KU Ecological Niche Modeling group. Many friends have been important for my success, but I would like to particularly recognize Kate Ingenloff, Jacob Cooper, and Jesse Grismer. They have been invaluable collaborators and companions as I finished my dissertation.

I would like to recognize my parents, Michael and Nancye, and my siblings, Abbie, Skyler, and Tim. They have always been my greatest fans and celebrated every bump along this long road with me. I dedicate this dissertation to the memory of my father, Michael. He always believed in me and encouraged me to take the honest and thoughtful path, wherever it may lead.

TABLE OF CONTENTS

INTRODUCTION

Animal movements are complex behaviors shaped by internal and external processes at multiple spatial and temporal scales. Animal movements can be broadly categorized into three classes: dispersal, home-range movements, and migration (Nathan et al. 2008). Within these classes, dispersal of invasive species and migratory movements of animals across international waters or over national borders are particularly important from a global policy perspective (Perrings et al. 2005; Martin et al. 2007). Invasions of non-native species present catastrophic risks for native ecosystems, endangering native species, disrupting ecosystem services and causing billions of dollars of damage to economies (Pimentel et al. 2005; Pejchar & Mooney 2009). On the other hand, conservation of species with international distributions necessitate cooperation between range-states; critical life stages of threatened species may occur in different countries or in neutral waters (Martin et al. 2007; Birnie et al. 2009).

Until recently, investigations of animal movements across landscapes often favored description over analyses or hypothesis testing (Holyoak et al. 2008). The field of movement ecology arose to address two major obstacles facing quantitative analyses of animal movements: limited data and the need for well-defined methods to test movement hypotheses (Nathan et al. 2008). Early efforts to systematically collect movement data required marking individual animals with physical tags and recapturing them at a later date (Bennetts et al. 2001). These data provided a coarse view of movements, but were highly susceptible to errors caused by low retrieval rates and limited size of study areas (Nathan et al. 2003; Morales et al. 2004). Modern tracking technology — including global relocation sensors (GLS), platform terminal transmitters (PTT), and global positioning system (GPS) devices — can now yield records of location, altitude, and speed at the resolution of minutes (Wakefield et al. 2009), opening up a host of new

research questions. Increased availability of high-quality tracking data led to the development of numerous analysis tools that often lead to conflicting interpretations of identical datasets (Turchin 1998; Fortin & Dale 2005; Driezen et al. 2007; Beier et al. 2011; Bridge et al. 2013; Ovaskainen et al. 2016).

Here I present novel movement ecology models to characterize movements of migrating and invasive birds species, and address international policy dimensions of migratory species conservation. The first chapter delivers novel applications of circular-linear regression and generalized linear models to relate remotely sensed oceanographic environments to tracking data (global location sensors, GLS) of 11 arctic terns (*Sterna paradisaea*) during the longest documented seasonal migration in the animal kingdom (Egevang et al. 2010). The second chapter extends applications of these movement models, testing for environmental drivers of turning angles and path tortuosity of 6 pelagic seabird species in order Procellariiformes. I compare differences in movement preferences between trans-equatorial migrations of 3 species in family Procellariidae and home-range movements of 3 species in family Diomedeidae. The third chapter describes a series of natal dispersal simulations of the invasion of Eurasian collared dove (*Streptopelia decaocto*) across North America from 1997 – 2016, incorporating Allee effects. I compared these simulations with estimated abundance surfaces derived from Breeding Bird Survey (BBS) data to identify changes in dispersal behavior on an inter-annual basis. In the final chapter, I summarize the party structure and species composition of the Convention on Migratory Species (CMS), suggesting pathways to improved species coverage under the convention.

Chapter 1

Environmental factors in migratory route decisions: a case study on Greenlandic Arctic Terns (*Sterna paradisaea*)[1]

[1] Hensz C.M. (2015). Environmental factors in migratory route decisions: a case study on Greenlandic Arctic Terns (Sterna paradisaea). *Animal Migration*, 2: 76-85.

Abstract

Identification and characterization of seasonal migration routes and stopover sites has been recognized as important to the conservation of migratory species. This project utilizes multiple regression models including circular-linear regression to identify associations between route choice, travel speed, and environmental preferences using trajectory data of migratory Arctic Terns (*Sterna paradisaea*) and environmental data obtained through remote-sensing techniques. Results of this study suggest that route choice on the southward post-breeding migration route may be more dependent on underlying environment than the northward post-wintering migration route. In contrast, travel speed was variably associated with underlying environment between southward and northward migrations, including several differences regarding the impact of interactions between environment variables. These results reveal the importance of using multiple metrics in the estimation of spatial resistance and highlight conflicts between the theoretical resistance framework of GIS and movement analysis methods.

Introduction

Animal movements occur under diverse circumstances and across spatial scales [1], the most spectacular being seasonal migration. Migratory animals may traverse great distances between breeding and wintering ranges, which may or may not be environmentally similar [2]. Characterizing the complex distributions of migratory species requires understanding of not only the breeding and wintering ranges, but also migratory pathways and stopover sites [3]. Animals navigating heterogeneous landscapes face difficult route choice decisions where a linear path is not always optimal; environmental differences in space have been shown to affect movement patterns in many species including Ovenbirds (*Seiurus aurocapilla*) [4], Hedgehogs (*Erinaceus*

europaeus) [5], Elk (*Cervus elaphus*) [6], Turkey Vultures (*Cathartes aura*) [7], and Caribou (*Rangifer tarandus caribou*) [8] to name a few.

For the past decade, cost-distance approaches have been popular to incorporate the impact of environment on optimal movement pathways [9, 5, 7, 10-14]. Cost-distances, calculated using geographic information systems (GIS) software, use estimates of travel difficulty across landscapes (resistance surfaces) to calculate the amount of effort required to take a given path across geography; a map of optimal travel corridors can then be generated using diffusion models [10, 11]. Resistance surfaces are critical parameters in cost-distance calculation; despite this, there is no standard methodology to generate resistance estimates. Of 24 different cost-distance analyses surveyed by Beier et al. [15] only 9 used empirical data to estimate resistance. The remaining 15 studies relied upon combinations of expert opinion and literature reviews; of the 9 empirical studies, 5 derived resistance estimates from ecological niche modeling (ENM), but none utilized actual movement track data obtained from tracking devices.

The development of modern tracking devices and growing availability of environmental data present an opportunity: by analyzing the movement of individual animals in relation to underlying environments, inferences can be made about the movement preferences of entire populations and even species [1, 9]. While there has been a recent growing usage of track data to study animal movement in the literature, how to appropriately analyze tracks remains contentious. While friction models may be appropriate for environmental resistances such as wind, water currents, or terrain ruggedness, they can misinterpret slow movements associated with foraging or stopover sites [7, 16-19]. Movement analysis approaches, an alternate methodology, provide a more ecological interpretation of track data where increased residence time indicates increased environmental suitability rather than resistance [19, 18]. Speed alone

does not determine residence time; a tortuous movement path, turning back on itself frequently, also increases residence time [19, 18]. The contrasting interpretations of identical movement behavior from resistance-conductance GIS models and movement analysis approaches reveal the need to incorporate multiple metrics when analyzing movement data. In this project, using environmental layers from remote sensing, I analyze trajectory data with two approaches, a novel circular-regression method and a linear regression of travel speed. These are applied to investigate movement decisions and environmental preferences of Arctic Terns (*Sterna paradisaea*).

Arctic Terns are ground-nesting seabirds which exhibit a broad, circum-polar breeding distribution in high northern latitudes and a wintering distribution in high southern latitudes [20]. Previous researchers have studied Arctic Tern migration [7, 21, 22], but only recently have complete tracking data of the circum-global migration from Greenland, Iceland, the Netherlands, and Alaska to Antarctic waters been collected [20, 23-25]. The massive scale of Arctic Tern migration makes it ideal for studying impacts of large-scale processes (e.g. global climate change) upon migration navigation, resistance factors, and timing choices. Egevang et al. [20] hypothesized that regions of high ocean productivity and prevailing favorable wind currents influence Arctic Tern migration. The importance of food resources and upwelling areas has been well documented for Arctic Terns during migration [24], and for other seabirds [26-30]; the relationship between sea surface winds and route choice has also been documented in other seabirds using predefined resistance models [17, 16, 27]. While both surface winds and food availability are assumed to be important, the degree to which they influence route choice and travel velocity in Arctic Terns has not been fully explored. The goals of this project are therefore to (1) identify associations between underlying environment on route choice of Arctic Terns; (2)

investigate the results of models of route choice and travel speed; and (3) develop methods that utilize track data directly without the need for predefined resistance models.

Methods

Tracking Data

Arctic Tern migration data were provided on request by Carsten Egevang [20], collected from August 2007 to June 2008. Tracks were obtained using leg-mounted light loggers (Mk14 geolocators, mass 1.4 g; British Antarctic Survey). The dataset included full migration paths for 9 individual birds, 8 from the eastern edge of Greenland (Sand Island; 74° 43′ N, 20° 27′ W) and 1 from Iceland (Flatey Island; 65° 22′N; 22° 55′W). Each migratory route was divided into a post-breeding southward component, from the breeding region in Greenland and Iceland to the overwintering region in Antarctica (August-December, Fig. 1, Table 1), and a post-wintering northward component, from Antarctica back towards Greenland and Iceland (April-June, Fig. 1, Table 1).

In each case, birds were trapped as adults in breeding areas and light-level geolocators were attached to their legs. Geolocators documented and stored light curves which were translated into latitude-longitude coordinates at midday and midnight, resulting in a roughly 12-hour temporal resolution in sampling. These data were processed following methods by Philips et al. [31, 20]. These tracking devices provide coarse geolocation (~185 km resolution) becoming increasingly inaccurate in variable periods around the equinoxes when day-night lengths are approximately the same across all latitudes [31]. Despite geolocation coarseness, these devices can be used to broadly describe the entire cycle of migration and are the only tracking devices currently usable on small birds (<100 g) on a continental scale. Additionally, while the

relationships between consecutive points are greatly influenced by geolocation error, it is not expected that this error will introduce a consistent directional bias [32, 33].

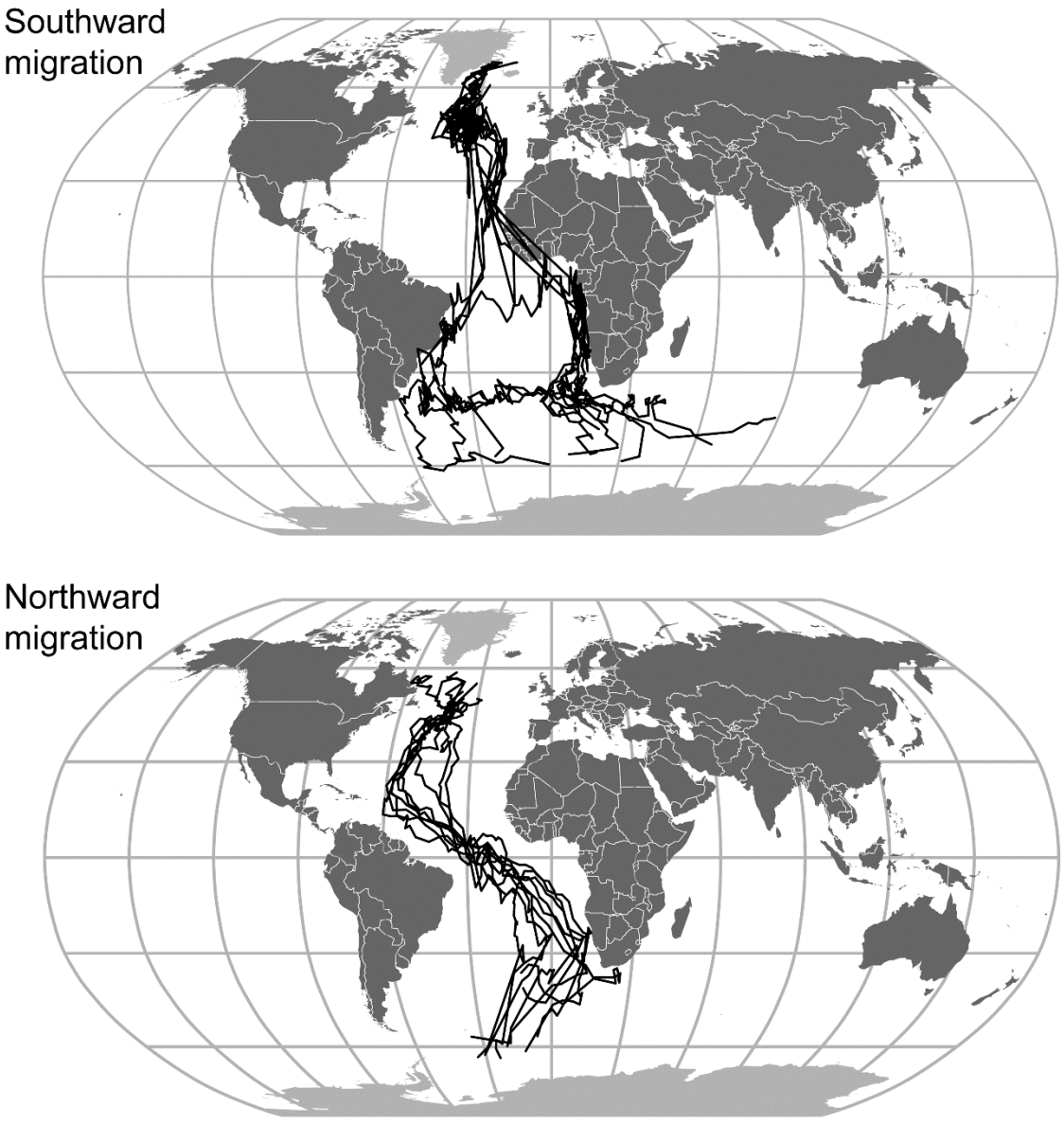

Figure 1.— Interpolated migration pathways of 9 Arctic Terns.

Table 1.— Dates of travel and sample size of track points for southward (post-breeding) and northward (post wintering) Arctic Terns.

Southward			Northward		
Start Date	**End Date**	**N**	**Start Date**	**End Date**	**N**
Aug 16, 2007	Nov 30, 2007	116	Apr 13, 2008	May 31, 2008	92
Aug 16, 2007	Nov 25, 2007	130	Apr 13, 2008	May 21, 2008	76
Aug 20, 2007	Nov 30, 2007	136	Apr 12, 2008	May 28, 2008	81
Aug 13, 2007	Dec 1, 2007	171	Apr 18, 2008	May 28, 2008	79
Aug 21, 2007	Nov 20, 2007	133	Apr 15, 2008	May 23, 2008	72
Aug 15, 2007	Nov 30, 2007	161	Apr 15, 2008	May 26, 2008	80
Aug 16, 2007	Nov 27, 2007	149	Apr 15, 2008	May 23, 2008	75
Aug 15, 2007	Nov 24, 2007	147	Apr 18, 2008	May 24, 2008	71
Aug 15, 2007	Nov 20, 2007	130	Apr 19, 2008	May 24, 2008	72

Tracking data from the overwintering period (December 2007 to April 2008) were removed, leaving only migration periods. As light-logging geolocators determine latitude position from the midpoint of the light curve, points recorded in the weeks surrounding equinoxes (from approximately September 11th – October 7th, 2007) show large error in latitude measurements, and were removed [20]. This excludes a portion of the mid-Atlantic southward migration, which limits the applicability of the analysis for post-breeding migration.

For each locality on each track, travel angles were calculated for the direction of travel to the next point and for the shortest path to destination (Fig. 2). The direction to destination was calculated for each locality as the nearest land-edge of Antarctica for the southward migration and the nearest land-edge of Greenland/Iceland for the northward migration. Distances between migration points were determined as Meeus great-circle distances. The above measures were calculated in R (version 3.2.0; R Development Core Team, http://www.R-project.org) utilizing the 'geosphere' package (version 1.3-13; R. Hijmans, http://CRAN.R-project.org/package=geosphere). Point velocities were calculated as travel distance divided by travel time between consecutive points.

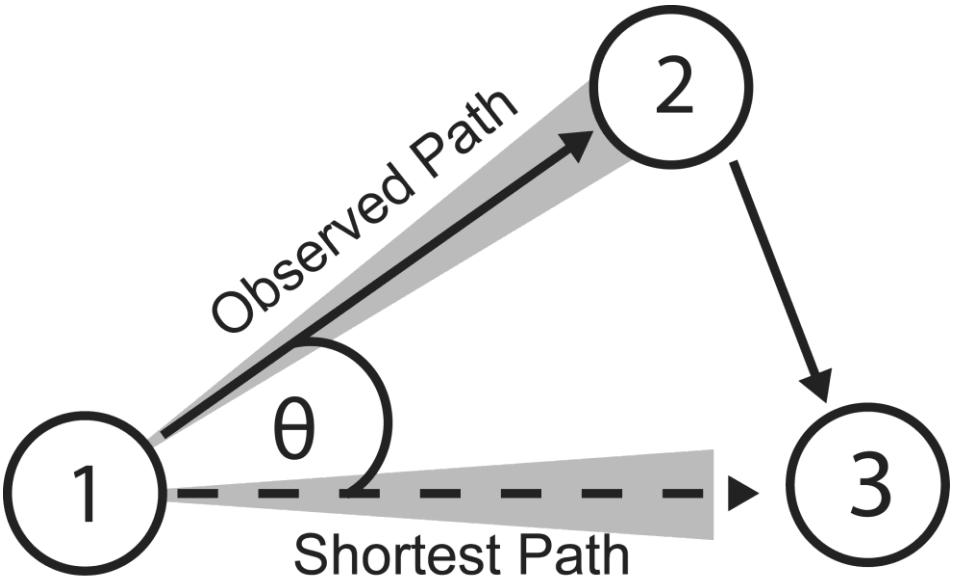

Figure 2.— Diagrammatic representation of sampling neighborhoods for the first point in a hypothetical 3-point trajectory. Solid gray fans indicate sampled regions along the shortest (dashed) and observed (solid) paths for point 1. Sampling regions are 10° fans with side length equal to 12 hours of travel at the velocity calculated between points 1 and 2. Deviation angle between shortest and observed paths is shown by θ.

Environmental Data

Multiple sources of environmental data were collected for the time period of migration. I used wind-speed data from the Cross-Calibrated Multi-Platform Ocean Surface Wind Velocity dataset containing interpolated wind speed measurements (in m/s) for u-wind (longitudinal component) and v-wind (latitudinal component) at 10 m above sea level [34]. This data product extends globally over oceans at 0.25° spatial resolution and 5 day temporal resolution. I used daytime sea surface temperature (SST) data (°C) from the NOAA Optimum Interpolation 1/4 Degree Daily Sea Surface Temperature Analysis dataset [35], which comprises spatially interpolated measurements for global daytime sea-surface temperatures at 0.25° spatial resolution. I also used a post-processed dataset of ocean net primary productivity (NPP, mg C/ m^2 / day, http://www.science.oregonstate.edu/ocean.productivity/index.php). The dataset is derived from a Vertically Generalized Production Model (VGPM) estimating chlorophyll based photosynthetic capacity [36] and NPP was used as a proximate measure of food availability. This dataset has a spatial resolution of 0.083°, and 8-day temporal resolution. Each environmental dataset was used in its native resolution.

For each sample point on each migratory trajectory 2 fan-shaped sampling neighborhoods of equal area were used to extract environmental values, one in the direction of the shortest path to the final destination (nearest land-edge of Antarctica for post-breeding tracks, nearest land-edge Greenland and Iceland for post-wintering tracks) and one in the observed direction to the next point in sequence. All fans radiated from sampling points with 10° interior angles. Because portions of the southward migration tracks were removed because of location error, the size of each set of sampling neighborhoods varied depending on speed: I defined the side length of each sampling neighborhood pair as the distance traveled in 12 hours at the speed calculated for the

sample point, equivalent to the temporal resolution of the tracking data (Fig. 2). Varying the size of sampling neighborhoods limited overlap of environmental sampling for points close together and prevented under-sampling of environments for points further apart. Mean environmental variables were sampled using a polygon extract operation in the 'geosphere' package in R. Extracted mean values of net primary productivity (NPP) were right skewed and were log transformed to reduce skew of values. Wind values were sampled as mean u-wind and mean v-wind values. Because wind is a directional variable, I used the scalar projection of the wind speed on the direction of the sampling fan, including only headwinds and tailwinds.

Circular dispersion models

To estimate which environmental variables, if any, presented migration resistance, I created a circular-linear regression model [37] of angular dispersion as a function of the difference between environments sampled for each point. Circular-linear regression assumes that some angular response variable θ is a function of a mean direction μ and a concentration parameter κ following a Von-Mises distribution. A circular-normal Von-Mises variable has a mean direction μ and concentration parameter κ with the following probability density function:

$$f(\theta;\mu,\kappa) = [2\pi I_0(\kappa)]^{-1} \exp[\kappa \cos(\theta - \mu)],\ -\pi < \theta,\ \mu \leq \pi,\ \kappa \geq 0$$

where I_0 is the modified Bessel function of order 0. When $\kappa = 0$, this function becomes the circular uniform distribution; for $\kappa \geq 2$ the density becomes tightly concentrated around μ and can be approximated by a normal distribution with variance $1/\kappa$ [37]. For this project the expected angle of travel is that of the shortest direct path to the destination, therefore $\mu = 0$ and θ is the angular deviation of the observed path from the expected. θ is a measure of deviation from the global axis [38] rather than an axis constructed from a local trend [7]. With this framework,

smaller vales of κ indicate greater average deviation from the shortest distance path to the destination. If Arctic Terns are following cost-optimal pathways during migration, deviation from the shortest path to destination may indicate a greater net cost to travel the direct route. Regressing differences in environmental neighborhoods onto θ estimates the impact of differences in environment on route decisions.

The log-likelihood for a circular-normal distribution with known mean and unknown concentration was proposed by Fisher and Lee [37]:

$$-\sum_{i=1}^{n} \log I_0(\kappa_i) + \sum_{i=1}^{n} \kappa_i \cos(\theta_i - \mu)$$

where the subscript i corresponds to the i^{th} data point in the regression. In this instance, i is a particular sample point on a migratory track. The predictor environmental variables were link-transformed using an exponential function:

$$\kappa_i = \exp(-\beta x_i + \alpha)$$

to wrap the linear predictors of the i^{th} environment x_i onto a prediction of the concentration parameter for that set of environments κ_i ranging from $[0, \infty)$. x_i is a vector containing the differences of the environmental values of the observed path and the shortest path. β is the vector of regression coefficients where positive values indicate differences in environments associated with deviation (i.e. environments less resistant than the shortest path) and α is the intercept. I maximized the log-likelihood model proposed by Fisher and Lee [37] using the "optim" function in R to determine the maximum-likelihood value of β.

Regression models were evaluated separately for the northward and southward tracks to evaluate differences in observed travel behavior between pre-breeding and post-breeding migration. All 2-way interaction terms were included in initial models, and were retained only when significant.

Linear velocity models

To contrast the circular-linear model of route direction, I constructed a mixed linear model of travel speed as a response to underlying environment with individual bird included as an intercept-only random effect:

$$V = \beta x + Bird + \alpha$$

where the independent variable V is travel speed, β is the vector of regression coefficients on the matrix of predictor variables x, and α is the intercept. The linear regression used only the environmental neighborhoods between consecutive points rather than the difference between observed and shortest path used in the circular regression because potential velocities in non-traveled environments are unknown. Predictor variables were mean-centered to reduce possible colinearity between main effects and interaction terms [39]. Initial model evaluation included all main effects from predictor variables, all potential 2-way interactions between effects, and random effect of individuals. Model coefficients were estimated using maximum-likelihood with the 'nlme' package in R (version 3.1-120, J. Pinheiro et al., http://CRAN.R-project.org/package=nlme). Backwards selection against uninformative model parameters was performed by comparing model AIC scores of the full model to subset models. When an included parameter failed to significantly decrease AIC ($\Delta AIC<2$) compared to simpler a model with fewer parameters, it was eliminated. Parameters were sequentially discarded until reducing the number of parameters lead to an increase in AIC [40, 41].

Table 2.— Model summary of circular-linear regressions of environment on route choice for both paths. Positive estimates indicate an association between dispersion and underlying environment. Statistically significant results ($p \leq 0.05$) are in bold.

Route	Parameter	Estimate	Std Err.	*t*	*p*
South	Wind[1]	**0.086**	0.019	4.572	**<0.001**
	SST	0.130	0.082	1.594	0.055
	NPP[2]	**1.006**	0.342	2.937	**0.002**
	Intercept	**0.682**	0.093	7.320	**<0.001**
North	Wind[1]	-0.027	0.017	1.565	0.058
	SST	**-0.092**	0.054	1.693	**0.045**
	NPP[2]	0.133	0.320	0.416	0.338
	Intercept	**0.165**	0.075	2.193	**0.014**

[1] Average scalar projection of wind

[2] Log-transformed average of NPP

Table 3.— Summary of models included in model selection. ΔAIC is the difference between the lowest AIC and the given model. AIC weight shows the relative evidence for each model given model. Final models are in bold.

Route	Model	AIC	ΔAIC	AIC Weight
South	Base[1]	10080.47	41.698	3.54E-10
	Base + Wind*SST	**10040.99**	**2.212**	**0.133**
	Base + Wind*NPP	10059.72	20.943	1.34E-10
	Base + SST*NPP	10078.5	39.722	9.53E-10
	Base + Wind*SST + Wind*NPP	10040.41	1.637	0.177
	Base + Wind*SST + SST*NPP	10039.44	0.667	0.288
	Base + Wind*NPP + SST*NPP	10057.67	18.896	3.17E-05
	Full Model	10038.78	0.000	0.402
North	Base	6119.878	13.343	9.43E-04
	Base + Wind*SST	6120.652	14.118	6.40E-04
	Base + Wind*NPP	6114.675	8.145	0.013
	Base + SST*NPP	6113.476	6.942	0.023
	Base + Wind*SST + Wind*NPP	6111.931	5.396	0.050
	Base + Wind*SST + SST*NPP	6113.712	7.180	0.021
	Base + Wind*NPP + SST*NPP	6109.771	3.230	0.148
	Full Model	**6106.535**	**0.000**	**0.744**

[1] Base = Wind + SST + NPP

Table 4.— Model summary of linear regressions of environment on velocity for both paths. Positive estimates indicate an association between faster travel speed and more positive environmental values. Statistically significant results ($p \leq 0.05$) are in bold.

Route	Parameter	Estimate	Std Err.	*t*	*p*	Individual Random Effect	
South	Wind[1]	0.011	0.085	0.132	0.895	**Std Dev :**	Intercept = 1.859
	SST	0.113	0.065	1.744	0.081		Residual = 13.821
	NPP[2]	**-1.770**	0.647	-2.735	**0.006**		
	Wind*SST	**-0.082**	0.013	-6.482	**<0.001**		
	Intercept	**18.590**	0.737	25.237	**<0.001**		
North	Wind[1]	0.052	0.216	0.241	0.809	**Std Dev :**	Intercept = 1.892
	SST	-0.232	0.121	-1.908	0.057		Residual = 19.254
	NPP[2]	**-7.083**	1.280	-5.535	**<0.001**		
	Wind*SST	**0.070**	0.030	2.287	**0.022**		
	Wind*NPP	**0.870**	0.287	3.034	**0.003**		
	SST*NPP	**0.389**	0.138	2.809	**0.005**		
	Intercept	**28.530**	1.013	28.168	**<0.001**		

[1] Average scalar projection of wind

[2] Log-transformed average of NPP

Results

In the circular-linear dispersion model, more favorable winds and higher values of NPP were significantly and positively related to increased dispersion on the southward migration route. For the northward migration route, only decreased sea surface temperature was significantly associated with increased dispersion (Table 2). For both northward and southward dispersion models, no interaction effects were found to be significant and were not included in final models.

In the southward linear regression model regarding travel speed, the full model was rejected as the final model despite performing best because it was indistinguishable from intermediate models including fewer parameters ($\Delta AIC < 2$, Table 3). The final model for the southward linear regression included all main effects (wind, SST, NPP) and the interaction between wind and SST. For the northward route, all interaction terms were included in final models; exclusion of any parameters from the full model resulted in an increase in AIC ($\Delta AIC \geq 3.263$, Table 3). For both southward and northward migration, high values of NPP were negatively associated with travel speed. Increased sea surface temperature was a marginally insignificant variable for both southward ($p = 0.081$) and northward models ($p = 0.057$). Wind speed was not a significant predictor of travel speed for either direction. Several interaction effects were significant and dissimilar comparing southward and northward models. For the southward model, only the negative interaction between wind and SST was significant. For the northward model, all interaction effects were significant and positive (Table 4).

Discussion

For the southward migration, circular-linear regression supports the hypothesis that Arctic Terns show preferential route choice based upon available environments. Southward migration paths divert from the shortest paths towards more favorable winds, and regions of higher NPP. These results support the popular hypothesis that food availability significantly influences the choice of travel route.

For northward migration, only colder sea surface temperature was significantly associated with dispersion in route choice, and only marginally. Despite being predicted as a major influence, wind was not significantly associated with route dispersion in this analysis. This negative result may be caused by the fact that the shortest direction of travel aligned well with the direction of favorable winds, eliminating any observable signal of selectivity. NPP was not a significant predictor of route choice on the northward route, which indicates that migration strategy may differ post-wintering. Arctic Terns travel more quickly on the northward, spring route (mean travel time of ~40 days) than on the southward, autumn route (mean travel time of ~97 days) which is a general trend for migratory birds [42].

Linear regressions of travel speed on environmental characteristics showed a different and highly complex picture. On both southward and northward routes, areas of high NPP were associated with slower travel speeds despite the fact that no association between food availability and route choice could be shown on the northward route using dispersion models. This may be a signal of opportunistic feeding in regions of high productivity. Northward and southward models differed highly in all other significant variables. Complex differences in interaction terms between northward and southward models are notably more difficult to explain with reasonable hypotheses. While wind alone was not predictive, at least one wind interaction term was

significant for both migration legs. It is possible that winds may be a secondary driver of travel speed, serving as a frictional force that mediates or supports choice of speed indirectly. It is apparent that the underlying decision-making process is highly complex and surprisingly variable.

The possible reliance of Arctic Terns on strong favorable winds is a troubling result for the species. Climate change is likely to reduce the strength of Hadley cells, in turn calming ocean winds in the future [43], which may have detrimental impacts on the migration success of Arctic Terns in the future. Other sea bird species, most notably albatrosses, have shown changes in migratory routes and habits in response to changes in wind pattern [44]. It remains to be seen if the response observed in albatrosses will be a consistent trend amongst species of sea bird, as Arctic Terns have a much longer migration route than albatrosses, relying more on large-scale wind patterns. Climate change may alter the shape, size and magnitude of important wind currents including the North Atlantic Oscillation and the East Atlantic pattern [45]. In other species with shorter migration routes, changes in wind patterns have affected breeding phenology, migration timing, and community composition [46, 47, 44]. This analysis includes only Arctic Terns over the Atlantic Ocean; application of these techniques onto Pacific Arctic Tern data [24, 25] would be necessary to support a consistent species wide trend.

More generally, the directional model of environmental suitability presented here provides a data-driven approach to estimate movement resistance across landscapes. Specifically for the southward migration route of Arctic Terns, the model shows that previously hypothesized factors related to tern flight preference proposed by Egevang et al. had detectable associations with route choice [20]. Additionally, this study highlights the risk of assuming that slower travel speeds indicate increased travel difficulty as per traditional GIS resistance/conductance

framework [48]. Arctic Terns in this analysis showed significant decreases in travel speed in regions of high NPP, a result that is not easily explained by resistance. Circular-linear models show considerable promise as an alternative and complementary tool to analyze animal movements.

Several limitations should be considered as regards to this analysis, however. Tracking data used in this study were obtained through light-level geolocation, which has notable limitations. Light-level data are susceptible to shading effects resulting in low spatial accuracy [31, 33]. Additionally, light-level data cannot decipher latitude for several weeks in proximity to equinoxes, which excluded several weeks of the southward migration from analysis [20]. While I do not expect that geolocation error introduced a consistent directional bias, it is likely that the signal of environment in the regression analyses was greatly reduced by noise. Results of analyzing light-logger data is best used at a broad spatial scale in the context of large-scale behavior [27]. The usage of circular-linear regression on travel trajectories is currently an exploratory exercise rather than a fully predictive tool. Circular-linear regression does not account for the fact that animal movements are often auto-correlated spatially and temporally; while alternate approaches can be used to account for autocorrelation, namely state-space or hidden-Markov models, incorporating environmental variables into these models is currently limited in scope [49]. Both the circular-linear and linear regressions only construct monotonic relationships between the underlying environment and travel direction or speed. Intuitively, the relationship would hold only in an optimal range, and the relationship may decay or reverse at extreme values. Response curves in physiology and functional mechanics are generally bell-shaped, such that extreme intermediate environments are favored: e.g., no wind is unfavorable, but extremely fast tailwinds generated from storm systems may be detrimental as well [50]. The

suitability curve approach has been investigated extensively as regards to distributions and scenopoetic ecological niches [51], and should be a next goal in movement analyses of this kind.

Conclusions

Calculation of resistance surfaces from regression coefficients for animal migrations is a complicated procedure. Resistance varies simultaneously in direction, time, and space and computations involved in projections are time-consuming and expensive. Future efforts should focus on expected velocities of migration across space to explore future migration events. Areas of reduced velocity have traditionally been used as an indication of high-friction, but may be the product of much more complex environmental decisions than previously hypothesized.

With increased availability of high-quality tracking data and the advent of new data-driven analytic techniques, it is possible to obtain more direct measurements of migration preference. These tools can estimate impacts of climate change on migration and illustrate suitable areas for migratory pathway conservation. In addition, track analysis may provide a link between migratory species and the environment for cross-taxonomic analyses. Track analyses can be generalized to any species with track data; temporal and taxonomic generalization of the track analysis approach is a sensible next step to study general patterns of migratory animal movements.

References

1. Nathan R., Getz W.M., Revilla E., Holyoak M., Kadmon R., Saltz D.*, et al.*, A movement ecology paradigm for unifying organismal movement research. Proc. Natl. Acad. Sci. U. S. A., 2008, 105(49), 19052-19059

2. Nakazawa Y., Martínez-Meyer E., Peterson A.T., Navarro-Sigüenza A.G., Evolution of seasonal ecological niches in the Passerina buntings (Aves: Cardinalidae). Proc. R. Soc. Lond. B Biol. Sci., 2004, 271(1544), 1151-1157

3. Crick H.Q.P. Migratory wildlife in a changing climate. Bonn: UNEP/CMS Secretariat2006.

4. Desrochers A., Belisle M., Morand-Ferron J., Bourque J., Integrating GIS and homing experiments to study avian movement costs. Landsc. Ecol., 2011, 26(1), 47-58

5. Driezen K., Adriaensen F., Rondinini C., Doncaster C.P., Matthysen E., Evaluating least-cost model predictions with empirical dispersal data: a case-study using radiotracking data of hedgehogs (Erinaceus europaeus). Ecol. Model., 2007, 209(2-4), 314-322

6. Forester J.D., Ives A.R., Turner M.G., Anderson D.P., Fortin D., Beyer H.L.*, et al.*, State-space models link elk movement patterns to landscape characteristics in Yellowstone National Park. Ecol. Monogr., 2007, 77(2), 285-299

7. Mandel J.T., Bohrer G., Winkler D.W., Barber D.R., Houston C.S., Bildstein K.L., Migration path annotation: cross-continental study of migration-flight response to environmental conditions. Ecol. Appl., 2011, 21(6), 2258-2268

8. O'Brien D., Manseau M., Fall A., Fortin M.-J., Testing the importance of spatial configuration of winter habitat for woodland caribou: an application of graph theory. Biol. Conserv., 2006, 130(1), 70-83

9. Schick R.S., Loarie S.R., Colchero F., Best B.D., Boustany A., Conde D.A.*, et al.*, Understanding movement data and movement processes: current and emerging directions. Ecol. Lett., 2008, 11(12), 1338-1350

10. Adriaensen F., Chardon J.P., De Blust G., Swinnen E., Villalba S., Gulinck H.*, et al.*, The application of 'least-cost' modelling as a functional landscape model. Landsc. Urban Plann., 2003, 64(4), 233-247

11. Beier P., Spencer W., Baldwin R.F., McRae B.H., Toward best practices for developing regional connectivity maps. Conserv. Biol., 2011, 25(5), 879-892

12. Chetkiewicz C.L.B., Boyce M.S., Use of resource selection functions to identify conservation corridors. J. Appl. Ecol., 2009, 46(5), 1036-1047

13. Epps C.W., Wehausen J.D., Bleich V.C., Torres S.G., Brashares J.S., Optimizing dispersal and corridor models using landscape genetics. J. Appl. Ecol., 2007, 44(4), 714-724

14. Spear S.F., Balkenhol N., Fortin M.-J., McRae B.H., Scribner K.I.M., Use of resistance surfaces for landscape genetic studies: considerations for parameterization and analysis. Mol. Ecol., 2010, 19(17), 3576-3591

15. Beier P., Majka D.R., Spencer W.D., Forks in the road: choices in procedures for designing wildland linkages. Conserv. Biol., 2008, 22(4), 836-851

16. Felicisimo A.M., Munoz J., Gonzalez-Solis J., Ocean surface winds drive dynamics of transoceanic aerial movements. PLoS One, 2008, 3(8), 7

17. González-Solís J., Felicísimo A., Fox J.W., Afanasyev V., Kolbeinsson Y., Muñoz J.s., Influence of sea surface winds on shearwater migration detours. Mar. Ecol. Prog. Ser., 2009, 391, 221-230

18. Turchin P. Quantitative analyiss of movement. Sinnauer Associates, Sunderland, MA, USA, 1998

19. Fortin M.-J., Dale M.R.T. Spatial analyisis: a guide for ecologists. Cambridge University Press, Cambridge, UK, 2005

20. Egevang C., Stenhouse I.J., Phillips R.A., Petersen A., Fox J.W., Silk J.R.D., Tracking of Arctic Terns Sterna paradisaea reveals longest animal migration. Proc. Natl. Acad. Sci. U. S. A., 2010, 107(5), 2078-2081

21. Gudmundsson G.A., Alerstam T., Larsson B., Radar observations of northbound migration of the Arctic tern, Sterna paradisaea, at the Antarctic Peninsula. Antarct. Sci., 1992, 4(2), 163-170

22. Møller A.P., Flensted-Jensen E., Mardal W., Dispersal and climate change: a case study of the Arctic tern Sterna paradisaea. Glob. Change Biol., 2006, 12(10), 2005-2013

23. Fijn R.C., Hiemstra D., Phillips R.A., Winden J.v.d., Arctic Terns Sterna paradisaea from the Netherlands migrate record distances across three oceans to Wilkes Land, East Antarctica. Ardea, 2013, 101(1), 3-12

24. McKnight A., Allyn A.J., Duffy D.C., Irons D.B., 'Stepping stone' pattern in Pacific Arctic tern migration reveals the importance of upwelling areas. Mar. Ecol. Prog. Ser., 2013, 491, 253-264

25. Duffy D.C., Mcknight A., Irons D.B., Trans-Andean passage of migrating Arctic Terns over Patagonia. Mar. Ornithol., 2013, 41, 155-159

26. Shaffer S.A., Tremblay Y., Weimerskirch H., Scott D., Thompson D.R., Sagar P.M., *et al.*, Migratory shearwaters integrate oceanic resources across the Pacific Ocean in an endless summer. Proc. Natl. Acad. Sci. U. S. A., 2006, 103(34), 12799-12802

27. Raymond B., Shaffer S.A., Sokolov S., Woehler E.J., Costa D.P., Einoder L., *et al.*, Shearwater foraging in the Southern Ocean: the roles of prey availability and winds. PLoS One, 2010, 5(6), e10960

28. Dias M.P., Granadeiro J.P., Phillips R.A., Alonso H., Catry P., Breaking the routine: individual Cory's shearwaters shift winter destinations between hemispheres and across ocean basins. Proc. R. Soc. Biol. Sci. Ser. B, 2011, 278(1713), 1786-1793

29. Croxall J.P., Silk J.R.D., Phillips R.A., Afanasyev V., Briggs D.R., Global circumnavigations: tracking year-round ranges of nonbreeding albatrosses. Science, 2005, 307(5707), 249-250

30. Catry P., Dias M.P., Phillips R.A., Granadeiro J.P., Different means to the same end: long-distance migrant seabirds from two colonies differ in behaviour, despite common wintering grounds. PLoS One, 2011, 6(10), e26079

31. Phillips R.A., Silk J.R.D., Croxall J.P., Afanasyev V., Briggs D.R., Accuracy of geolocation estimates for flying seabirds. Mar. Ecol., 2004, 266, 265-272

32. Bridge E.S., Kelly J.F., Contina A., Gabrielson R.M., MacCurdy R.B., Winkler D.W., Advances in tracking small migratory birds: a technical review of light-level geolocation. J. Field Ornithol., 2013, 84(2), 121-137

33. Lisovski S., Hewson C.M., Klaassen R.H.G., Korner-Nievergelt F., Kristensen M.W., Hahn S., Geolocation by light: accuracy and precision affected by environmental factors. Methods Ecol. Evol., 2012, 3(3), 603-612

34. Atlas R., R.N. Hoffman, S.C. Bloom, J.C. Jusem, Ardizzone J., A multiyear global surface wind velocity data set using SSM/I wind observations. Bull. Am. Met. Soc., 1996, 77, 869-882

35. Reynolds R.W., Smith T.M., Liu C., Chelton D.B., Casey K.S., Schlax M.G., Daily high-resolution-blended analyses for sea surface temperature. J. Clim., 2007, 20(22), 5473-5496

36. Behrenfeld M.J., Falkowski P.G., Photosynthetic rates derived from satellite-based chlorophyll concentration. Limnol. Oceanogr., 1997, 42(1), 1-20

37. Fisher N.I., Lee A.J., Regression models for an angular response. Biometrics, 1992, 48(3), 665-677

38. Thorup K., Bisson I.-A., Bowlin M.S., Holland R.A., Wingfield J.C., Ramenofsky M.*, et al.*, Evidence for a navigational map stretching across the continental U.S. in a migratory songbird. Proc. Natl. Acad. Sci. U. S. A., 2007, 104(46), 18115-18119

39. Zuur A.F., Ieno E.N., Smith G.M. Analysing ecological data. Statistics for biology and health. Springer-Verlag, New York, 2007

40. Lewis F., Butler A., Gilbert L., A unified approach to model selection using the likelihood ratio test. Methods Ecol. Evol., 2011, 2(2), 155-162

41. Arnold T.W., Uninformative parameters and model selection using Akaike's Information Criterion. The Journal of Wildlife Management, 2010, 74(6), 1175-1178

42. Nilsson C., Klaassen R.H.G., Alerstam T., Differences in speed and duration of bird migration between spring and autumn. Am. Nat., 2013, 181(6), 837-845

43. Gastineau G., Le Treut H., Li L., Hadley circulation changes under global warming conditions indicated by coupled climate models. Tellus Ser. A-Dyn. Meterol. Oceanol., 2008, 60(5), 863-884

44. Weimerskirch H., Louzao M., de Grissac S., Delord K., Changes in wind pattern alter albatross distribution and life-history traits. Science, 2012, 335(6065), 211-214

45. Woollings T., Blackburn M., The North Atlantic jet stream under climate change and its relation to the NAO and EA patterns. J. Clim., 2012, 25(3), 886-902

46. Drent R.H., The timing of birds' breeding seasons: the Perrins hypothesis revisited especially for migrants. Ardea, 2006, 94(3), 305-322

47. Møller A.P., Rubolini D., Lehikoinen E., Populations of migratory bird species that did not show a phenological response to climate change are declining. Proc. Natl. Acad. Sci. U. S. A., 2008, 105(42), 16195-16200

48. van Etten J., Hijmans R.J., A geospatial modelling approach integrating archaeobotany and genetics to trace the origin and dispersal of domesticated plants. PLoS One, 2010, 5(8), e12060

49. Jonsen I.D., Basson M., Bestley S., Bravington M.V., Patterson T.A., Pedersen M.W.*, et al.*, State-space models for bio-loggers: a methodological road map. Deep-Sea Res. Part II-Top. Stud. Oceanogr., 2013, 88-89, 34-46

50. Newton I., Weather-related mass-mortality events in migrants. Ibis, 2007, 149(3), 453-467

51. Peterson A., Soberón J., Pearson R.G., Anderson R.P., Martínez-Meyer E., Nakamura M.*, et al.* Ecological niches and geographic distributions. Monographs in population biology. Princeton University Press, Princeton, NJ, USA, 2011

Chapter 2

Environmental influences on macro scale movement patterns of six pelagic seabird species[2]

[2] Hensz C.M., Ingenloff K. (2018). Environmental influence on macro scale movement patterns of six pelagic seabird species.

Abstract

Pelagic seabirds are model organisms for biologists interested in macro scale animal movements. Seabird movements can extend thousands of kilometers across diverse oceanographic environments. Tracking of individual birds with light level geolocator tags provide detailed records of individual seabird movements, offering critical insight into migration pathways, stopover sites, and foraging behavior. We explored circular regression as a bridge between fine-scale movement ecology models and coarse-scale distributional ecology models. We used tracking data for six pelagic seabird species (Tristan Albatross, Black-Browed Albatross, Sooty Albatross, Sooty Shearwater, Cook's Petrel, and Bugio Petrel) to test for environmental effects on macro scale movement patterns. Variations in bathymetry and sea surface temperature significantly influenced turning angles for 3 species; the other half showed little to no directional relationship at the macro-scale. Travel speed showed more consistent environmental relationships across species with reduced travel speeds over areas of warm, productive waters. These results are limited by coarse resolution tracking data, but may suggest broad species level movement preferences.

Introduction

Pelagic seabirds are among the most mobile animals on the planet, spending at least half of their time at sea, traveling between breeding colonies and conspicuous foraging areas on a seasonal-to-annual basis. Seabird migrations can extend thousands of kilometers, connecting breeding and wintering grounds as distant as Arctic and Antarctic regions. As such, seabirds serve as model organisms for marine biologists interested in migration, foraging at the macro-scale (Phillips et al. 2005). Effective conservation of pelagic seabirds requires an understanding

of the drivers of movement behavior as well as knowledge and protection of areas of importance (e.g., breeding, staging, and wintering/stopover sites). Because pelagic seabird breeding colonies are often constrained to small islands highly affected by novel invaders, limited access to resources, and human intervention, they are disproportionally threatened when compared to other major groups of birds (Cuthbert et al. 2005, Suryan et al. 2008, Wakefield et al. 2011, Croxall et al. 2012).

Historically, observations of seabirds were limited to singular records of individuals at a particular location; however, tracking technology now provides detailed records of individual seabird movements, offering critical insight into migration pathways, stopover sites, and foraging behavior (Burger & Shaffer 2008, Schick et al. 2008, Wakefield et al. 2009, Bridge et al. 2013). While collecting tracking data remains a difficult and expensive endeavor, insights gleaned from these data are invaluable (Pettorelli et al. 2014). Tracking tags provide estimates of location without significantly impacting survival or reproductive success of the birds they are attached to, allowing for unobtrusive records of movement behaviors (Phillips et al. 2003, Adams et al. 2009).

Despite extensive representation in scientific publications, Holyoak et al. found that the majority of more than 26,000 peer-reviewed movement ecology manuscripts was almost exclusively descriptive, with only 34% containing measurements or explicitly tested hypotheses (2008). One possible explanation for the bias towards description is the lack of an accepted and standardized methodology for analyzing movement data. Methods of analyzing movement data are numerous and include state-space modeling (Patterson et al. 2008, Jonsen et al. 2013), regression approaches (Mandel et al. 2011), least-cost surfaces (Adriaensen et al. 2003, Desrochers et al. 2011), and process-based modeling (Felicísimo et al. 2008, González-Solís et

al. 2009, Hays et al. 2014). Each of these methods has strengths, weaknesses, and assumptions, and address different spatial, temporal, and biological levels of organization. Further, incomplete, non-existent, inaccessible, or poor quality environmental data can also impede attempts at analysis (Burger & Shaffer 2008, Wakefield et al. 2009).

At the landscape scale, distribution ecology models of point density (Ramírez et al. 2013) and ecological niche models (Peterson et al. 2011) focus on correlations between occurrence data and environmental covariates. These models estimate environmental suitability at the landscape scale but are insensitive to anisotropic (i.e. directional) variables, such as wind, that may greatly impact movements of migratory bird species (Felicísimo et al. 2008). In contrast, fine-scale analyses such as state-space models (Patterson et al. 2008, Schick et al. 2008, Jonsen et al. 2013) can incorporate movement parameters such as turning angles and step lengths in addition to environmental variation. However, state-space models are heavily focused upon localized behavioral states of individual animals rather than broad environmental drivers of movement (Bailey et al. 2009).

This project presents a midpoint approach between distribution ecology and state space-methodology. We explore regression models utilizing movement track data at the macro scale (hundreds to thousands of kilometers), focused upon broad environmental associations at the population and species level. We test a suite of circular linear regression and linear regression models on turning angles, path tortuosity, and travel speed to characterize macroscale movement preferences from tracking data with examples for 6 species of pelagic seabirds in the order Procellariiformes. We hypothesize that differences in available environments influence macro scale movements of these species.

Materials and methods: Environmental Data

We incorporated four environmental variables in our analyses: sea surface temperature (SST; °C), net primary productivity (NPP; mg C m-2 day-1), wind speed and direction (m s-1), and bathymetry (m below sea level). We used daily NOAA Optimum Interpolation Sea Surface Temperature data at 0.25° spatial resolution from the NOAA National Centers for Environmental Information (Reynolds et al. 2007); https://www.ncdc.noaa.gov/oisst; accessed 14 November 2015). Net primary productivity data were obtained from the Oregon State University Ocean Productivity lab, serving as a proximate measure of food availability (http://www.science.oregonstate.edu/ocean.productivity; accessed 29 July 2015). These data use a vertically generalized production model (VGPM) to derive 8-day estimates of chlorophyll-based photosynthetic capacity at 0.083° spatial resolution (Behrenfeld & Falkowski 1997). We used the Cross-Calibrated Multi-Platform Ocean Surface Wind Velocity dataset to derive daily velocities for longitudinal (u-wind) and latitudinal (v-wind) components 10 m above sea level at 0.25° spatial resolution (Atlas et al. 1996; http://rda.ucar.edu/datasets/ds744.9; accessed 12 November 2015). Lastly, we retrieved high-resolution ocean bathymetry data from the NASA Visible Earth dataset (http://visibleearth.nasa.gov/grid.php; accessed 6 January 2016).

All environmental data were converted from netCDF format to geoTIFF and left at their native spatial and temporal resolutions except bathymetry; bathymetry data were aggregated from six 90° x 90° tiles into a single global file and aggregated from 0.0083° to 0.0416° using package '*raster*' in R (Hijmans 2016 v.2.5-8, R Core Team 2016 v.3.4.0). NPP data, restricted to January 2002 – December 2011, were the most limited of all input data temporally. Thusly our analyses were restricted to this time period.

Seabird Movement Data

We obtained pelagic seabird movement data through the BirdLife International Seabird Tracking Database (http://www.seabirdtracking.org; requested 13 July 2015). We requested all tracking data for 17 species in the order Procellariiformes collected using global location sensors (GLS; see "Requested Species" in Supplemental). Of the 17 species for which GLS data were requested (Table S1), we were granted access to data for seven (Table S2). Tracking data for six of the seven species were available for the time period corresponding to our environmental data (January 2002 – December 2011) and included: Tristan Albatross (*Diomedea dabbenena*), Black-Browed Albatross (*Thalassarche melanophris*), Sooty Albatross (*Phoebetria fusca*), Sooty Shearwater (*Ardenna grisea*), Cook's Petrel (*Pterodroma cookii*), and Bugio Petrel (*Pterodroma deserta*). All six study species are colonial, island breeders. Three species—those in the family Diomedeidae (*D. dabbenena, T. melanophris,* and *P. fusca*)—have Antarctic circumpolar distributions (Figure 1, a – c). These species exhibit high breeding site fidelity, returning to the same breeding colonies each season (Cuthbert et al. 2005, Phillips et al. 2005, Pinaud & Weimerskirch 2007). Outside the breeding season, these circumpolar species engage in 'wandering forage' tracking optimal environmental conditions (Croxall et al. 2005, Cuthbert et al. 2005, Phillips et al. 2005, Weimerskirch 2007, Suryan et al. 2008, Wakefield et al. 2011). All three Procellariidae species included in our study (*A. grisea, P. cookii,* and *P. deserta*) are transequatorial migrants, moving annually between breeding colonies and known wintering sites (Figure 1, d – f; Shaffer et al. 2006, Shaffer et al. 2009, Raymond et al. 2010, Rayner et al. 2011, Ramírez et al. 2013). These differences in life-history traits provide an opportunity to contrast potential environmental associations between different movement strategies.

GLS devices attached to the legs of seabirds measure light levels at regular time intervals. When GLS devices are retrieved from recaptured birds, stored data are summarized into light curves, which provide estimates of day length and time of midday. These estimates are subsequently used to calculate longitude and latitude coordinates, which for our study species translated to roughly 12-hour resolution for all except *A. grisea*, which was measured in 24-hour intervals. GLS data depend on light levels, making them susceptible to error caused by shadowing of devices. Further, because GLS devices depend on day length, latitude estimates become inaccurate near equinoxes when day lengths are approximately uniform across all latitudes (Phillips et al. 2004, Lisovski et al. 2012). While coordinates obtained from GLS data are relatively coarse spatially (~185 km resolution), the lifespan of GLS devices is longer than more accurate tracking devices that utilize satellite telemetry (on the order of months-to-years as opposed to weeks-to-months). GLS devices provide long-term seasonal movement datasets (Wakefield et al. 2009), which are necessary to characterize macroscale movement patterns of non-breeding birds.

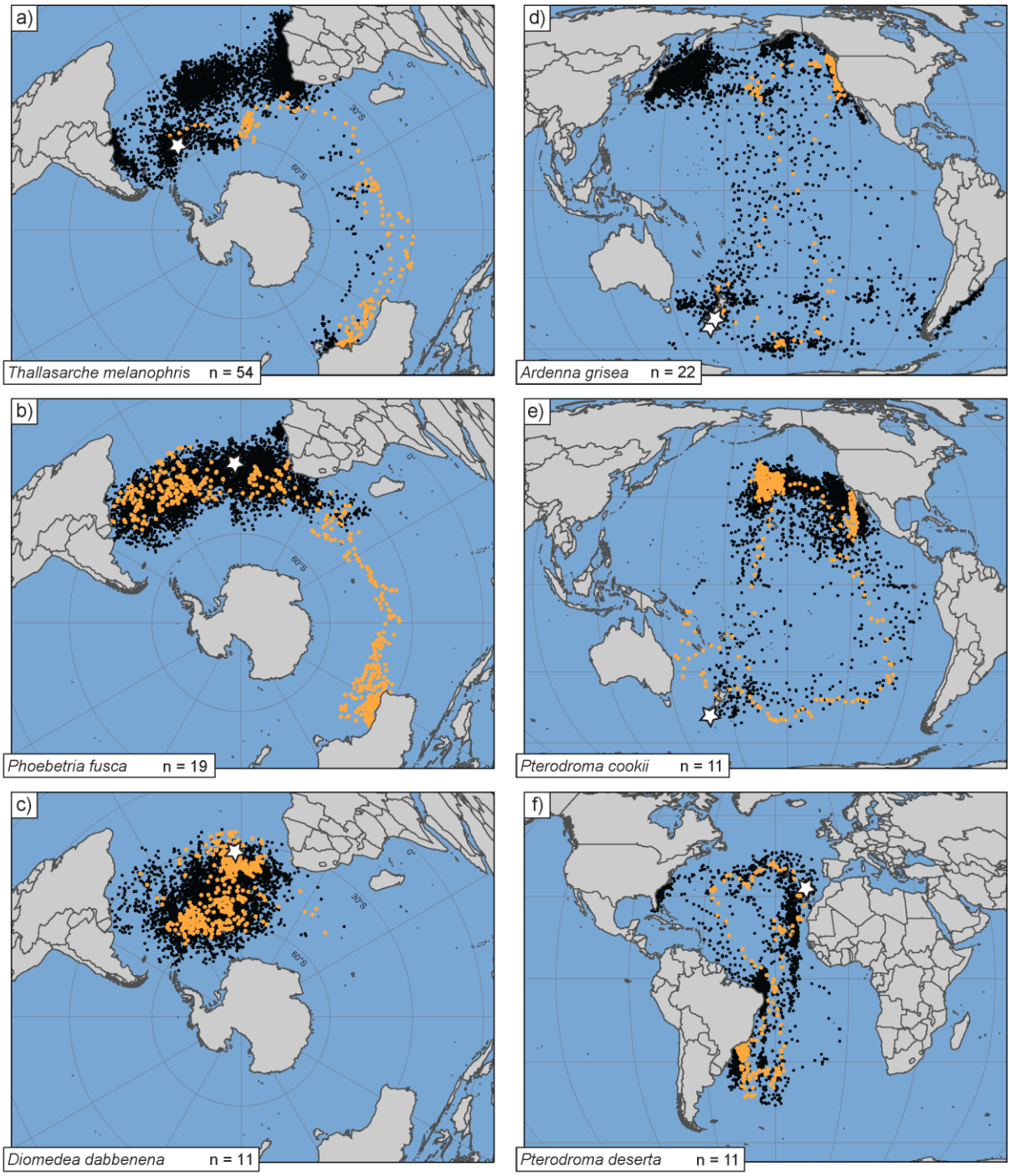

Figure 1. Cleaned seabird tracking data (black points) and number of individual tracks (n) used in analyses for each species. White stars denote breeding colonies of tracked birds. A single example track is highlighted by orange points for each species. Study species included members of the family Diomedeidae (a, *Thalassarche melanophris*; b, *Phoebetria fusca*; c, *Diomedea*

dabbenena) and family Procellariidae (d, *Ardenna grisea*; e, *Pterodroma cookii*; f, *Pterodroma deserta*). Plots are projected in (a – c) South Pole Lambert Equal Area, (d – e) Eckert IV, and (f) Robinson.

All movement data were cleaned and standardized prior to analysis as follows. We first excluded all tracks falling outside the temporal range of our environmental data (2002 - 2011) and/or including fewer than 50 data points. We then removed all location data points occurring within two weeks of an equinox to reduce geolocation error. Next, we removed juveniles and failed breeders so as to include only known non-breeding, adult birds in our analyses, focusing on macroscale landscape movements rather more localized movements associated with breeding and juvenile birds. Finally, we excluded points within staging/wintering regions for transequatorial species. This process yielded a final total of 132 movement tracks across the six species suitable for analyses (Figure S1).

Environmental Extractions

As our aim was to investigate the interaction between marine environments and movement behavior, we generated a series of sampling neighborhoods to compare environmental differences between observed and hypothetical travel paths. We defined observed paths by the shortest geodesic route between consecutive points on an individual movement track. We created diamond-shaped sampling neighborhoods by expanding the observed path using a 'stretch' parameter which extended the observed path by 10% at each end and defined a minor axis at the midpoint equal to 20% of the observed path distance (Figure 2).

We then created two sets of comparison neighborhoods to test if underlying environment was related to path choice. The first set of comparison neighborhoods was generated by rotating the observed neighborhoods in the average travel direction over the previous 12-hours, and 1, 2, and 3 days to measure turning angle (e.g., how much the current direction differed from the direction of previous steps; Figure 2). The second set of neighborhoods was made by rotating the observed path neighborhood directly towards the shortest path to location points 3 days and 7 days into the future. These neighborhoods indicate whether tortuous paths, those with many turns, highlight differences in environmental preference to straight-line paths. We generated environmental sampling neighborhoods using the '*geosphere*' package in R (Hijmans et al. 2016 v1.5-5). Mean travel directions were calculated using the '*circular*' package in R (Agostinelli & Lund 2017 v.0.4-93).

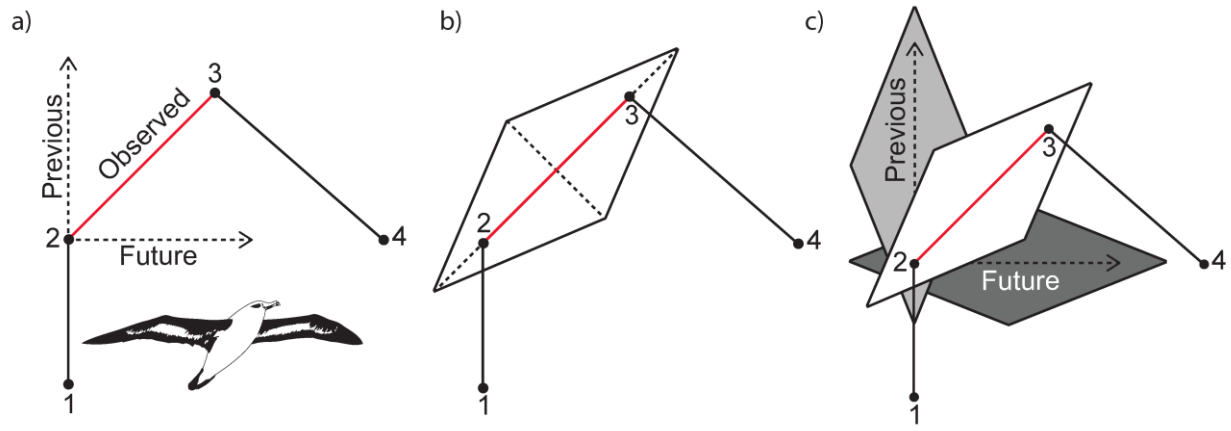

Figure 2. Schematic example of comparison neighborhoods between two points within a hypothetical movement track of four consecutive geolocator measurements, 1 – 4. The red line denotes the observed path between points 2 – 3. a) Dashed lines indicate potential alternative travel paths away from point 2, either minimizing turning angle from 1 – 2 (i.e. previous direction), or taking the least tortuous path two steps into the future from 2 – 4 (i.e. future destination). b) Extraction neighborhood for the observed path between points 2 – 3. Length

dashed lines from the solid red line are equal to 1/10 the length of the observed path (exaggerated to 1/3 for this illustration). c) Two comparison neighborhoods for environmental extraction were generated for each observed travel path by rotating the observed travel neighborhood in the average previous travel direction and towards the shortest path to the future locality.

Environments in extraction neighborhoods were evaluated using raster extraction operations in the '*raster*' package in R (Hijmans et al. 2016 v.2.5-8). For wind data, we measured the scalar projection of wind on travel direction. We log transformed NPP data post-extraction to account for heavy skew in measured environmental values. Any neighborhood occurring outside the extent of the environmental data were excluded from analysis.

Statistical analyses

Discrete movement data consists of two components: directions and step lengths. For the directional component, we used maximum-likelihood circular-linear regression to test the relationship between path choice, the angle between observed paths and comparison neighborhoods, and the difference in environments between those neighborhoods (Fisher & Lee 1992, Hensz 2015). Circular-linear regression assumes that angles θ are drawn from a von Mises distribution. Specifically, we estimated the effect of variation across environmental neighborhoods on the concentration parameter of the von Mises distribution. The von Mises distribution, often referred to as the 'circular normal' distribution from $[-2\pi, 2\pi]$, has 2 parameters: mean angle μ, and a concentration parameter, κ, with the following the probability density function:

$$f(\theta;\mu,\kappa) = \left[2\pi\, I_0(\kappa)\right]^{-1} \exp\left[\kappa\cos(\theta-\mu)\right];\ \theta > -\pi,\ \mu \le \pi,\ \kappa \ge 0$$

The value of κ, which ranges from zero to infinity, defines the shape of the distribution. When $\kappa = 0$, the von Mises distribution is equivalent to the circular uniform distribution. For $\kappa \geq 2$, the von Mises distribution is approximately equal to a normal distribution with mean μ and variance κ^{-1} (Figure 3).

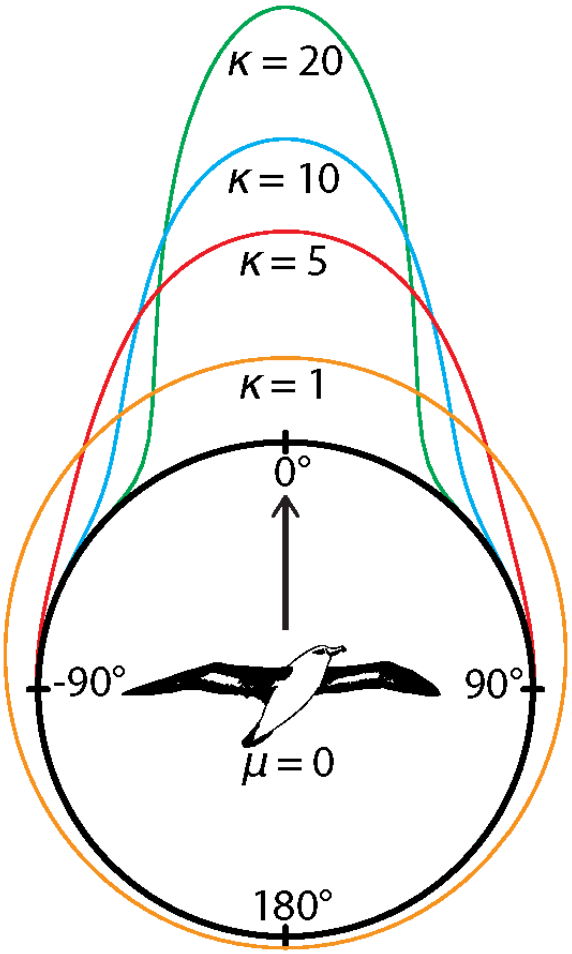

Figure 3. Four von Mises distributions with mean travel angle, $\mu = 0$, and different values of the concentration parameter, κ. For $\kappa \geq 2$, the von Mises distribution is approximately equal to a normal distribution with variance $1/\kappa$.

We assume mean deviation values $\mu \approx 0$, such that larger regression coefficients indicate a relationship between environmental differences and increased deviation (i.e. smaller κ) from comparison neighborhoods. Significant regression results indicate a quantifiable association between environment and the direction of observed travel paths. The relationship between environmental neighborhoods and κ is related using exponential link function:

$$\kappa = \exp(-\beta x + \alpha)$$

where β is the vector of model parameters, x is the matrix of environmental differences, and α is the intercept. Maximum-likelihood circular-linear models were estimated using the '*circular*' package in R (Agostinelli & Lund 2017 v.0.4-93).

To complement these directional models, we used linear regression to test for relationships between travel speed (derived from step lengths) and underlying environments as follows:

$$V = -\beta x + \alpha$$

where V is observed travel speed travel speed, β is the vector of model parameters, x is the matrix of environmental measurements, and α is the intercept. Appropriate interpretations of travel speed models depend on the environmental variable in question. For variables related to movement costs such as wind, water currents, or terrain ruggedness, slow travel speeds may indicate resistance to movement (van Etten & Hijmans 2010). In the case of environmental variables related to habitability such as NPP, slow travel speeds may be associated with highly favorable foraging areas including stopover sites (Turchin 1998, Fortin & Dale 2005).

Results

Among models for each species, differences arising from the time scale of the sampling neighborhood were relatively minor. Most model variation was observed between species and between classes of comparison neighborhoods rather than across time periods. Circular models of route choice were generally less informative than linear models of travel speed. Of 12 circular models using tortuosity neighborhoods, only half indicated significant relationships for any environmental variables. Comparisons based upon turning angles were equally uninformative; only 15 of 29 contained any significant relationships.

Relationships between environment and travel angle varied extensively across species. Circular models performed poorly for *Phoebetria fusca*, *Diomedea dabbenena*, and *Ardenna grisea*, yielding one or no significant models for each species. Mean turning angles > 30° caused most models of *P. fusca* and *D. dabbenena* to be uninformative, as variability in movements rendered them unsuitable to be fitted to a von Mises distribution.

Circular model results for *Thalassarche melanophris*, *Pterodroma cookii*, and *Pterodroma deserta* were more informative, indicating significant relationships in at least 6 of 7 models for each species (Tables 1 and S3). Across these species, bathymetry, SST, and NPP were most significant, but magnitude and direction of these relationships varied. *T. melanophris* showed consistent, increased dispersion towards greater turning angles in association with deeper ocean waters, though these results should be taken with caution as the mean turning angles were significantly greater than 0 (~30°). *P. cookii* showed significant turning behavior towards warmer and, surprisingly, less productive waters. *P. deserta* turned towards deeper waters and exhibited more tortuous paths away when towards warmer regions.

Models of travel speed indicated at least one significant environmental variable for 5 of 6 species, excluding *P. fusca*. Unlike the models of turning angle, environmental associations with travel speed were fairly consistent across species; slower travel speeds were commonly associated with warmer, deeper, and more productive waters excepting *D. dabbenena* which travelled faster over colder ocean waters (Table 2).

Table 1. Selected circular-linear model results for *Thalassarche melanophris*, *Pterodroma cookii*, and *Pterodroma deserta*. Positive estimates indicate an association between increased dispersion and greater values in the comparison neighborhood than the traveled path. Statistically significant results ($p \leq 0.05$) are in bold. T-value (T), mean angular deviation of comparison neighborhoods in degrees (μ), and the total number of geolocation points used in regression (N) are presented for each model

Species	Neighborhood	Variable	Estimate	SE	T	p	μ (deg)	N
Thalassarche melanophris	Past trend (12h)	**SST**	**0.043**	**0.02**	**1.77**	**0.038**	1.60	4241
		NPP	0.057	0.09	0.61	0.272		
		Bathymetry	**0.005**	**0.00**	**3.53**	**<0.001**		
		Wind	-0.002	0.00	0.52	0.302		
		Intercept	0.163	0.03	5.55	<0.001		
	Tortuosity (72h)	SST	-0.003	0.03	0.09	0.464	-2.44	3197
		NPP	0.074	0.10	0.74	0.228		
		Bathymetry	**-0.003**	**0.00**	**1.79**	**0.037**		
		Wind	0.006	0.00	1.20	0.115		
		Intercept	-0.030	0.03	1.03	0.151		
Pterodroma cookie	Past trend (12h)	**SST**	**0.064**	**0.03**	**2.49**	**0.006**	-32.46	596
		NPP	**-1.799**	**0.60**	**2.98**	**0.001**		
		Bathymetry	-0.001	0.02	0.05	0.480		
		Wind	**0.060**	**0.03**	**2.27**	**0.011**		
		Intercept	0.871	0.16	5.33	<0.001		
	Tortuosity (72h)	**SST**	**0.044**	**0.02**	**2.35**	**0.009**	-2.55	652
		NPP	0.001	0.37	0.00	0.499		
		Bathymetry	4.80E-04	0.01	0.06	0.476		
		Wind	-0.012	0.01	1.02	0.154		
		Intercept	0.052	0.07	0.74	0.230		
Pterodroma Deserta	Past trend (12h)	SST	0.017	0.02	0.82	0.206	-3.33	391
		NPP	-0.460	0.40	1.15	0.125		
		Wind	**0.037**	**0.02**	**1.66**	**0.048**		
		Bathymetry	**0.014**	**0.01**	**2.60**	**0.005**		
		Intercept	0.455	0.14	3.36	<0.001		
	Tortuosity (72h)	**SST**	**0.027**	**0.01**	**2.29**	**0.011**	-8.53	457
		NPP	0.110	0.29	0.38	0.353		
		Bathymetry	0.006	0.01	1.12	0.130		
		Wind	0.004	0.02	0.25	0.402		
		Intercept	-0.217	0.07	3.05	0.001		

.

Table 2. Results of linear regression of travel speed by species. Positive estimates indicate an association between faster travel speed and more positive environmental values. Statistically significant results ($p \leq 0.05$) are in bold. T-value (T), adjusted R-sqaured value, and the total number of geolocation points used in regression (N) are presented for each model.

Species	Variable	Estimate	SE	T	p	Adj. R-Squared	N
Thalassarche melanophris	**SST**	**1.604**	**0.24**	**6.68**	**< 0.001**	0.110	5180
	NPP	**-2.230**	**0.34**	**-6.59**	**< 0.001**		
	Bathymetry	**-3.839**	**0.31**	**-12.37**	**< 0.001**		
	Wind	0.287	0.21	1.35	0.176		
	Intercept	19.579	0.21	92.40	< 0.001		
Phoebetria Fusca	SST	-3.701	4.10	-0.90	0.367	0.001	3346
	NPP	-4.255	4.11	-1.06	0.289		
	Bathymetry	1.488	2.90	0.51	0.607		
	Wind	1.180	2.72	0.43	0.665		
	Intercept	56.701	2.72	20.83	< 0.001		
Diomedea dabbenena	**SST**	**-1.282**	**0.40**	**-3.17**	**0.002**	0.018	4387
	NPP	**-2.787**	**0.40**	**-6.88**	**< 0.001**		
	Bathymetry	-0.174	0.38	-0.45	0.650		
	Wind	-0.494	0.38	-1.30	0.194		
	Intercept	29.987	0.38	78.86	< 0.001		
Pterodroma cookie	**SST**	**6.652**	**0.62**	**10.73**	**< 0.001**	0.179	674
	NPP	**-1.414**	**0.71**	**-2.00**	**0.046**		
	Bathymetry	1.131	0.68	1.66	0.098		
	Wind	0.046	0.59	0.08	0.938		
	Intercept	25.181	0.58	43.21	< 0.001		
Pterodroma Deserta	**SST**	**4.988**	**0.68**	**7.39**	**< 0.001**	0.154	474
	NPP	-1.229	0.74	-1.67	0.096		
	Bathymetry	**-1.821**	**0.70**	**-2.61**	**0.009**		
	Wind	-0.543	0.61	-0.88	0.377		
	Intercept	22.103	0.61	36.25	< 0.001		
Ardenna Grisea	**SST**	**7.552**	**0.55**	**13.77**	**< 0.001**	0.309	472
	NPP	**-2.474**	**0.65**	**-3.81**	**< 0.001**		
	Bathymetry	0.965	0.68	1.41	0.158		
	Wind	0.192	0.52	0.37	0.711		
	Intercept	20.481	0.51	40.30	< 0.001		

Discussion

Pelagic seabirds navigate marine environments based upon a suite of internal and external factors. Using remotely sensed environmental data and tracking data from light-level geolocators, we found support for the hypothesis that differences in available environments influence macroscale movements of several pelagic seabird species. We also found support for the hypothesis that these species show different responses to the same oceanic environments. Specific environmental relationships were mixed across species. Bathymetry and SST may be associated with path turning in half of the species in this study. However, the other half showed little to no directional relationship at the macroscale. In contrast, travel speed seemed to show more consistent relationship with environments across species with reduced travel speeds over areas of warm, productive waters.

Despite well-documented associations between seabird movements and wind patterns in multiple seabird species (Felicísimo et al. 2008, González-Solís et al. 2009, Wakefield et al. 2009, Raymond et al. 2010), our analyses did not indicate a significant effect of wind for any of our study species. This result is likely a reflection of the coarse resolution of the study, as wind is less likely to be a dominant distributional driver in the context of modeling at moderately coarse spatio-temporal resolutions (Wakefield et al. 2009). We utilized relatively coarse light logger tracking data to characterize movement at the macroscale because of limitations in the temporal range of more accurate spatial tracking devices. Additionally, these data are more available for study as they are the result of simpler and more accessible technology (Phillips et al. 2004, Holyoak et al. 2008, Lisovski et al. 2012).

Observed differences in navigation tactics across our study species are unsurprising given huge differences in wing morphology and breeding habits (Bridge 2006). Albatross species

within Diomedeidae are at least 20 - 30 times heavier and have wingspans at least 3 - 4 times wider than species from Procellariidae (Warham 1977). The unique exaggerated wing morphology of albatrosses expends very little energy in flight, resulting in different flight patterns than smaller birds with narrower, broader wings such as our two gadfly petrel (Pterodroma) species. In addition, the albatrosses are limited to a polar distribution in southern waters; species within Procellariidae showed drastic changes in movement modes from relatively static periods of foraging to directed transequatorial migrations to and from these regions (Pinaud & Weimerskirch 2007, González-Solís et al. 2009, Shaffer et al. 2009, Raymond et al. 2010, Rayner et al. 2011, Ramírez et al. 2013).

The models in this study assume a monotonic relationship between environmental differences and route decisions. Monotonic relationships are sensible for variables like NPP, where increased access food resources is generally assumed preferable. However, environmental tolerances often have upper and lower limits depending on species ecologies, behaviors, and physiologies (Peterson et al. 2011). Future studies of macroscale movement ecology may benefit from developing new modeling methods to incorporate these non-linear relationships.

We included only environmental variables in this study for simplification, but movement decisions are highly complex, based upon many factors. Group movements and human interference (especially from fishing vessels) can also greatly influence seabird behavior (Cuthbert et al. 2005, Pinaud & Weimerskirch 2007, Croxall et al. 2012, Tremblay et al. 2014). Accounting for the influence of these variables is notoriously difficult without detailed individual surveillance of movements (Tremblay et al. 2014).

Movement ecology is a rapidly developing field with many researchers focusing on different spatiotemporal scales of movement behavior (Turchin 1998, Fortin & Dale 2005,

Nathan et al. 2008, Schick et al. 2008). At fine spatial resolutions, state-space methods have been highly successful in characterizing seabird movements (Nathan et al. 2008, Patterson et al. 2008, Schick et al. 2008, Jonsen et al. 2013). However, while these methods provide much more detailed information on movement patterns, they require prior knowledge of movements to inform models. At coarser scales, stable isotopes have been used to broadly characterize foraging regions and individual differences within populations of seabirds (Bearhop et al. 2006, Phillips et al. 2009, Jaeger et al. 2010) but these analyses are blind to the effects of physical variables such as wind.

Using circular linear regression on track data to characterize species level seabird movements at the macroscale, we explored a bridge between fine-scale movement ecology models and coarse-scale distributional ecology models (Peterson et al. 2011, Ramírez et al. 2013). Macroscale studies construct a general picture of species that complement finer-scale assessments, allowing more informed conservation decisions, invaluable for highly threatened groups of species.

Acknowledgements

We thank Ross Wanless and Richard Philips at the British Antarctic Survey, Matt Rayner, Victor Paiva, Ivan Ramirez, Francis Zino, Manuel Biscoito, Scott Shaffer, David Thompson, and the curators of the Bird Life International Seabird Tracking Database for providing data and feedback for this project.

References

Adams J, Scott D, McKechnie S, Blackwell G, Shaffer SA, Moller H (2009) Effects of geolocation archival tags on reproduction and adult body mass of sooty shearwaters (Puffinus griseus). NZ J Zool 36:355-366

Adriaensen F, Chardon JP, De Blust G, Swinnen E, Villalba S, Gulinck H, Matthysen E (2003) The application of 'least-cost' modelling as a functional landscape model. Landsc Urban Plann 64:233-247

Atlas R, Hoffman RN, Bloom SC, Jusem JC, Ardizzone J (1996) A multiyear global surface wind velocity data set using SSM/I wind observations. Bull Am Meteorol Soc 77:869-882

Bailey H, Mate BR, Palacios DM, Irvine L, Bograd SJ, Costa DP (2009) Behavioural estimation of blue whale movements in the Northeast Pacific from state-space model analysis of satellite tracks. Endanger Species Res 10:1

Bearhop S, Phillips RA, McGill R, Cherel Y, Dawson DA, Croxall JP (2006) Stable isotopes indicate sex-specific and long-term individual foraging specialisation in diving seabirds. Mar Ecol Prog Ser 311:157-164

Behrenfeld MJ, Falkowski PG (1997) Photosynthetic rates derived from satellite-based chlorophyll concentration. Limnol Oceanogr 42:1-20

Bridge ES (2006) Influences of morphology and behavior on wing-molt strategies in seabirds. Mar Ornithol 34:7-19

Bridge ES, Kelly JF, Contina A, Gabrielson RM, MacCurdy RB, Winkler DW (2013) Advances in tracking small migratory birds: a technical review of light-level geolocation. J Field Ornithol 84:121-137

Burger AE, Shaffer SA (2008) Perspectives in ornithology application of tracking and data-logging technology in research and conservation of seabirds. Auk 125:253-264

Croxall JP, Butchart SH, Lascelles B, Stattersfield AJ, Sullivan B, Symes A, Taylor P (2012) Seabird conservation status, threats and priority actions: a global assessment. Bird Conserv Int 22:1-34

Croxall JP, Silk JRD, Phillips RA, Afanasyev V, Briggs DR (2005) Global circumnavigations: tracking year-round ranges of nonbreeding albatrosses. Science 307:249-250

Cuthbert R, Hilton G, Ryan P, Tuck GN (2005) At-sea distribution of breeding Tristan albatrosses Diomedea dabbenena and potential interactions with pelagic longline fishing in the South Atlantic Ocean. Biol Conserv 121:345-355

Desrochers A, Belisle M, Morand-Ferron J, Bourque J (2011) Integrating GIS and homing experiments to study avian movement costs. Landsc Ecol 26:47-58

Dodge S, Bohrer G, Bildstein K, Davidson SC, Weinzierl R, Bechard MJ, Barber D, Kays R, Brandes D, Han J (2014) Environmental drivers of variability in the movement ecology of turkey vultures (Cathartes aura) in North and South America. Philos Trans R Soc B 369:20130195

Felicísimo ÁM, Muñoz J, González-Solis J (2008) Ocean surface winds drive dynamics of transoceanic aerial movements. PLOS ONE 3:e2928

Fisher NI, Lee AJ (1992) Regression models for an angular response. Biometrics 48:665-677

Fortin M-J, Dale MRT (2005) Spatial analyisis: a guide for ecologists. Cambridge University Press, Cambridge, UK

González-Solís J, Felicísimo A, Fox JW, Afanasyev V, Kolbeinsson Y, Muñoz Js (2009) Influence of sea surface winds on shearwater migration detours. Mar Ecol Prog Ser 391:221-230

Hays GC, Christensen A, Fossette S, Schofield G, Talbot J, Mariani P (2014) Route optimisation and solving Zermelo's navigation problem during long distance migration in cross flows. Ecol Lett 17:137-143

Hensz CM (2015) Environmental factors in migratory route decisions: a case study on Greenlandic Arctic Terns (Sterna paradisaea). Anim Mig 2:76-85

Holyoak M, Casagrandi R, Nathan R, Revilla E, Spiegel O (2008) Trends and missing parts in the study of movement ecology. Proc Natl Acad Sci USA 105:19060-19065

Jaeger A, Connan M, Richard P, Cherel Y (2010) Use of stable isotopes to quantify seasonal changes of trophic niche and levels of population and individual specialisation in seabirds. Mar Ecol Prog Ser 401:269-277

Jonsen ID, Basson M, Bestley S, Bravington MV, Patterson TA, Pedersen MW, Thomson R, Thygesen UH, Wotherspoon SJ (2013) State-space models for bio-loggers: A methodological road map. Deep Sea Res Part II 88:34-46

Lisovski S, Hewson CM, Klaassen RHG, Korner-Nievergelt F, Kristensen MW, Hahn S (2012) Geolocation by light: accuracy and precision affected by environmental factors. Methods Ecol Evol 3:603-612

Mandel JT, Bohrer G, Winkler DW, Barber DR, Houston CS, Bildstein KL (2011) Migration path annotation: cross-continental study of migration-flight response to environmental conditions. Ecol Appl 21:2258-2268

Nathan R, Getz WM, Revilla E, Holyoak M, Kadmon R, Saltz D, Smouse PE (2008) A movement ecology paradigm for unifying organismal movement research. Proc Natl Acad Sci USA 105:19052-19059

Patterson TA, Thomas L, Wilcox C, Ovaskainen O, Matthiopoulos J (2008) State–space models of individual animal movement. Trends Ecol Evol 23:87-94

Peterson A, Soberón J, Pearson RG, Anderson RP, Martínez-Meyer E, Nakamura M, Araújo MB (2011) Ecological niches and geographic distributions (Vol. 49). Princeton University Press, Princeton, NJ, USA

Pettorelli N, Safi K, Turner W (2014) Satellite remote sensing, biodiversity research and conservation of the future. Philos Trans R Soc B 369: 20130190

Phillips RA, Bearhop S, Mcgill RAR, Dawson DA (2009) Stable isotopes reveal individual variation in migration strategies and habitat preferences in a suite of seabirds during the nonbreeding period. Oecologia 160:795-806

Phillips RA, Silk JRD, Croxall JP, Afanasyev V, Bennett VJ (2005) Summer distribution and migration of nonbreeding albatrosses: individual consistencies and implications for conservation. Ecology 86:2386-2396

Phillips RA, Silk JRD, Croxall JP, Afanasyev V, Briggs DR (2004) Accuracy of geolocation estimates for flying seabirds. Mar Ecol 266:265-272

Phillips RA, Xavier JC, Croxall JP (2003) Effects of satellite transmitters on albatrosses and petrels. Auk 120:1082-1090

Pinaud D, Weimerskirch H (2007) At- sea distribution and scale- dependent foraging behaviour of petrels and albatrosses: a comparative study. J Anim Ecol 76:9-19

Ramírez I, Paiva VH, Menezes D, Silva I, Phillips RA, Ramos JA, Garthe S (2013) Year-round distribution and habitat preferences of the Bugio petrel. Mar Ecol Prog Ser 476:269-284

Raymond B, Shaffer SA, Sokolov S, Woehler EJ, Costa DP, Einoder L, Hindell M, Hosie G, Pinkerton M, Sagar PM, Scott D, Smith A, Thompson DR, Vertigan C, Weimerskirch H (2010) Shearwater foraging in the Southern Ocean: the roles of prey availability and winds. PLOS ONE 5:e10960

Rayner MJ, Hauber ME, Steeves TE, Lawrence HA, Thompson DR, Sagar PM, Bury SJ, Landers TJ, Phillips RA, Ranjard L (2011) Contemporary and historical separation of transequatorial migration between genetically distinct seabird populations. Nat Commun 2:332

Reynolds RW, Smith TM, Liu C, Chelton DB, Casey KS, Schlax MG (2007) Daily high-resolution-blended analyses for sea surface temperature. Journal of Climate 20:5473-5496

Schick RS, Loarie SR, Colchero F, Best BD, Boustany A, Conde DA, Halpin PN, Joppa LN, McClellan CM, Clark JS (2008) Understanding movement data and movement processes: current and emerging directions. Ecol Lett 11:1338-1350

Shaffer SA, Tremblay Y, Weimerskirch H, Scott D, Thompson DR, Sagar PM, Moller H, Taylor GA, Foley DG, Block BA, Costa DP (2006) Migratory shearwaters integrate oceanic resources across the Pacific Ocean in an endless summer. Proc Natl Acad Sci USA 103:12799-12802

Shaffer SA, Weimerskirch H, Scott D, Pinaud D, Thompson DR, Sagar PM, Moller H, Taylor GA, Foley DG, Tremblay Y (2009) Spatiotemporal habitat use by breeding sooty shearwaters Puffinus griseus. Mar Ecol Prog Ser 391:209-220

Suryan RM, Anderson DJ, Shaffer SA, Roby DD, Tremblay Y, Costa DP, Sievert PR, Sato F, Ozaki K, Balogh GR (2008) Wind, waves, and wing loading: morphological specialization may limit range expansion of endangered albatrosses. PLOS ONE 3:e4016

Tremblay Y, Thiebault A, Mullers R, Pistorius P (2014) Bird-borne video-cameras show that seabird movement patterns relate to previously unrevealed proximate environment, not prey. PLOS ONE 9:e88424

Turchin P (1998) Quantitative analyiss of movement. Sinnauer Associates, Sunderland, MA, USA

van Etten J, Hijmans RJ (2010) A geospatial modelling approach integrating archaeobotany and genetics to trace the origin and dispersal of domesticated plants. PLOS ONE 5:e12060

Wakefield ED, Phillips RA, Matthiopoulos J (2009) Quantifying habitat use and preferences of pelagic seabirds using individual movement data: a review. Mar Ecol Prog Ser 391:165-182

Wakefield ED, Phillips RA, Trathan PN, Arata J, Gales R, Huin N, Robertson G, Waugh SM, Weimerskirch H, Matthiopoulos J (2011) Habitat preference, accessibility, and competition limit the global distribution of breeding Black- browed Albatrosses. Ecol Monogr 81:141-167

Warham J (1977) Wing loadings, wing shapes, and flight capabilities of procellariiformes. NZ J Zool 4:73-83

Weimerskirch H (2007) Are seabirds foraging for unpredictable resources? Deep Sea Res Part II 54:211-223

SUPPLEMENTAL MATERIAL

Table S1. Procellarid global location sensor data requested 13 July 2015 through the BirdLife International Seabird Tracking Database (http://www.seabirdtracking.org/) by species.

Order: Procellariiformes

Family: Diomedeidae (albatrosses**)**

Common Name	**Scientific Name**	
Antipodean albatross	*Diomedea antipodensis*	
Tristan albatross	*Diomedea dabbenena*	+
Wandering albatross	*Diomedea exulans*	
Short-tailed albatross	*Phoebastria albatrus*	
Sooty albatross	*Phoebetria fusca*	+
Buller's albatross	*Thalassarche bulleri*	
Shy albatross	*Thalassarche cauta*	
Grey-headed albatross	*Thalassarche chrysostoma*	+*
Black-browed albatross	*Thalassarche melanophris*	+

Family: Procellariidae (fulmarine petrels, gadfly petrels, prions, shearwaters**)**

Common Name	**Scientific Name**	
Sooty shearwater	*Ardenna grisea*	+
Cory's shearwater	*Calonectris borealis*	
Scopoli's shearwater	*Calonectris diomedea*	
Southern giant petrel	*Macronectes giganteus*	
Northern giant petrel	*Macronectes halli*	
Westland petrel	*Procellaria westlandica*	
Cook's petrel	*Pterodroma cookii*	+
Bugio petrel	*Pterodroma deserta*	+

+ Access to (some) tracking data granted
* All available movement data fall outside range of environmental data

Table S2. Pelagic seabird global location sensor (GLS) data made available for, and utilized in, these analyses by species name, species colony site, dataset owner, total number of tracks in the dataset used, date range of the dataset, and corresponding BirdLife International dataset identification number.

Species	Colony Site(s)	Data Contributor(s)	Tracks Used	Year(s)	BirdLife ID
Diomedea dabbenena	Gough Is. (40.32°S 9.94°W)	Ross Wanless; British Antarctic Survey	13	2004 - 06	423
	Tristan da Cunha (37.07°S 12.32°W)				
Phoebetria fusca	Gough Is. (40.32°S 9.94°W)	Ross Wanless; British Antarctic Survey	19	2003 - 06	424
	Tristan da Cunha (37.07°S 12.32°W)				
Thalassarche melanophris	Bird Is. (54.01°S 38.05°W)	Richard Philips; British Antarctic Survey	56	2002 - 03	493
Pterodroma cookie	Little Barrier Is. (36.20°S 175.08°E)	Matt J. Rayner	0	2007 - 09	637
	Codfish Is. (46.78°S 167.63°E)		11		639
Pterodroma deserta	Madeira Is. (32.65°N 16.91°W)	Victor Paiva; Ivan Ramirez	0	2008 - 13	824
		Francis Zino; Manuel Biscoito	11	2009 - 12	825
Ardenna grisea	Mana Is. (41.09°S 174.78°E)	Scott Shaffer; David Thompson	6	2005 - 06	517
	Codfish Is. (46.78°S 167.63°E)		16		518

Table S3. Complete circular model results of past directional trend and path tortuosity for *Thalassarche melanophris*, *Phoebetria fusca, Diomedea dabbanena, Pterodroma cookii*, *Pterodroma deserta, and Ardenna grisea*. Positive estimates indicate an association between increased dispersion and greater values in the comparison neighborhood than the traveled path. Statistically significant results ($p \leq 0.05$) are in bold. T-value (T), p-value (p), Mean angular deviation of comparison neighborhoods in degrees (μ) and the total number of geolocation points used in regression (N) are presented for each model. Models discarded due to large values of μ (> 90°) are highlighted in red.

Species	Neighborhood	Variable	Estimate	SE	T	p	mu (deg)	N
Thalassarche melanophris	Past trend (12h)	**SST**	**0.043**	**0.02**	**1.77**	**0.038**	1.60	4241
		NPP	0.057	0.09	0.61	0.272		
		Bathymetry	**0.005**	**0.00**	**3.53**	**<0.001**		
		Wind	-0.002	0.00	0.52	0.302		
		Intercept	0.163	0.03	5.55	0.000		
	Past trend (24h)	SST	0.043	0.03	1.37	0.085	0.32	3769
		NPP	0.019	0.13	0.15	0.441		
		Bathymetry	**0.007**	**0.00**	**3.59**	**<0.001**		
		Wind	-0.002	0.01	0.34	0.368		
		Intercept	0.531	0.04	12.55	<0.001		
	Past trend (48h)	SST	0.058	0.04	1.40	0.081	-3.52	3366
		NPP	0.078	0.16	0.48	0.315		
		Bathymetry	**0.006**	**0.00**	**2.36**	**0.009**		
		Wind	-0.005	0.01	0.65	0.257		
		Intercept	0.855	0.06	14.22	<0.001		
	Past trend (72h)	SST	0.070	0.05	1.30	0.098	-4.49	3039
		NPP	0.156	0.21	0.75	0.225		
		Bathymetry	**0.005**	**0.00**	**1.69**	**0.046**		
		Wind	-0.003	0.01	0.27	0.394		
		Intercept	1.067	0.08	13.80	<0.001		
	Past trend (96h)	SST	0.093	0.06	1.62	0.053	-11.42	2756
		Bathymetry	0.004	0.00	1.33	0.092		
		NPP	0.112	0.21	0.53	0.298		
		Wind	-0.006	0.01	0.61	0.271		
		Intercept	1.051	0.08	13.15	<0.001		
	Tortuosity (72h)	SST	-0.003	0.03	0.09	0.464	-2.44	3197
		NPP	0.074	0.10	0.74	0.228		
		Bathymetry	**-0.003**	**0.00**	**1.79**	**0.037**		
		Wind	0.006	0.00	1.20	0.115		
		Intercept	-0.030	0.03	1.03	0.151		
	Tortuosity (7d)	SST	-0.007	0.05	0.14	0.444	-4.38	2168
		NPP	0.031	0.14	0.22	0.412		
		Bathymetry	-0.002	0.00	0.73	0.232		
		Wind	0.005	0.01	0.70	0.242		
		Intercept	0.315	0.05	6.86	<0.001		

Species	Neighborhood	Variable	Estimate	SE	T	P	mu (deg)	N
Phoebetria Fusca	Past trend (12h)	**SST**	**-0.106**	**0.06**	**1.83**	**0.033**	8.28	2695
		Bathymetry	-0.002	0.01	0.35	0.362		
		NPP	0.686	0.43	1.60	0.055		
		Wind	0.005	0.02	0.32	0.373		
		Intercept	1.648	0.15	11.14	<0.001		
	Past trend (24h)	SST	0.206	0.02	9.82	<0.001	**-174.32**	2564
		NPP	-0.667	0.15	4.37	<0.001		
		Bathymetry	0.005	0.00	1.58	0.057		
		Wind	-0.122	0.01	11.88	<0.001		
		Intercept	2.310	0.21	10.82	<0.001		
	Past trend (48h)	SST	0.286	0.02	11.62	<0.001	**-175.26**	2331
		NPP	-0.759	0.16	4.63	<0.001		
		Bathymetry	0.005	0.00	1.31	0.095		
		Wind	0.132	0.01	10.37	<0.001		
		Intercept	2.745	0.27	10.08	<0.001		
	Past trend (72h)	SST	0.020	0.02	0.91	0.180	**175.46**	2222
		Bathymetry	-0.008	0.00	2.10	0.018		
		NPP	-2.656	0.28	9.58	<0.001		
		Wind	-0.118	0.01	9.19	<0.001		
		Intercept	2.801	0.30	9.29	<0.001		
	Past trend (96h)	SST	0.112	0.02	5.59	<0.001	**-179.82**	2050
		NPP	-3.177	0.32	10.05	<0.001		
		Bathymetry	-0.009	0.00	2.11	0.017		
		Wind	0.094	0.01	7.43	<0.001		
		Intercept	2.794	0.32	8.78	<0.001		
	Tortuosity (72h)	SST	0.008	0.02	0.37	0.354	1.04	2387
		NPP	-0.047	0.16	0.29	0.386		
		Bathymetry	5.08E-05	0.00	0.02	0.493		
		Wind	-0.003	0.01	0.62	0.268		
		Intercept	0.262	0.04	6.25	< 0.001		
	Tortuosity (7d)	SST	0.021	0.03	0.73	0.232	0.09	1809
		NPP	-0.247	0.22	1.12	0.131		
		Bathymetry	-0.001	0.00	0.21	0.417		
		Wind	-0.002	0.01	0.35	0.362		
		Intercept	0.494	0.06	8.44	< 0.001		

Species	Neighborhood	Variable	Estimate	SE	T	P	mu (deg)	N
Diomedea dabbenena	Past trend (12h)	SST	0.009	0.03	0.33	0.372	-3.10	3785
		NPP	0.311	0.20	1.58	0.057		
		Bathymetry	-0.007	0.00	1.93	0.027		
		Wind	-0.009	0.01	1.13	0.129		
		Intercept	0.951	0.06	15.31	<0.001		
	Past trend (24h)	SST	-0.014	0.15	0.09	0.463	-52.60	3582
		NPP	0.339	0.98	0.34	0.365		
		Bathymetry	-0.008	0.02	0.47	0.319		
		Wind	-0.004	0.04	0.11	0.455		
		Intercept	2.648	0.34	7.77	<0.001		
	Past trend (48h)	SST	-0.370	0.04	9.33	<0.001	**-134.14**	3415
		NPP	0.796	0.18	4.37	<0.001		
		Bathymetry	-0.003	0.00	0.61	0.272		
		Wind	0.100	0.01	7.98	<0.001		
		Intercept	2.962	0.32	9.40	<0.001		
	Past trend (72h)	SST	-0.289	0.06	5.03	<0.001	**-101.34**	3243
		NPP	0.800	0.34	2.34	0.010		
		Bathymetry	-0.030	0.01	3.92	<0.001		
		Wind	0.097	0.02	4.50	<0.001		
		Intercept	3.417	0.56	6.11	<0.001		
	Past trend (96h)	SST	0.024	0.21	0.11	0.456	-14.39	3093
		Bathymetry	-0.008	0.03	0.31	0.378		
		NPP	0.346	1.49	0.23	0.408		
		Wind	0.002	0.05	0.03	0.489		
		Intercept	2.984	0.51	5.82	<0.001		
	Tortuosity (72h)	SST	0.008	0.02	0.38	0.353	1.83	3388
		NPP	-0.085	0.13	0.63	0.264		
		Bathymetry	0.002	0.00	0.70	0.241		
		Wind	0.005	0.00	1.10	0.135		
		Intercept	0.281	0.04	7.88	<0.001		
	Tortuosity (7d)	SST	0.015	0.03	0.51	0.307	4.47	2778
		NPP	-0.234	0.18	1.29	0.098		
		Bathymetry	0.004	0.00	1.35	0.089		
		Wind	0.005	0.01	0.82	0.206		
		Intercept	0.514	0.05	10.68	<0.001		

Species	Neighborhood	Variable	Estimate	SE	T	p	mu (deg)	N
Pterodroma cookie	Past trend (12h)	**SST**	**0.064**	**0.03**	**2.49**	**0.006**	-32.46	596
		NPP	**-1.799**	**0.60**	**2.98**	**0.001**		
		Bathymetry	-0.001	0.02	0.05	0.480		
		Wind	**0.060**	**0.03**	**2.27**	**0.011**		
		Intercept	0.871	0.16	5.33	<0.001		
	Past trend (24h)	SST	0.051	0.03	1.50	0.067	-33.78	571
		NPP	**-1.713**	**0.56**	**3.08**	**0.001**		
		Bathymetry	0.003	0.01	0.18	0.429		
		Wind	**0.064**	**0.03**	**2.43**	**0.008**		
		Intercept	0.822	0.16	5.14	<0.001		
	Past trend (48h)	SST	0.055	0.04	1.49	0.068	-33.18	533
		NPP	-0.804	0.66	1.21	0.113		
		Bathymetry	-0.002	0.02	0.12	0.454		
		Wind	**0.072**	**0.03**	**2.66**	**0.004**		
		Intercept	0.733	0.15	4.82	<0.001		
	Past trend (72h)	**SST**	**0.092**	**0.03**	**3.65**	**<0.001**	-29.28	520
		Bathymetry	-0.001	0.02	0.03	0.488		
		NPP	-0.625	0.63	0.99	0.160		
		Wind	**0.064**	**0.03**	**2.52**	**0.006**		
		Intercept	0.652	0.14	4.61	<0.001		
	Past trend (96h)	SST	0.052	0.03	1.52	0.064	-24.28	497
		NPP	**-1.039**	**0.62**	**1.66**	**0.048**		
		Bathymetry	-0.006	0.02	0.32	0.373		
		Wind	**0.071**	**0.03**	**2.51**	**0.006**		
		Intercept	0.751	0.16	4.65	<0.001		
	Tortuosity (72h)	**SST**	**0.044**	**0.02**	**2.35**	**0.009**	-2.55	652
		NPP	0.001	0.37	0.00	0.499		
		Bathymetry	4.80E-04	0.01	0.06	0.476		
		Wind	-0.012	0.01	1.02	0.154		
		Intercept	0.052	0.07	0.74	0.230		
	Tortuosity (7d)	**SST**	**0.041**	**0.02**	**2.39**	**0.008**	-2.54	620
		NPP	0.081	0.42	0.20	0.423		
		Bathymetry	0.002	0.01	0.27	0.393		
		Wind	0.010	0.01	0.83	0.204		
		Intercept	0.100	0.08	1.33	0.092		

Species	Neighborhood	Variable	Estimate	SE	T	p	mu (deg)	N
Pterodroma Deserta	Past trend (12h)	SST	0.017	0.02	0.82	0.206	-3.33	391
		NPP	-0.460	0.40	1.15	0.125		
		Bathymetry	**0.014**	**0.01**	**2.60**	**0.005**		
		Wind	**0.037**	**0.02**	**1.66**	**0.048**		
		Intercept	0.455	0.14	3.36	< 0.001		
	Past trend (24h)	SST	0.029	0.02	1.45	0.073	-1.29	398
		NPP	-0.143	0.43	0.33	0.369		
		Bathymetry	**0.008**	**0.00**	**1.65**	**0.049**		
		Wind	0.029	0.02	1.32	0.093		
		Intercept	0.478	0.13	3.60	< 0.001		
	Past trend (48h)	SST	0.019	0.02	0.83	0.203	0.09	379
		NPP	-0.248	0.40	0.63	0.265		
		Bathymetry	**0.009**	**0.01**	**1.80**	**0.036**		
		Wind	0.016	0.02	0.74	0.230		
		Intercept	0.468	0.14	3.43	< 0.001		
	Past trend (72h)	SST	-0.007	0.03	0.19	0.424	1.97	385
		NPP	-0.530	0.43	1.22	0.111		
		Bathymetry	0.005	0.01	0.91	0.181		
		Wind	0.028	0.02	1.24	0.107		
		Intercept	0.519	0.14	3.73	< 0.001		
	Past trend (96h)	SST	-0.053	0.11	0.46	0.322	-1.01	369
		NPP	-0.722	0.41	1.77	0.039		
		Bathymetry	**0.010**	**0.01**	**2.02**	**0.022**		
		Wind	0.022	0.02	0.98	0.164		
		Intercept	0.477	0.14	3.47	< 0.001		
	Tortuosity (72h)	**SST**	**0.027**	**0.01**	**2.29**	**0.011**	-8.53	457
		Bathymetry	0.006	0.01	1.12	0.130		
		NPP	0.110	0.29	0.38	0.353		
		Wind	0.004	0.02	0.25	0.402		
		Intercept	-0.217	0.07	3.05	0.001		
	Tortuosity (7d)	**SST**	**0.058**	**0.02**	**3.25**	**0.001**	-15.16	437
		NPP	0.023	0.29	0.08	0.468		
		Bathymetry	0.001	0.01	0.17	0.433		
		Wind	-0.014	0.02	0.91	0.182		
		Intercept	-0.082	0.08	1.00	0.158		

Species	Neighborhood	Variable	Estimate	SE	T	p	mu (deg)	N
Ardenna Grisea	Past trend (24h)	SST	-0.070	0.08	0.84	0.202	5.86	354
		NPP	0.544	0.51	1.06	0.145		
		Bathymetry	0.009	0.01	0.92	0.180		
		Wind	0.010	0.02	0.64	0.262		
		Intercept	0.204	0.11	1.91	0.028		
	Past trend (48h)	SST	-0.102	0.10	1.04	0.150	1.13	310
		Bathymetry	0.005	0.01	0.44	0.331		
		NPP	0.413	0.55	0.76	0.225		
		Wind	0.001	0.02	0.05	0.478		
		Intercept	0.365	0.13	2.82	0.002		
	Past trend (72h)	SST	-0.089	0.10	0.89	0.187	3.65	269
		NPP	0.594	0.56	1.07	0.142		
		Bathymetry	0.007	0.01	0.60	0.274		
		Wind	0.006	0.02	0.26	0.397		
		Intercept	0.384	0.14	2.71	0.003		
	Past trend (96h)	SST	-0.109	0.10	1.04	0.150	-0.94	230
		NPP	0.785	0.68	1.16	0.124		
		Bathymetry	0.006	0.01	0.44	0.330		
		Wind	-0.016	0.02	0.69	0.244		
		Intercept	0.303	0.14	2.09	0.018		
	Tortuosity (48h)	**SST**	**0.045**	**0.02**	**2.22**	**0.013**	-1.36	380
		NPP	-0.404	0.41	0.97	0.165		
		Bathymetry	0.003	0.01	0.38	0.351		
		Wind	-0.003	0.01	0.22	0.415		
		Intercept	-0.647	0.07	9.94	< 0.001		
	Tortuosity (7d)	SST	0.013	0.03	0.45	0.328	-1.31	267
		NPP	-0.352	0.44	0.80	0.212		
		Bathymetry	-0.002	0.01	0.26	0.397		
		Wind	-0.020	0.02	1.15	0.125		
		Intercept	-0.546	0.08	6.88	< 0.001		

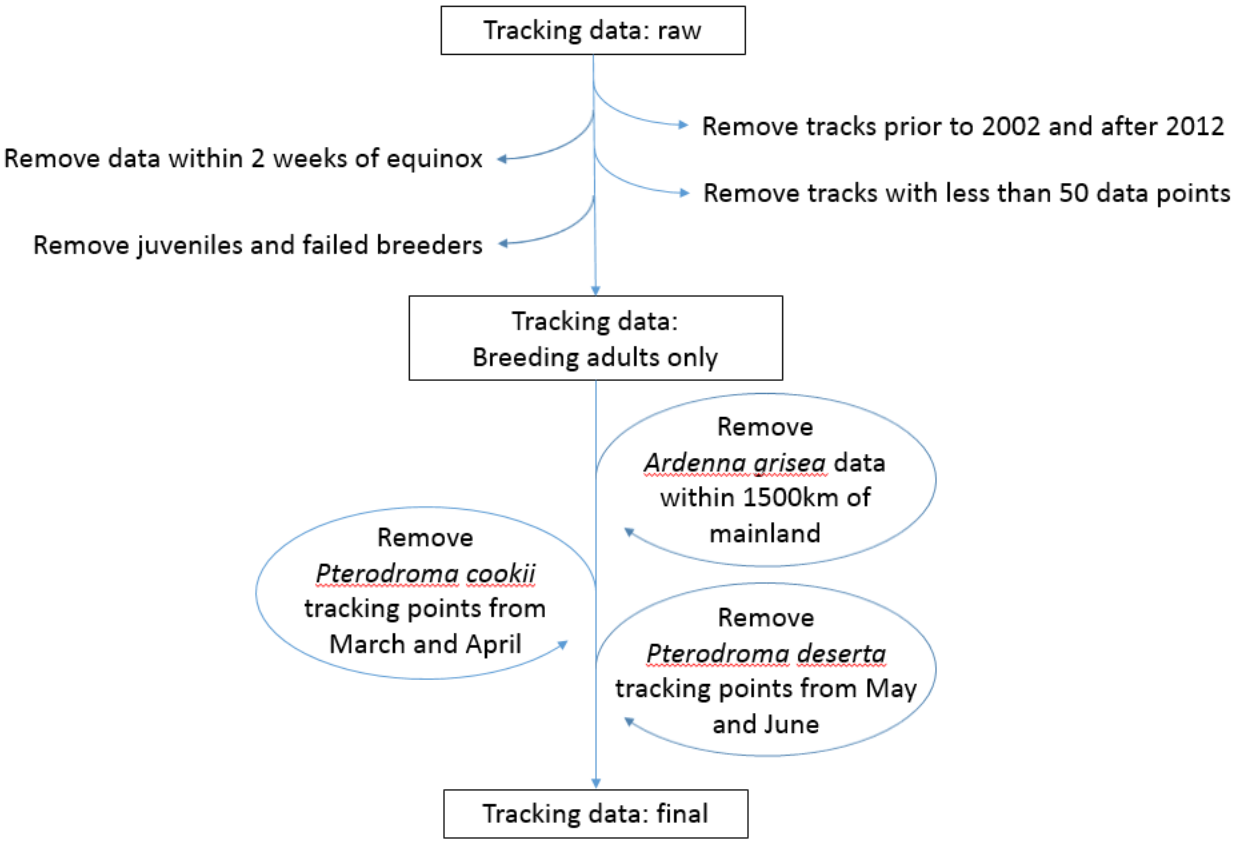

Figure S1. Generalized cleaning workflow for seabird tracking data obtained through the BirdLife International Seabird Tracking Database (http://www.seabirdtracking.org/).

APPENDIX. R Code

```
# Hensz, C. M. & K. Ingenloff. "Environmental influences on macro
scale movement patterns of six pelagic seabird species."

# Scripts developed by: Christopher Hensz and Kate Ingenloff#

#Call relevant packages#
library(circular)
library(raster)
library(rgeos)
library(geosphere)

#Function to generate a vector of dates from BirdLife tracking data#
pointdates = function(x) {
  y = vector(mode = "character")
  y = strptime(paste(as.character(x$date_gmt),
as.character(x$time_gmt), sep =
                       " "),
               format = "%Y-%m-%d %H:%M:%S",
               tz = "UTC")
  y
}

#Function to generate the time between consecutive dates in a vector#
datediff = function(timelist) {
  v = list()
  for (i in 1:(length(timelist) - 1)) {
    v[i] = difftime(timelist[i + 1], timelist[i], units = "hours")
  }
  v = c(v, NA)
  v = unlist(v)
  v = as.numeric(as.character(v))
  v
}

#Function to calculate the bearings between each point in sequence
from BirdLife tracking data#
migbear = function(x) {
  require(circular)
  result = vector(mode = "numeric", length = (nrow(x) - 1))
  for (i in 1:((nrow(x) - 1))) {
    result[i] = bearing(c(x$longitude[i], x$latitude[i]),
                        c(x$longitude[i + 1], x$latitude[i + 1]))
  }
  result = c(result, NA)
  result
}

#Function to calculate the curved earth distance between each point in
sequence
```

```
migdist = function(x) {
  y = vector(mode = "numeric", length = (nrow(x) - 1))
  for (i in 1:((nrow(x) - 1))) {
    y[i] = distMeeus(
      c(x$longitude[i], x$latitude[i]),
      c(x$longitude[i + 1], x$latitude[i + 1]),
      a = 6378137,
      f = 1 / 298.257223563
    )
  }
  y = c(y, NA)
  y
}

#Generates a table of basic parameters using tracking data#
Table = function(x) {
  result = data.frame(
    cbind(
      "SPECIES" = as.character(x$common_name),
      "TRACKID" = x$track_id,
      "POINTID" = 1:nrow(x),
      "DATE" = as.character(pointdates(x)),
      "TDIFF" = datediff(pointdates(x)),
      "LON" = x$longitude,
      "LAT" = x$latitude,
      "LONNEXT" = c(x$longitude[-1], NA),
      "LATNEXT" = c(x$latitude[-1], NA),
      "VEL" = migdist(x) / datediff(pointdates(x)),
      "MIG" = migbear(x),
      "MIGDIST" = migdist(x)
    )
  )
  result[, 1] = as.character(result[, 1])
  for (i in 5:12) {
    result[, i] = as.numeric(as.character(result[, i]))
  }
  result
}


#Function to calcuate the time between a point and a point a number of
'steps' in the past#
#Uses tables generated by the function 'Table'#
lasttime = function(x, steps = 1) {
  y = vector(mode = "numeric", length = (nrow(x) - steps))
  for (i in (steps + 1):nrow(x)) {
    y[i] = sum(x$TDIFF[i - 1:steps])
  }
  y
}

#Function to calcuate the time between a point and a bumber of
```

```
'steps' in the future#
#Uses tables generated by the function 'Table'#
nexttime = function(timelist, steps = 1) {
  v = list()
  for (i in 1:(length(timelist) - steps)) {
    v[i] = difftime(timelist[i + steps], timelist[i], units = "hours")
  }
  v = c(v, rep(NA, steps))
  v = unlist(v)
  v = as.numeric(as.character(v))
  v
}

#Function to calcuate the shortest direction between a point and a
point a bumber of 'steps' in the past#
#Uses tables generated by the function 'Table'#
lastdir = function(x, steps = 1) {
  y = vector(mode = "numeric", length = (nrow(x) - steps))
  for (i in (steps + 1):nrow(x)) {
    y[i] = mean.circular(circular(
      x$MIG[i - 1:steps],
      units = "degrees",
      zero = pi / 2,
      rotation = "clock"
    ))
  }
  y
}

#Function to calcuate the shortest direction between a point and a
point a bumber of 'steps' in the future#
#Uses tables generated by the function 'Table'#
nextdir = function(x, steps = 1) {
  y = vector(mode = "numeric", length = nrow(x))
  for (i in 1:(nrow(x) - steps)) {
    y[i] = bearing(c(x[i, 1], x[i, 2]), c(x[i + (steps - 1), 3], x[i +
(steps -

1), 4]))
  }
  y
}


## Function uses output of function 'Table' as input#
TableComps = function(x) {
  result = x
  # we add on directions and times for forward (tortuousity) and
backward (turning angle) steps#
  result2 = cbind(
    result,
    "LAST1TIME" = lasttime(result, steps = 1),
```

```
    "LAST1DIR" = lastdir(result,
                         steps = 1),
    "LAST2TIME" = lasttime(result, steps = 2),
    "LAST2DIR" = lastdir(result,
                         steps = 2),
    "LAST3TIME" = lasttime(result, steps = 3),
    "LAST3DIR" = lastdir(result,
                         steps = 3),
    "LAST4TIME" = lasttime(result, steps = 4),
    "LAST4DIR" = lastdir(result,
                         steps = 4),
    "LAST6TIME" = lasttime(result, steps = 6),
    "LAST6DIR" = lastdir(result,
                         steps = 6),
    "LAST8TIME" = lasttime(result, steps = 8),
    "LAST8DIR" = lastdir(result,
                         steps = 8),
    "NEXT3TIME" = nexttime(result$DATE, steps = 3),
    "NEXT3DIR" = nextdir(result[, 6:9], steps = 3),
    "NEXT6TIME" = nexttime(result$DATE, steps = 6),
    "NEXT6DIR" = nextdir(result[, 6:9], steps = 6),
    "NEXT7TIME" = nexttime(result$DATE, steps = 7),
    "NEXT7DIR" = nextdir(result[, 6:9], steps = 7),
    "NEXT14TIME" = nexttime(result$DATE, steps = 14),
    "NEXT14DIR" = nextdir(result[, 6:9], steps = 14)
  )

  # We calculate and append the lat-long coordinates for comparison
neighborhoods onto the table#
  output = result2
  for (i in seq(14, 24, by = 2)) {
    LASTLON = vector()
    LASTLAT = vector()
    for (j in 1:nrow(result3)) {
      LASTLON[j] = destPoint(
        p = c(result3$LON[j], result3$LAT[j]),
        b = result3[j, i],
        d = result3$MIGDIST[j]
      )[, 1]
      LASTLAT[j] = destPoint(
        p = c(result3$LON[j], result3$LAT[j]),
        b = result3[j, i],
        d = result3$MIGDIST[j]
      )[, 2]
    }
    output = cbind(output, LASTLON, LASTLAT)
  }
  names(output) = c(
    names(result3),
    "LAST1LON",
    "LAST1LAT",
    "LAST2LON",
```

```
    "LAST2LAT",
    "LAST3LON",
    "LAST3LAT",
    "LAST4LON",
    "LAST4LAT",
    "LAST6LON",
    "LAST6LAT",
    "LAST8LON",
    "LAST8LAT"
  )
  result4 = output
  for (i in seq(26, 32, by = 2)) {
    NEXTLON = vector()
    NEXTLAT = vector()
    for (j in 1:nrow(result3)) {
      NEXTLON[j] = destPoint(
        p = c(result3$LON[j], result3$LAT[j]),
        b = result3[j, i],
        d = result3$MIGDIST[j]
      )[, 1]
      NEXTLAT[j] = destPoint(
        p = c(result3$LON[j], result3$LAT[j]),
        b = result3[j, i],
        d = result3$MIGDIST[j]
      )[, 2]
    }
    output = cbind(output, NEXTLON, NEXTLAT)
  }
  names(output) = c(
    names(result4),
    "NEXT3LON",
    "NEXT3LAT",
    "NEXT6LON",
    "NEXT6LAT",
    "NEXT7LON",
    "NEXT7LAT",
    "NEXT14LON",
    "NEXT14LAT"
  )
  return(output)
}

###Environmental extractions###

## Function: DestinationsSB ##
# The four points bounding the extraction neighborhood for raster
extraction polygons are calculated using destPoint ('geosphere'
package) within the DestinationsSB function. The function returns a
spatial curved-earth polygon generated from these four points. See
figure 2

# Required function inputs include:
```

```
## lonlat1: lon-lat of point 1
## lonlat2: lon-lat of point 2
## bearing: direction in degrees
## dist: distance in meters
## stretch: the size of the buffer around points as a fraction of
distance

DestinationsSB = function(lonlat1,
                         lonlat2,
                         bearing,
                         dist,
                         stretch = 1 / 10) {
  POINTS = rbind(
    as.vector(destPoint(lonlat1, bearing - 180, stretch * dist, r =
6378137)),
    as.vector(destPoint(
      midPoint(lonlat1, lonlat2), bearing - 90, stretch * dist, r =
6378137
    )),
    as.vector(destPoint(lonlat2, bearing, stretch * dist, r =
6378137)),
    as.vector(destPoint(
      midPoint(lonlat1, lonlat2), bearing + 90, stretch * dist, r =
6378137
    ))
  )
  makePoly(POINTS, sp = T)
}


# load list of rasters for all dates in range
## Rotation: -180 to 180, used for points in the atlantic, away from
the international dateline
EnvRas <-
  list.files("XXXXXXXX", full.names = T) # Filepath for folder
containing raster files

## Rotation: 0 to 360, used for points in the pacific near the
international dateline
EnvRasRot <- list.files("XXXXXX", full.names = T)

# Prepare a file with the date range for each raster layer
#each row contains: a filename, the start date, and end date for that
layer
EnvDates = read.csv("XXXXXX")

#This function extracts all neighborhoods for a single environmental
variable for a single track#
#input:
#track: a track data.frame object passed through 'Table' and
'TableComps'
#rasterlist: a nested list where the first element contains the list
```

```
of -180 to 180 rasters and
#the second element contains the 0 - 360 rasters
#EnvDates: data.frame described above
#Neighborhood: the neighborhood of interest
#Varname: the name of the variable
SBAveExtract = function(track,
                        rasterlist = list(EnvRas, EnvRasRot),
                        EnvDates,
                        neighborhood = "LAST1TIME",
                        Varname = "") {
  #check which files are in range for each point
  times = as.Date(strptime(as.character(track$DATE),
                           format = "%F %T", tz = "UTC"))
  datecheck = sapply(
    times,
    FUN = function(x) {
      which(x[1] >= as.Date(EnvDates[, 2]) & x[1] < as.Date(EnvDates[,
3]))
    }
  )
  result = vector(mode = "numeric", length = (nrow(track) - 1))
  extrcol = which(grepl(names(track), pattern = neighborhood))
  print(paste("Extracting", neighborhood, sep = " "))
  progress = txtProgressBar(min = 1,
                            max = nrow(track),
                            style = 3)
  for (j in 1:(nrow(track) - 1)) {
    setTxtProgressBar(progress, j)
    # data prior to the first environmental dataset is skipped over
and the environments are treated as NA
    if (times[j] < "2002-07-04") {
      result[j] = "NA"
    } else{
      # if the time between two points is 0 or NA, return 'NA'
      if (track[j, extrcol] == 0 |
          is.na(track[j, extrcol]) |
          (neighborhood == "LAST2TIME" & is.na(track$LAST2DIR[j]))) {
        result[j] = "NA"
      } else{
        #
        poly = DestinationsSB(c(sba$LON[j], sba$LAT[j]),
                              c(sba[j, (extrcol + 20)], sba[j,
(extrcol + 21)]),
                              sba$MIG[j],
                              sba$MIGDIST[j])
        if (extent(poly)@xmin < (-170) & extent(poly)@xmax > 170) {
          poly = recenter(poly)
          EnvR <-
            raster(rasterlist[[2]][datecheck[[j]]], varname = Varname)
          EnvRas2 = crop(EnvR, poly)
          result1 = mask(EnvRas2, poly)
          result[j] = mean(getValues(result1), na.rm = T)
```

```
        } else{
          EnvR <- raster(rasterlist[[1]][datecheck[[j]]], varname =
Varname)
          EnvRas2 = crop(EnvR, poly)
          result1 = mask(EnvRas2, poly)
          result[j] = mean(getValues(result1), na.rm = T)
        }
      }
    }
  }
  close(progress)
  result[sapply(result, is.null)] = "NA"
  return(result)
}

##Statistics functions##

#This function returns a table to be used for circular-linear
regressions
#input:
#tracks = a list of track data.frames
#neighborhood = the direction and time frame of the comparison
neighborhood
#vars = a list of the environmental variables to compare
#timestep = the size of the comparison neighborhoods in numbers of
steps
#resolution = the time-step resolution of the tracking data in hours
SBDataCirc = function(tracks,
                      neighborhood = c("LAST1DIR", "LAST1TIME"),
                      vars = c("UWNDLAST1", "VWNDLAST1", "SSTLAST1",
"BATHYLAST1", "NPPLAST1"),
                      timestep = 1,
                      resolution = 12) {
  require(circular)
  Data = tracks
  Data2 = cbind(
    Data[, 1:12],
    "ComparDir" = Data[, which(names(Data) == neighborhood[1])],
    "ComparTime" = Data[, which(names(Data) == neighborhood[2])],
    "UWNDAVE" = Data[, which(names(Data) == vars[1])],
    "VWNDAVE" = Data[, which(names(Data) == vars[2])],
    "SSTAVE" = Data[, which(names(Data) == vars[3])],
    "BATHYAVE" = Data[, which(names(Data) == vars[4])],
    "NPPAVE" = Data[, which(names(Data) == vars[5])],
    "WINDU" = Data[, which(names(Data) == "WINDU")],
    "WINDV" = Data[, which(names(Data) == "WINDV")],
    "SST" = Data[, which(names(Data) == "SST")],
    "NPP" = Data[, which(names(Data) == "NPP")],
    "BATHY" = Data[, which(names(Data) == "BATHY")]
  )
```

```
#Calculate the environmental comparsions for all variables and
aggregate into a table
  Stat1 = cbind(
    "THETA" = Data2[, 11] - Data2[, 13],
    "TDIFF" = Data2[, 5],
    "LASTTIME" = Data2[, 14],
    "VEL" = Data2[, 10],
    "SST" = Data2[, 22],
    "BATHY" = Data2[, 24],
    "NPP" = Data2[, 23],
    "WINDPROJ" = Data2[, 20] * cos(rad(90 - Data2[, 11])) + Data2[,
21] *
      cos(rad(Data2[, 11])),
    "SSTAVE" = Data2[, 17],
    "BATHYAVE" = Data2[, 18],
    "NPPAVE" = Data2[, 19],
    "WINDPROJAVE" = Data2[, 15] * cos(rad(90 - Data2[, 13])) + Data2[,
16] *
      cos(rad(Data2[, 13]))
  )
  #Clean table for empty records for any environment
  Stat1 = na.omit(Stat1)
  Stat2 = Stat1
  #simplify angular differences to be within -180 to 180
  Stat2[, 1][which(Stat1[, 1] > 180)] = Stat1[, 1][which(Stat1[, 1] >
180)] -
    360
  Stat2[, 1][which(Stat1[, 1] < (-180))] = Stat1[, 1][which(Stat1[, 1]
<
                                                          (-180))]
+ 360
  Stat3 = Stat2
  #remove points with time between points greater than 1.5 times the
resolution
  #this eliminates neighborhoods missing points in the middle
  Stat3 = Stat2[-which(Stat2[, 2] > resolution * 1.5 |
                         Stat2[, 3] == 0 | Stat2[, 3] >
                         (resolution * timestep + 0.5 * resolution)),
]
  result = cbind(
    Stat3[, 1:4],
    "DELTASST" = Stat3[, 5] - Stat3[, 9],
    "DELTABATHY" = Stat3[, 6] - Stat3[, 10],
    "LOGDELTANPP" = log(Stat3[, 7]) - log(Stat3[, 11]),
    "DELTAWINDPROJ" = Stat3[, 8] - Stat3[, 12]
  )
  return(result)
}

#This function returns a table for linear regression

#input:
```

```
#tracks = a list of track data.frames
#resolution = the time-step resolution of the tracking data in hours

SBDataVel = function(tracks, resolution = 12) {
  require(circular)
  Data = tracks[[1]]
  for (i in 2:length(tracks)) {
    Data = rbind(Data, tracks[[i]])
  }
  Data2 = cbind(
    Data[, 1:12],
    "WINDPROJ" =
      Data[, which(names(Data) == "WINDU")] * cos(rad(90 - Data[,
11])) + Data[, which(names(Data) ==

"WINDV")] * cos(rad(Data[, 11])),
    "SST" = Data[, which(names(Data) == "SST")],
    "NPP" = Data[, which(names(Data) == "NPP")],
    "BATHY" = Data[, which(names(Data) == "BATHY")]
  )
  Data2 = (na.omit(Data2))
  result = Data2[-which(Data2[, 5] > resolution * 1.5), ]
  result
}

##Circular Statistics Function##

#conducts circular-linear regresion of the concentration parameter
kappa from Fisher (1992)
#input:
#track = data passed through the 'SBDataCirc' function
#nvar = the number of variables in the model
#columns = the columns of the input containing those variables

CircStats = function(track,
                     nvar = 4,
                     columns = 5:8) {
  sbgamma = optim(
    par = c(rep(0.01, nvar), 1),
    fn = function(sbgamma) {
      y = rad(track[, 1])
      x = as.matrix(cbind(track[, columns], 1))
      mu = mean.circular(y)
      result = -sum(log(besselI(exp(
        -as.vector(x %*% sbgamma)
      ),
      nu = 0))) +
        sum(exp(-as.vector(x %*% sbgamma)) *
              cos(y - mu))
      result
    },
    control = list(maxit = 100000, fnscale = -1)
```

```
  )$par
  resids = as.matrix(cbind(track[, columns], 1))
  link = exp(-as.vector(resids %*% sbgamma))
  se.gamma = sqrt(diag(solve(t(resids) %*% #t(x)
                             (diag(
                               link ^ 2 * (1 - A1(link) ^ 2 -
A1(link) /  link)
                             )) %*% #W
                             resids))) #x
  tval = abs(sbgamma / (se.gamma))
  p = 1 - pnorm(tval)
  result = cbind(
    "Parameter Estimate" = sbgamma,
    "SE" = se.gamma,
    "TValue" = tval,
    "P Value" = p
  )
  result
}
```

Chapter 3

Temporal variation in dispersal habits of invasive Eurasian collared doves in North America

Introduction

A major goal of invasive species research is to predict rates of spread and invasion potential of newly colonized regions. Invasion processes are highly complex, driven by a combination of landscape configurations, environmental suitability, dispersal capability, and population dynamics (Hengeveld 1989, Veit & Lewis 1996, Simberloff 1997, Courchamp et al. 1999, Keitt et al. 2001, Peterson 2003, Johnson et al. 2006, Baguette & Van Dyck 2007); each of these factors must be considered when attempting to model changes in invasive species geographic ranges.

Ecological niches have been used to characterize potential species distributions for over a century (Grinnell 1917, Hutchinson 1959, Peterson et al. 2011) describing the biotic conditions (competitive exclusion, obligate or facilitative mutualisms, etc.) and abiotic conditions (climate, topography, landscape type, etc.) necessary to establish stable populations. Peterson et al. (2011) presented a theoretical framework where ecological niches can be broken down into 'fundamental', 'existing', and 'realized' niches. A species' fundamental niche defines the region in environmental space suitable for population growth. The existing niche is the subset of the environments in the fundamental niche that is represented in geographical space. The realized niche is the subset of the existing niche that is represented in the observed distribution of the species. Differences between existing and realized niches can be used to investigate undocumented areas of an animal's potential distribution or transferred onto new landscapes to predict areas susceptible to biological invasions (Peterson 2003, Peterson et al. 2011). Differences between existing and realized niches can be caused by many factors related to geographic accessibility, including limited dispersal capabilities, "hard" geographical barriers such as mountains or rivers, and "soft" barriers such as expansive inhospitable regions. Soberón

and Peterson (2005) presented the 'BAM' conceptual framework summarizing how biotic factors, abiotic factors, and mobility interact to define species distributions (Figure 1). The observed geographic distribution of a species, denoted G_O, is found at the intersection of all three factors. The invadable geographic area (i.e. suitable, unoccupied areas), denoted G_I are restricted by factors related to mobility.

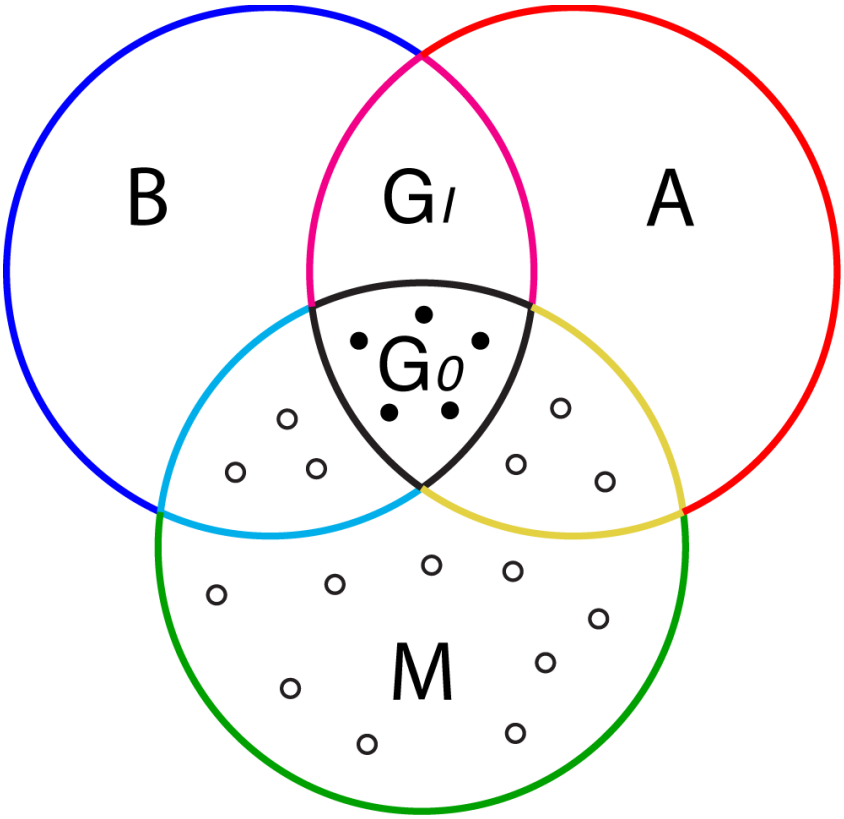

Figure 1 — 'BAM' diagram representing a simplified ecological niche in geographic space. Areas of suitable biotic conditions are defined by ***B.*** Areas of suitable abiotic conditions are defined by ***A***. Areas accessible to the species are represented by ***M***. $\boldsymbol{G_O}$ defines the observed geographic distribution. $\boldsymbol{G_I}$ represents suitable, but currently unoccupied areas in geography caused by limitations in mobility. Hollow points represent accessible, but unsuitable habitats that would result in sink populations. Solid black points are stable, source populations.

Natal dispersal capabilities greatly influence the rate of spread of invasive species across new landscapes. Despite the importance of dispersal to distributional patterns, estimating the dispersal capabilities of a species remains challenging given the inherent randomness present in the natal dispersal process. Dispersal is divided into two modes: short-distance diffusion processes, and long-distance "jump" dispersal (Simberloff 1997, Higgins et al. 2003, Nathan et al. 2003, Trakhtenbrot et al. 2005). Modeling short-distance dispersal is relatively straight-forward using diffusion models (Bled et al. 2011), but rare, long-distance dispersal is less predictable. To account for this randomness, dispersal kernels (probability distributions of dispersal distances) are usually leptokurtic or "fat tailed" to include more long-distance dispersal events than the normal distribution (Morales 2002, Nathan et al. 2012). In these cases, spread of a species distribution may consist of a few large jumps followed by backfill (Veit & Lewis 1996, Johnson et al. 2006, Scheidt & Hurlbert 2014).

Many models of invasive species movements also include demographic factors such as the Allee effect (Veit & Lewis 1996, Courchamp et al. 1999, Stephens & Sutherland 1999, Keitt et al. 2001, Johnson et al. 2006). The Allee effect describes the negative impact of small population size for overall population growth, effectively establishing a minimum population size before conventional growth models, such as logistic growth, take effect (Stephens & Sutherland 1999). The Allee effect is especially influential on invasive species, potentially slowing or stopping range expansion entirely (Keitt et al. 2001). Simulated invasions of the gypsy moth (*Lymantria dispar*) and the house finch (*Haemorhous mexicanus*) across regions of North America found significant improvements to invasion models when including the Allee effect (Veit & Lewis 1996, Johnson et al. 2006).

In this contribution, I present a model of the invasion of Eurasian collared doves (*Streptopelia decaocto*) across North America from 1997 – 2016. The Eurasian collared dove is an invasive bird with a broad distribution across Europe, Asia, and North America. The collared dove is a cosmopolitan invasive species, having spread across Europe in the 1930's and later across North America from the 1980's – present day (Ingenloff et al. 2017). The spread of the Eurasian collared dove has been extensively studied and documented in both Europe (Robertson 1990, Eraud et al. 2007, Eraud et al. 2011) and North America (Romagosa & Labisky 2000, Beckett et al. 2007, Fujisaki et al. 2010, Bled et al. 2011, Scheidt & Hurlbert 2014, Ingenloff et al. 2017). The collared dove specializes in disturbed habitats on the periphery of developed urban regions, preferring areas highly modified by human activity over pristine forested landscapes (Fujisaki et al. 2010). Despite being invasive, there is no data to suggest that collared doves have a large negative impact on native species of doves in North America, but the effect of high-density breeding populations are still not well-understood (Poling & Hayslette 2006). The extensive documentation of Eurasian collared doves provides an opportunity to characterize the underlying drivers of this invasion process.

My goal is to investigate the relationship between inter-annual dispersal behavior of collared doves in North America and underlying environmental conditions. I argue that differences in environmental suitability influence both population abundance and natal dispersal patterns using a combination of ecological niche models, population abundance estimates, and dispersal simulations.

Materials and Methods

Abundance Estimation

Abundance data for the Eurasian collared dove were obtained through the North American Breeding Bird Survey (BBS) dataset (Pardieck et al. 2017). The BBS maintains 4647 active survey routes; abundance data are recorded for all observed bird species at 0.5 mile intervals (~0.8 km) along each 24.5 mile (~39.4 km) transect each year. Each BBS track is assigned a single set of coordinates (longitude and latitude) without providing the exact location for each stop. For this reason, I associated the sum of all observations along each BBS route to the singular corresponding georeferenced locations provided.

I used all 4647 active BBS routes to estimate the abundance of collared doves across the United States and Canada from 1997 – 2016. Of the 4647 active BBS routes, 1586 contained at least one observation of the collared dove in the range of the dataset. I used simple kriging to interpolate abundance of collared doves onto a 10km x 10km grid in Albers Equal Area Conic map projection with packages 'gstat' (v. 1.1 – 5) and 'raster' (v. 2.5 – 8) in R (R Core Team 2017). Kriging was performed using the spherical model with linear interpolation for each year 1997 – 2016 producing annual estimates of population abundance across North America. To represent Allee effects of varying intensity, I applied a set of three minimum abundance thresholds to the annual abundance estimations (2, 5, and 10 individuals per 10km x 10km cell); for each of these values, cells containing fewer individuals than the defined threshold were treated as non-breeding territory for the purpose of simulations (Figure 2). I used these breeding distribution grids to characterize inter-annual changes in distributional area from 1997 – 2015. I compared the estimated distributions of sequential years and summarized these comparisons into

three groups: 1) cells retained in the next year, 2) new cells gained in the next year, and 3) cells lost in the next year.

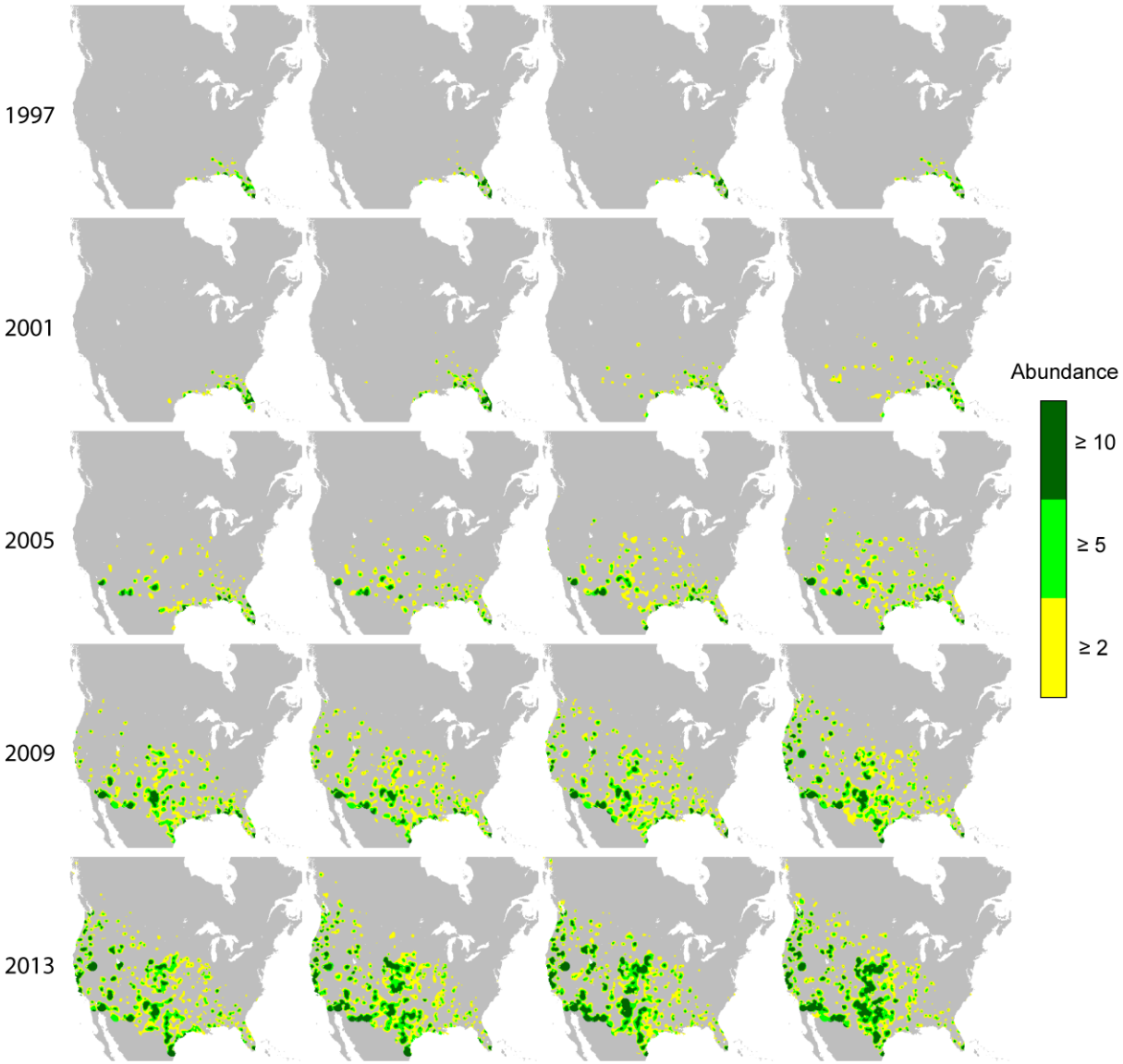

Figure 2 — Distribution of Eurasian collared dove in North America from 1997 - 2016. Population sizes were derived for each year by kriging abundance values of Eurasian collared dove from 4647 active Breeding Bird Survey (BBS) routes in the United States and Canada onto a 10km x 10km grid (Albers equal area conic map projection).

Niche centrality and population abundance

I used a minimum volume ellipsoid (MVE) model (Qiao et al. 2015) of the fundamental niche of old-world Eurasian collared doves from Ingenloff et al. (2017) to estimate environmental suitability values across North America. Based upon this ellipsoidal fundamental niche, the relative suitability of each region in geography was determined by the relative distances to the niche centroid; regions near the niche centroid are highly suitable while those on the periphery are less suitable. This relationship between niche centrality and population abundance is supported by a number of studies reporting a negative relationship between distance to niche centroid and abundance of populations (VanDerWal et al. 2009, Kulhanek et al. 2011, Martínez-Meyer et al. 2013, Osorio-Olvera et al. 2016).

I used a zero-inflated regression model (Zuur et al. 2009) to evaluate the relationship between population abundances obtained from BBS surveys in 2016 and distances to the niche centroid. Zero-inflated regression is a useful tool for datasets containing many 'zero' values, which violate assumptions of traditional logistic regression models. Zero-inflated regression is a mixed modeling process with two components: 1) a regression of count data (in this case a Poisson regression with a log link function) and 2) a binary model to capture the probability of zero-inflation, zeroes within the dataset resulting from external factors (in this case a binomial regression with a logit link function). These regression analyses were performed in R using the 'pscl' package (Zeileis et al. 2008; v. 1.5.1).

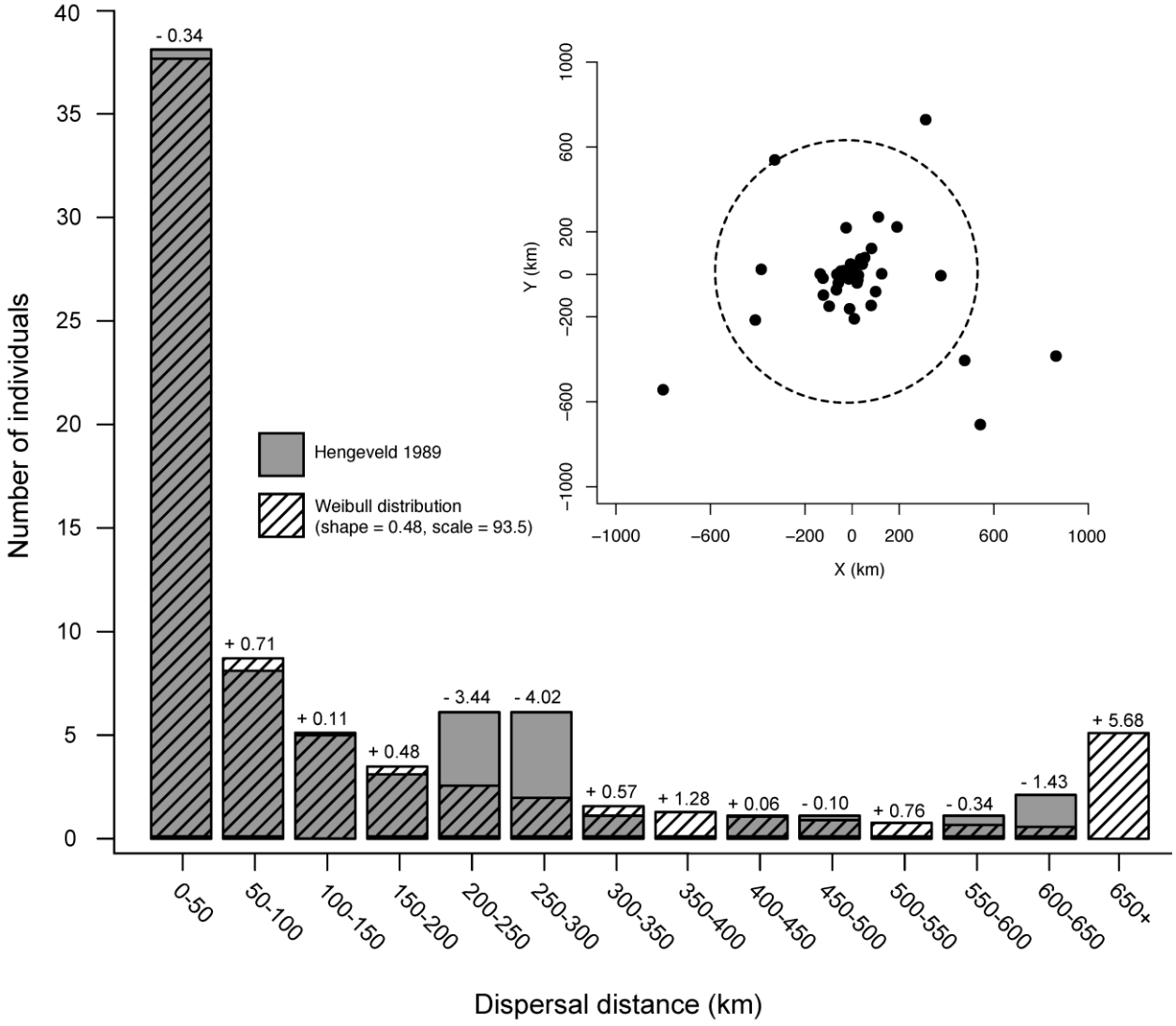

Figure 3 — Natal dispersal kernel for Eurasian collared doves parameterized using dispersal distances of 72 birds in Western Europe (gray bars; Hengeveld 1989). Hatched bars are the expected proportions of the best-fit Weibull distribution. Numbers above each bar show the difference between the expected values and the original dispersal dataset. Inset plot (upper right) shows a representative random dispersal simulation of 72 individuals. For each point, distance from the origin was drawn from the fitted Weibull dispersal kernel and travel direction was drawn from a uniform (0, 2π]. The dashed circle marks the maximum observed value for the original dispersal dataset.

Dispersal kernel estimation

I used mark-recapture data for Eurasian collared doves from central Europe (Hengeveld 1989) to fit a dispersal kernel for simulations. These data include the dispersal distances of 72 juvenile birds binned into 50 km intervals ranging from 0 – 650km. These data provide a more liberal estimate of collared dove dispersal capability than more recent datasets in Europe (Eraud et al. 2011), but overly conservative estimates of dispersal capability may significantly under-represent long-distance dispersal on the landscape scale. I chose a Weibull probability density function to serve as the dispersal kernel; the Weibull distribution is 'fat-tailed' (Nathan et al. 2012) and has been utilized in other spread models of invasive birds (Veit & Lewis 1996). The Weibull distribution is represented by the following probability density equation:

$$f(x) = (a/b)(x/b)^{a-1} \exp\left[-(x/b)^{a}\right]$$

where x is dispersal distance, a is the 'shape' parameter, and b is the 'scale' parameter. I estimated the 'shape' and 'scale' parameters of the dispersal kernel by minimizing the sum of squared distances between the binned observed dispersal distances and the predicted values from the probability distribution using the 'optim' function in R (R Core Team 2017; v. 3.3.3). The resulting Weibull kernel (shape = 0.48, scale = 93.5; Figure 3) was used to generate random dispersal distances for all natal dispersal simulations.

Dispersal Simulations

I performed dispersal simulations for each year from 1997 – 2015 using the breeding distribution maps derived from BBS abundance data. For each year, juvenile dispersal was simulated from each 10km x 10km cell above the Allee threshold. Based upon demographic data of Eurasian collared doves collected by Robertson (1990), I assumed that each pair of doves in the defined breeding range produced 3.1 successful fledging offspring per year (1.55 per individual, rounded down). I assumed that the direction of dispersal for each fledging was random; dispersal angles were randomly drawn from the circular uniform distribution from (0, 2π]. Dispersal distances for each juvenile were drawn from the Weibull distribution (Fig 2).

For each year from 1997 – 2015, I ran 100 replicate simulations of juvenile dispersal. For each replicate, I counted the number of dispersing juveniles that arrived into each 10km x 10km cell. I estimated overall dispersal probabilities for each grid cell — the likelihood that a grid cell would receive a sufficient number of individuals to establish a new breeding population — by taking the proportion of simulations that each grid cell received enough individuals to overcome the Allee threshold.

I compared the dispersal patterns generated by these simulations to distribution maps derived from BBS data. For each year and Allee threshold, I calculated the mean dispersal probability and mean distance to niche centroid for areas that represented gains, retention, and loss of distributional area (Figure 4). This provides a measurement of dispersal strategy, where small mean dispersal probabilities indicate increased frequencies of long distance dispersal.

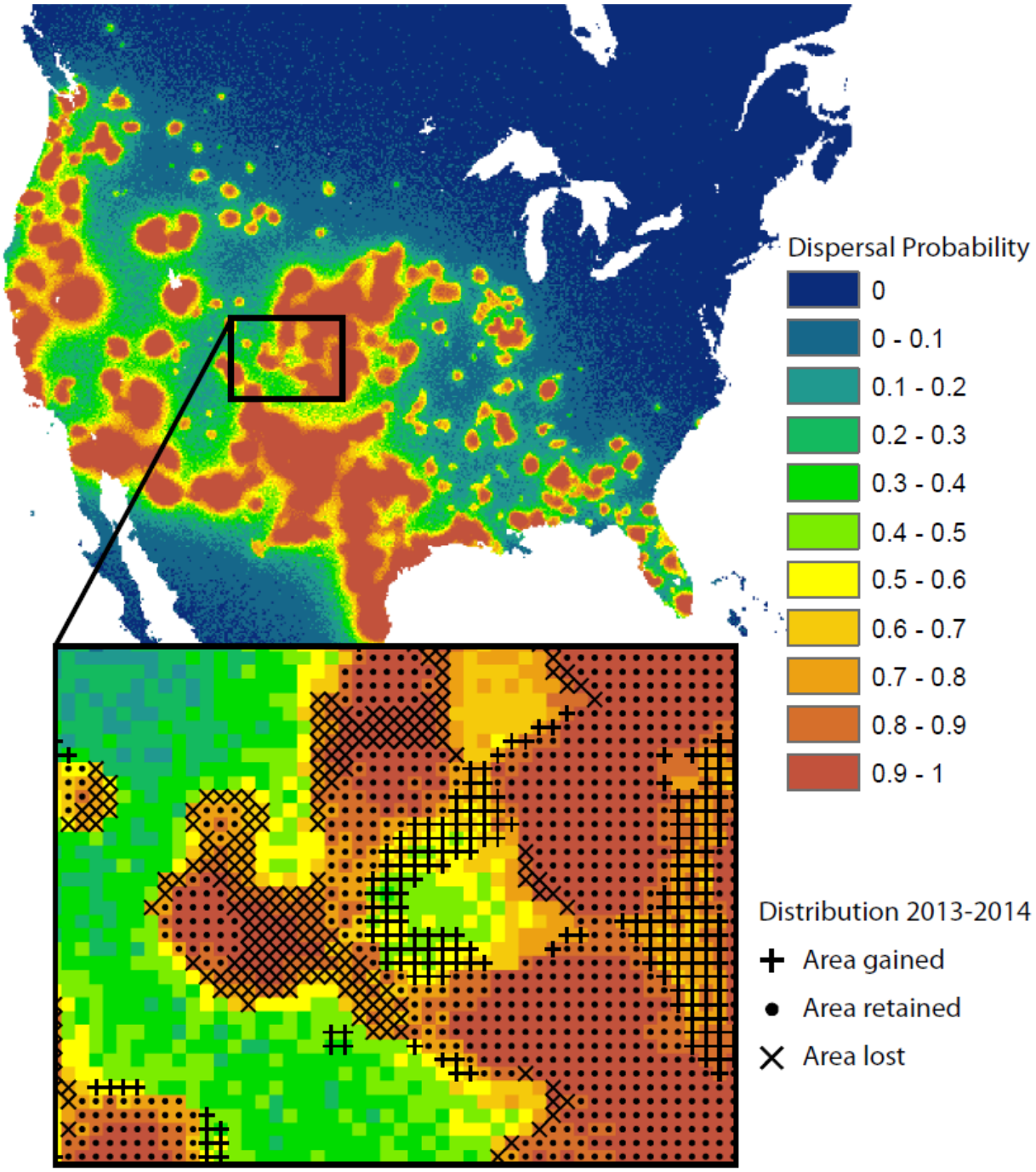

Figure 4 — Map of dispersal probabilities for Eurasian collared doves from 2013 – 2014 with an Allee threshold of 2. Dispersal probabilities are the proportion of simulations where each grid cell received enough individuals to overcome the Allee threshold. The lower plot indicates changes in geographic distribution according to interpolated population estimates from the

Breeding Bird Survey. Plus symbols represent distribution expansion. Circles represent retained areas. X symbols represent lost distributional area.

Results

Population abundances of the Eurasian collared doves in North America were significantly affected by variation in underlying environmental conditions (Figure 5). Zero-inflated regression revealed that increased distance to the niche centroid was associated with reduced population abundance ($p < 0.001$) and increased likelihood of zero inflation ($p < 0.001$).

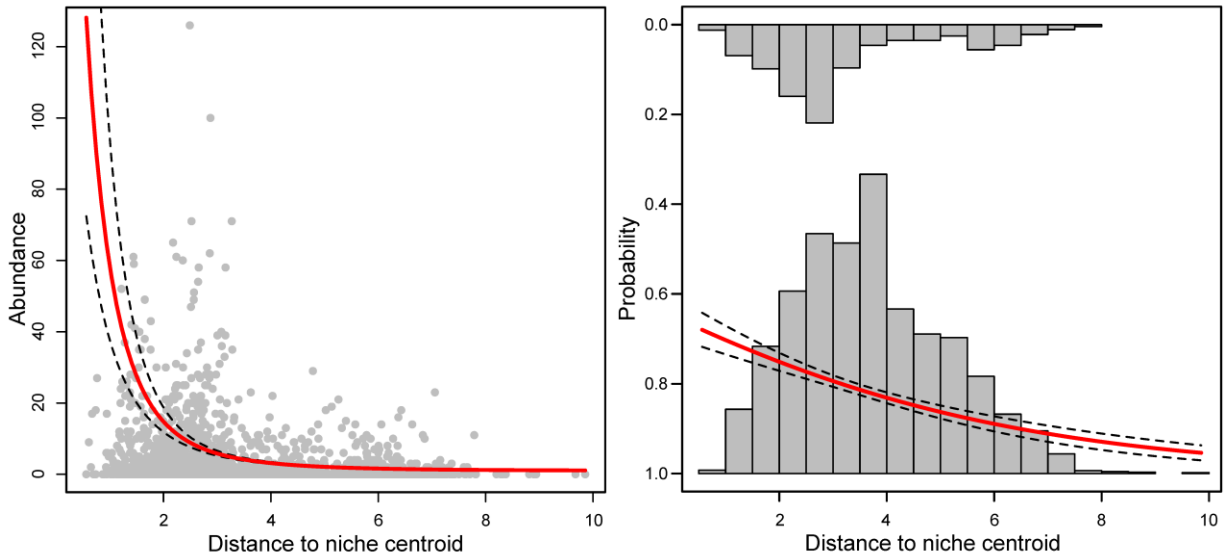

Figure 5 — Graphical representation of zero-inflated regression of Eurasian collared dove population abundance in each active Breeding Bird Survey (BBS) route in 2016 (left) and probability of zero inflation (right) with respect to distance to environmental niche centroid. Upper histogram represents non-zero values. Red lines show the predicted values for mean population abundance (left) and direction of zero-inflation (right). Dashed lines are 95% confidence intervals.

Comparing the results of simulations with thresholded maps derived from BBS data revealed similar year-to-year patterns for both mean dispersal probability and distance to niche centroid across all Allee thresholds (Figure 6). Mean dispersal probabilities were generally parabolic. Higher mean dispersal probabilities were observed in the first and last years of the Eurasian collared dove invasion. Lower mean dispersal probabilities were observed in during the middle period of invasion (2003 – 2009). Mean dispersal probabilities were greatly affected by Allee threshold. Stronger Allee effects (5, 10 individuals per 10km x10km cell) showed greatly reduced dispersal probabilities overall. The mean distance to niche centroid increased slightly during the initial years of invasion (1997 – 2003) and slowly decreased thereafter.

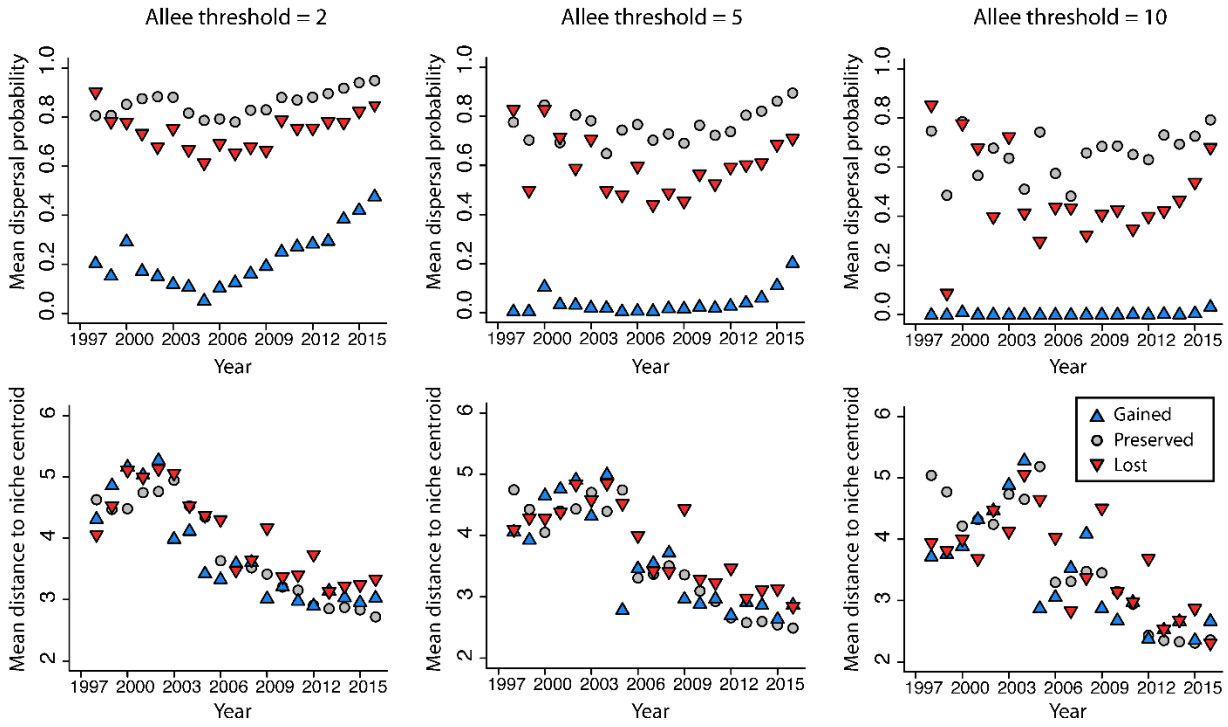

Figure 6 — Mean dispersal probability (upper) and mean distance to niche centroid (lower) of Eurasian collared dove distributions in North America from 1997 – 2016. Blue triangles represent areas that were gained from previous years. Gray circles represent areas that were retained from previous years. Red triangles represent areas that were lost.

Discussion

The spread of Eurasian collared doves across North America occurred in patterns of long distance dispersal followed by subsequent infilling of connecting regions (Scheidt & Hurlbert 2014). In many attempts to predict invasion patterns across landscapes, modeling patterns of jump dispersal is problematic (Ingenloff et al. 2017), Given this difficulty, I used a probabilistic approach to estimate the likelihood of expansion patterns rather than attempt to replicate dispersal patterns directly. Using a model of juvenile dispersal incorporating empirical measurements of dispersal capability (Hengeveld 1989) and pertinent life history characteristics (Robertson 1990), I found variation in the dispersal behavior of collared dove from 1997 – 2016. Specifically, I observed increased levels of low probability dispersal in from 2003 – 2009 when the collared dove spread across the central region of the United States. As the distribution of collared doves stabilized, the amount of long-distance (and rare) dispersal events decreased, supporting the hypothesis that long-distance natal dispersal is more common in colonizing populations and on the boundaries of distributions (Morales 2002).

This project relied upon Breeding Bird Survey abundance estimates which may not adequately sample the disturbed habitats where collared doves are found in large numbers (Fujisaki et al. 2010). More accurate estimates of collared dove abundance should include surveys of disturbed habitats on the periphery of urban areas (Beckett et al. 2007, Scheidt & Hurlbert 2014). Underestimation of collared dove breeding populations reduces the probability of observing rare dispersal events and may lead to overly conservative estimates of dispersal potential.

Mark-recapture data is often used to inform dispersal models but is susceptible to errors caused by non-detection of rare jump dispersal events (Kareiva 1983, Bennetts et al. 2001,

Nathan et al. 2003, Morales et al. 2004, Ovaskainen 2004). Mark-recapture studies are influenced by constrained study areas and small sample sizes. Theoretically, non-detection errors in mark-recapture studies could be overcome with the use of direct surveillance (e.g. radiotracking) but efforts to directly characterize movements of collared doves have yielded overly constrained dispersal estimates (Eraud et al. 2007, Eraud et al. 2011).

Clearly, the usage of one kernel for all natal dispersal simulations in this study was a simplification of actual dispersal processes. It is expected that dispersal patterns will be shaped by topography, climate, and habitat configuration (Baguette & Van Dyck 2007, Driezen et al. 2007). Incorporating differences in landscape resistance requires multiple requires multiple measurements of movement potential across difference landscapes, which are not currently available for Eurasian collared doves. For simplicity, I also assumed a uniform distribution of dispersal angles from breeding sources. In a natural setting, directional bias in movements are common, depending on landscape configurations (Ovaskainen et al. 2016). These simulations assume that natal dispersal occurs independently for each juvenile, but social breeding behavior in collared doves present a difficult conundrum (Eraud et al. 2011). Despite the widespread influence of social behavior in animal movements, properly incorporating social effects into population models is largely unexplored (Nathan et al. 2012). Given these considerations, it is possible that simulations in the project give a conservative view of dispersal potential.

Geographic distributions are often depicted as continuous and relatively static regions. It is clear that this pattern is not found in the highly fragmented and mutable distribution on the collared dove in North America. While dispersal is clearly an important factor for range expansion, I found that these dispersal simulations could not account for breeding areas lost due to fluctuations of the geographic distribution on an inter-annual basis. Generally, breeding areas

lost from previous years were assigned much higher dispersal probabilities than areas that represented range expansion. This result indicates that dispersal alone is a necessary, but not sufficient, condition to establish new breeding populations. Establishment requires suitable population demographics and habitat conditions post-dispersal (Greenwood & Harvey 1982, Courchamp et al. 1999, Stephens & Sutherland 1999, Ovaskainen 2004, Eraud et al. 2011). It is also clear that a relationship exists between population abundance and ecological niche for the Eurasian collared dove, but it is unclear if similar environmental factors influence dispersal behavior directly.

This project is a post-hoc interpretation of dispersal patterns and can only depict the relative likelihood of future dispersal patterns, rather than provide any kind of prediction.

These dispersal simulations serve as a null model to investigate changes in dispersal behavior; inter-annual variation in dispersal probabilities may identify changes in dispersal mode across a landscape. Future investigations of dispersal can incorporate similar probabilistic approach to identify landscape and/or environmental features that may be associated with changes in dispersal behavior.

References

Baguette, M., and H. Van Dyck. 2007. Landscape connectivity and animal behavior: functional grain as a key determinant for dispersal. Landscape Ecology 22:1117-1129.

Beckett, S. M., N. Komar, and P. F. Doherty Jr. 2007. Population estimates for Eurasian collared-dove in northeastern Colorado. The Wilson Journal of Ornithology 119:471-475.

Bennetts, R. E., J. D. Nichols, R. Pradel, J. Lebreton, and W. Kitchens. 2001. Methods for estimating dispersal probabilities and related parameters using marked animals.

Bled, F., J. A. Royle, and E. Cam. 2011. Hierarchical modeling of an invasive spread: the Eurasian collared-dove Streptopelia decaocto in the United States. Ecological Applications 21:290-302.

Courchamp, F., T. Clutton-Brock, and B. Grenfell. 1999. Inverse density dependence and the Allee effect. Trends in Ecology & Evolution 14:405-410.

Driezen, K., F. Adriaensen, C. Rondinini, C. P. Doncaster, and E. Matthysen. 2007. Evaluating least-cost model predictions with empirical dispersal data: a case-study using radiotracking data of hedgehogs (Erinaceus europaeus). Ecological Modelling 209:314-322.

Eraud, C., J. M. Boutin, D. Roux, and B. Faivre. 2007. Spatial dynamics of an invasive bird species assessed using robust design occupancy analysis: the case of the Eurasian collared dove (Streptopelia decaocto) in France. Journal of Biogeography 34:1077-1086.

Eraud, C., A. Jacquet, and P. Legagneux. 2011. Post-fledging movements, home range, and survival of juvenile Eurasian Collared-Doves in Western France. The Condor 113:150-158.

Fujisaki, I., E. V. Pearlstine, and F. J. Mazzotti. 2010. The rapid spread of invasive Eurasian Collared Doves Streptopelia decaocto in the continental USA follows human-altered habitats. Ibis 152:622-632.

Greenwood, P. J., and P. H. Harvey. 1982. The natal and breeding dispersal of birds. Annual Review of Ecology and Systematics 13:1-21.

Grinnell, J. 1917. The niche-relationships of the California Thrasher. The Auk 34:427-433.

Hengeveld, R. 1989. Dynamics of biological invasions. Chapman and Hall, London, UK.

Higgins, S., R. Nathan, and M. Cain. 2003. Are long-distance dispersal events in plants usually caused by nonstandard means of dispersal? Ecology 84:1945-1956.

Hutchinson, G. E. 1959. Homage to Santa Rosalia or why are there so many kinds of animals? The American Naturalist 93:145-159.

Ingenloff, K., C. M. Hensz, T. Anamza, V. Barve, L. P. Campbell, J. C. Cooper, E. Komp, L. Jimenez, K. V. Olson, and L. Osorio-Olvera. 2017. Predictable invasion dynamics in North American populations of the Eurasian collared dove Streptopelia decaocto. Page 20171157 *in* Proc. R. Soc. B. The Royal Society.

Johnson, D. M., A. M. Liebhold, P. C. Tobin, and O. N. Bjornstad. 2006. Allee effects and pulsed invasion by the gypsy moth. Nature 444:361-363.

Kareiva, P. 1983. Local movement in herbivorous insects: applying a passive diffusion model to mark-recapture field experiments. Oecologia 57:322-327.

Keitt, T. H., M. A. Lewis, R. D. Holt, and F. Associate Editor: Lenore. 2001. Allee effects, invasion pinning, and species' borders. The American Naturalist 157:203-216.

Kulhanek, S. A., B. Leung, and A. Ricciardi. 2011. Using ecological niche models to predict the abundance and impact of invasive species: application to the common carp. Ecological Applications 21:203-213.

Martínez-Meyer, E., D. Díaz-Porras, A. T. Peterson, and C. Yáñez-Arenas. 2013. Ecological niche structure and rangewide abundance patterns of species. Biology Letters 9.

Morales, J. M. 2002. Behavior at habitat boundaries can produce leptokurtic movement distributions. The American Naturalist 160:531-538.

Morales, J. M., D. T. Haydon, J. Frair, K. E. Holsinger, and J. M. Fryxell. 2004. Extracting more out of relocation data: building movement models as mixtures of random walks. Ecology 85:2436-2445.

Nathan, R., E. Klein, J. J. Robledo-Arnuncio, and E. Revilla. 2012. Dispersal kernels: review. Page 496 *in* J. Clobert, M. Baguette, T. G. Benton, and J. M. Bullock, editors. Dispersal Ecology and Evolution. Oxford University Press, Oxford, UK.

Nathan, R., G. Perry, J. T. Cronin, A. E. Strand, and M. L. Cain. 2003. Methods for estimating long-distance dispersal. Oikos 103:261-273.

Osorio-Olvera, L. A., M. Falconi, and J. Soberón. 2016. Sobre la relación entre idoneidad del hábitat y la abundancia poblacional bajo diferentes escenarios de dispersión. Revista Mexicana de Biodiversidad 87:1080-1088.

Ovaskainen, O. 2004. Habitat-specific movement parameters estimated using mark-recapture data and a diffusion model. Ecology 85:242-257.

Ovaskainen, O., H. J. de Knegt, and M. del Mar Delgado. 2016. Quantitative ecology and evolutionary biology: integrating models with data. Oxford University Press, Oxford, UK.

Pardieck, K. L., D. J. Z. Jr., M. Lutmerding, K. Campbell, and M.-A. R. Hudson. 2017. North American Breeding Bird Survey Dataset 1966 - 2016. *in* U. S. G. Survey, editor., Patuxent Wildlife Research Center.

Peterson, A. T., J. Soberón, R. G. Pearson, R. P. Anderson, E. Martínez-Meyer, M. Nakamura, and M. B. Araújo. 2011. Ecological niches and geographic distributions. Princeton University Press, Princeton, NJ, USA.

Peterson, A. T. 2003. Predicting the geography of species' invasions via ecological niche modeling. The quarterly review of biology 78:419-433.

Poling, T. D., and S. E. Hayslette. 2006. Dietary overlap and foraging competition between mourning doves and Eurasian collared-doves. Journal of Wildlife Management 70:998-1004.

Qiao, H., J. Soberón, and A. T. Peterson. 2015. No silver bullets in correlative ecological niche modelling: insights from testing among many potential algorithms for niche estimation. Methods in Ecology and Evolution 6:1126-1136.

R Core Team. 2017. R: a language an environments for statistical computing. R Foundation for Statistical Computing, Vienna, Austria.

Robertson, H. A. 1990. Breeding of Collared Doves Streptopelia decaocto in rural Oxfordshire, England. Bird Study 37:73-83.

Romagosa, C. M., and R. F. Labisky. 2000. Establishment and dispersal of the Eurasian Collared-Dove in Florida. Journal of Field Ornithology 71:159-166.

Scheidt, S. N., and A. H. Hurlbert. 2014. Range expansion and population dynamics of an invasive species: the Eurasian Collared-Dove (Streptopelia decaocto). PLoS One 9:e111510.

Simberloff, D. 1997. The biology of invasions. Strangers in paradise: impact and management of nonindigenous species in Florida. Island Press, Washington, DC:3-17.

Soberón, J., and A. T. Peterson. 2005. Interpretation of models of fundamental ecological niches and species' distributional areas. Biodiversity Informatics 2:1-10.

Stephens, P. A., and W. J. Sutherland. 1999. Consequences of the Allee effect for behaviour, ecology and conservation. Trends in Ecology & Evolution 14:401-405.

Trakhtenbrot, A., R. Nathan, G. Perry, and D. M. Richardson. 2005. The importance of long-distance dispersal in biodiversity conservation. Diversity and Distributions 11:173-181.

VanDerWal, J., L. P. Shoo, C. N. Johnson, and S. E. Williams. 2009. Abundance and the environmental niche: environmental suitability estimated from niche models predicts the upper limit of local abundance. The American Naturalist 174:282-291.

Veit, R. R., and M. A. Lewis. 1996. Dispersal, population growth, and the Allee effect: dynamics of the house finch invasion of eastern North America. The American Naturalist 148:255-274.

Zeileis, A., C. Kleiber, and S. Jackman. 2008. Regression models for count data in R. Journal of statistical software 27:1-25.

Zuur, A. F., E. N. Ieno, N. J. Walker, A. A. Saveliev, and G. M. Smith. 2009. Zero-truncated and zero-inflated models for count data. Pages 261-293 Mixed effects models and extensions in ecology with R. Springer.

Supplemental Material

```
##Population estimation and expansion estimation of Eurasian collared doves
##By: Chris Hensz

#All active BBS routes from 1997 - 2016

#Route is a string of country, state, and route code as a unique identifier
#Count is the total number of collared doves observed on each route in 2016
#MVEDist is the distance to ecological niche centroid (Ingenloff et al. 2017)

#head(doves)
#       Lon      Lat       Route Count  MVEDist
# -121.6885 49.29488  C124S11R10     0 2.126593
# -123.5985 48.75744 C124S11R101    14 1.986806
# -116.4784 50.92435  C124S11R17     0 1.948948
# -118.7433 50.44063  C124S11R19     2 1.638410
# -119.3209 50.67375  C124S11R20     2 1.637038
# -121.0993 50.02257  C124S11R22     0 1.459695

#Zero inflated regression of dove count data

library(pscl)

dove.mod <- zeroinfl(Count ~ MVEDist, data = doves, dist = "poisson")
summary(dove.mod)

#Call:
#zeroinfl(formula = Count ~ MVEDist, data = doves, dist = "poisson")
#
#Pearson residuals:
#    Min      1Q  Median      3Q     Max
#-0.6534 -0.4842 -0.4195 -0.3205 28.7740
#
#Count model coefficients (poisson with log link):
#             Estimate Std. Error z value Pr(>|z|)
#(Intercept)  2.855954   0.027696  103.12   <2e-16 ***
#MVEDist     -0.236892   0.009141  -25.91   <2e-16 ***
#
#Zero-inflation model coefficients (binomial with logit link):
#            Estimate Std. Error z value Pr(>|z|)
#(Intercept)   0.6232     0.1020   6.109    1e-09 ***
#MVEDist       0.2411     0.0285   8.461   <2e-16 ***
#---
#Signif. codes:  0 '***' 0.001 '**' 0.01 '*' 0.05 '.' 0.1 ' ' 1
#
#Number of iterations in BFGS optimization: 15
#Log-likelihood: -7574 on 4 Df
#Spatial interpolation of dove populations from 1997 - 2016 from BBS data
library(raster)
library(gstat)

#for each year, we projected all BBS routes from longitude and latitude
#into Alber's Equal Area Conic projection for North America

dove.spat <-
```

```
  SpatialPointsDataFrame(doves[, 1:2],
                         doves[, 3:4],
                         proj4string = CRS("+proj=longlat +ellps=GRS80
+datum=NAD83 +no_defs "))
dove.aea <-
  spTransform(
    dove.spat,
    CRS(
      "+proj=aea +lat_1=20 +lat_2=60 +lat_0=40 +lon_0=-96 +x_0=0 +y_0=0
+ellps=GRS80 +datum=NAD83 +units=m +no_defs"
    )
  )

#variograms were created for each year to interpolate BBS routes onto a
#raster grid
dove.vgm <- variogram(Count ~ 1, dove.aea, width = 50000)
dove.fit <-
  fit.variogram(dove.vgm,
                vgm(
                  psill = 5,
                  model = "Sph",
                  range = 1900000
                ),
                fit.method = 1)

#create an empty raster with the desired properties for interpolation
output.rast <- raster()
#convert raster to points object
output.pts <- rasterToPoints(output.rast, spatial = T)
output.aea <-
  SpatialPoints(
    output.pts,
    proj4string = CRS(
      "+proj=aea +lat_1=20 +lat_2=60 +lat_0=40 +lon_0=-96 +x_0=0 +y_0=0
+ellps=GRS80 +datum=NAD83 +units=m +no_defs +towgs84=0,0,0"
    )
  )

#kriging models for a single year in raster form
dove.krige <-
  krige(
    Count ~ 1,
    dove.aea,
    output.aea,
    model = dove.fit,
    debug.level = -1,
    nmax = 10,
    maxdist = 100000
  )
dove.krige.rast <-
  rasterFromXYZ(
    cbind(dove.krige@coords, dove.krige$var1.pred),
    res = c(10000, 10000),
    crs = CRS(
      "+proj=aea +lat_1=20 +lat_2=60 +lat_0=40 +lon_0=-96 +x_0=0 +y_0=0
+ellps=GRS80 +datum=NAD83 +units=m +no_defs +towgs84=0,0,0"
    )
```

```
  )

#Dispersal simulation function:

#type is either 'flat' for Euclidean distances or 'curved' for curved earth
distance
#start is the coordinates of the source of dispersal
#npoints is the number of points simulated
#distscale is a numeric scaling factor for distances
#angle is the probability function used to simulate dispersal angles
#angleargs is a list of parameters to feed into the function defined by
#'angle'
#kernel is a probability function used to simulated dispersal distances
#kernelargs is a list of parameters to feed into the function defined by
#'kernel'

disperse <-
  function(type = c('flat', 'curved'),
           start,
           npoints,
           distscale,
           angle,
           angleargs = list(),
           kernel,
           kernelargs = list()) {
    if (class(start) != 'numeric' |
        length(start) != 2)
      stop('start must be a vector containing x and y coordinates')
    if (type == 'flat') {
      theta <- do.call(angle, c(npoints, angleargs))
      dist <- do.call(kernel, c(npoints, kernelargs))
      dist <- dist * distscale
      x <- dist * cos(theta) + start[1]
      y <- dist * sin(theta) + start[2]
      result <- cbind('Distance' = dist,
                      'X' = x,
                      'Y' = y)
      warning('angle is assumed to be in radians')
    }
    if (type == 'curved') {
      if (suppressWarnings(require(geosphere))) {
        theta <- do.call(angle, c(npoints, angleargs))
        dist <- do.call(kernel, c(npoints, kernelargs))
        result <-
          cbind(dist, destPoint(p = start, b = theta, d = dist))
        warning('angle is assumed to be a bearing from 0 to 360 degrees')
        warning('kernel is assumed to be in meters')
        colnames(result) <- c('Distance', 'Longitude', 'Latitude')
      } else
        stop('package geosphere not detected')
    }
    return(result)
  }

#Collared dove dispersal simulation with an Allee threshold of 5 individuals
#per 10x10 km cell
require(plyr)
```

```
#Dispersal was simulated for each raster cell containing at least 5
#individuals
allee <- 5
for (i in 1:length(doves.krige.rast)) {
  outputras = output.rast #empty raster to summarize results of dispersal
simulations
  for (j in 1:100) {
    #100 iterations
    cat("\r", paste(i + 1996, "simulation", j, "of 100"))
    run = adply(
      .data = doves.krige.rast[[i]],
      .margins = 1,
      .fun = function(x) {
        disperse(
          type = 'flat',
          start = as.numeric(x[1:2]),
          npoints = as.numeric(floor(1.55 * x[3])),
          distscale = 1000,
          angle = runif,
          angleargs = list(min = 0, max = 2 * pi),
          kernel = rweibull,
          kernelargs = list(shape = 0.48, scale = 93.45)
        )
      }
    )[, 5:6]
    runras = rasterize(run, output.rast, fun = "count", background = 0) >=
      allee
    outputras = outputras + runras
  }
  #output is a designated output folder
  writeRaster(outputras / 100,
              paste0(output, "100SpreadProb", i + 1996, ".asc"))
                                      }
```

Chapter 4

Participation in the Convention on Migratory Species: a biogeographic assessment[3]

[3] Hensz, C.M., Soberón, J.S. (2018) Participation in the Convention on Migratory Species: a biogeographic assessment. *AMBIO*. doi: 10.1007/s13280-018-1024-0

Abstract

The Convention on the Conservation of Migratory Species of Wild Animals (CMS) is a Multilateral Environmental Agreement (MEA) focused on species that regularly travel across international borders. Despite covering an important group of species, CMS is under-utilized compared to other conservation-focused MEAs. CMS suffers from a lack of participation across North America and most of Asia. Our goal is to illustrate differences in species richness and average range-size across signatory and non-signatory nation-states using range-diversity plots. We also show differences in the cost of CMS membership relative to species patterns to highlight which countries may be discouraged from becoming CMS signatories. Despite containing many CMS species, large economies such as the United States, Russia, and China are not members of the convention. To facilitate migratory species conservation into the future, CMS should seek to fill gaps in participation, potentially directing recruitment efforts toward non-signatory states that would receive the largest benefit at the lowest relative cost.

Introduction

Multilateral Environmental Agreements (MEAs) are legally binding instruments between two or more nation-states that address environmental issues (Dodds et al., 2007). Approximately 700 international agreements can be identified as MEAs (Kim, 2013). According to Koester (2002), the most important MEAs concerning biodiversity conservation are the Convention on Biological Diversity (CBD 1992), the Convention on International Trade in Endangered Species of Fauna and Flora (CITES 1973), the Convention on Wetlands of International Importance (RAMSAR 1971), the Convention Concerning the Protection of the World Cultural and Natural Heritage (WHC 1972), and the Convention on the Conservation of Migratory Species of Wild

Animals (CMS 1979). Of these, the CBD is regarded as the most politically salient, and CITES the most operative in administrative regulation (Guruswamy, 1999). Despite the ecological importance of transboundary species movements (Clobert et al., 2012), CMS is the only MEA focused broadly on migratory species across taxonomic divisions. Unlike CITES, CMS lacks stringent participation requirements for party states. Instead, CMS operates by facilitating the creation of smaller cooperative agreements (Seelarbokus, 2014), including as many as 106 "action plans" across 7 major conservation agreements and 19 non-binding Memoranda of Understanding (MoUs). These agreements under CMS administration have helped to stabilize populations of migratory species including Wadden Sea seals (*Phoca vitulina vitulina* and *Helichoerus grypus*) and the Bukhara deer (*Cervus elaphus bactrianus*) despite being non-binding (Baldwin, 2011). Since its initial signing in 1979, CMS membership increased from 29 signatories to 126 party states by 2017 (Birnie et al., 2009, Guruswamy and Doran, 2007).

CMS defines migratory species as those "whose members cyclically and predictably cross one or more national jurisdictional boundaries" (CMS, 1979). CMS also covers several species that cross international borders but are non-migratory such as marine otters (*Lontra felina*) and mountain gorillas (*Gorilla gorilla*). CMS lists migratory species in 2 appendices as agreed upon by party states: Appendix I includes endangered species restricted from taking (harvesting, hunting, etc.), appendix II lists species with unfavorable conservation status that may benefit from international cooperation, but are not restricted from taking. Several levels of biological organization are listed in each appendix (genera, species, sub-species, and populations) and these groups may be included in either or both appendices (CMS Appendix I and II, updated October 2017).

Becoming a party to CMS represents a large investment of expertise and time. CMS signatories agree to (i) undertake active conservation of migratory species under the first appendix of the agreement, (ii) form additional international agreements to conserve species in the second appendix, (iii) participate in the tri-annual Conference of the Parties, and (iv) financially support the CMS secretariat (CMS, 1979). A significant obstacle to encouraging large, economically powerful states to joining the convention is the cost of being a signatory. Similar to the General Assembly of the United Nations, the cost of participation in CMS is weighted by the gross domestic product (GDP) of signatory states (UNEP/CMS Res 12.2).

In this contribution, we aim to describe CMS from a biogeographic perspective to identify which countries may be most amenable to becoming signatories. We analyze the geographic structure of the species covered under CMS Appendix I and II using range-diversity plots (Arita et al., 2008) and relate the results of these plots to United Nations (UN) economic indices as a measure of participation cost. We aim to provide international policy-makers the tools to evaluate the potential conservation benefits of joining CMS.

Materials and Methods

We obtained the full record of 1115 CMS species through Species+, a database of CMS and CITES species (http://speciesplus.net; accessed March 2nd 2017). We aggregated the data to include a single record for each species, consolidating all species with multiple listed sub-populations and species under both CMS appendices. Sixty-two species included no range data and were excluded from this analysis. Species+ lists the countries where each species is found, but has no data for geographic range size by country, limiting analysis to the country scale.

The Holy See and South Sudan were excluded from analysis for poor data quality: The Holy See contains zero records and South Sudan could not be completely distinguished from Sudan in the database. Consequently, the maps we present depict a single united Sudan, reflecting the resolution of species data rather than political reality. Greenland was excluded from analysis as it has no established relationship with CMS and is independent of Denmark in its conservation decisions. The Cook Islands and Niue, while technically in association with New Zealand, have signed CMS independently and are thus treated as independent for this study (http://www.cms.int/en/parties-range-states; accessed March 2nd 2017). For all other countries we aggregated species data to the level of sovereign states, including all territories under each country (including American Samoa for the United States, French Guiana for France, etc.).

We used two sources of data to determine economic cost of being a party to CMS. For most signatory states, the expected financial contribution of each country from 2018 – 2020 is presented in reports from the 12th Conference of Parties in 2017 (COP12; UNEP/CMS/Resolution 12.2, pg 5–8). Parties to CMS contribute funding proportional to the size of their respective economies, measured in gross domestic product (GDP). To estimate the cost for a non-party to become a member of CMS, we added proportional 2018 GDP estimates for individual non-party states obtained from the United Nations General Assembly (UNGA Res A/70/416/Add.1, pg 3–8) to the CMS document and calculated cost based on the new proportional GDP. We obtained the signatory status of each country and designation of sovereign territories through the CMS web page (http://www.cms.int/en/parties-range-states; accessed March 2nd 2017).

We characterized species patterns for each country using richness-diversity diagrams, a biogeographic exploratory tool (Arita et al., 2008, Soberón and Ceballos, 2011) grouping the plots by: (i) k-means clustering (MacQueen, 1967) and (ii) CMS geographic region. K-means clustering of the range-diversity plots divides countries into groups that have similar properties based upon species-level patterns. Alternatively, grouping by the 6 CMS geographic regions (North America, Europe, Asia, Australia and Oceania, Africa, and South America and the Caribbean) indicates whether or not geographic proximity plays a dominant role in CMS species patterns. Richness-diversity diagrams use presence-absence data to describe species compositions of each recorded location in a dataset. From these diagrams it is possible to extract biodiversity indices including alpha and beta diversity (Soberón and Cavner, 2015). The horizontal axis shows the proportional mean range size, also called the dispersal field, of the species in each location (Graves and Rahbek, 2005). Proportional mean range size (referred from here on as simply 'range-size'), indicates how cosmopolitan species are for each location. For example if a country has a relatively large range-size value (e.g., > 0.75), species within that country occur in at least 75% of countries on average; further, a range-size value of 1 means that all species in that country are represented globally. The minimum possible range-size value, 1/n, (where n is the number of sites) indicates that all species present in a country are endemic and thus non-migratory. Calculations were performed in R (R Core Team, 2017) and resulting maps were created in ArcGIS (ESRI, 2011).

Results and Discussion

K-means clustering analyses identified 4 distinct groups of countries (referred to as groups A, B, C, and D; Figure 1). Group A includes 32 countries with the largest number of CMS species, the five with the most species being France, China, Great Britain, Russia, and India (Table 1). Both Great Britain and France are sovereign over territories in multiple hemispheres (including sub-Antarctic island territories), inflating the overall number of species observed for those countries. India, Russia, and China also contain a large number of CMS species (> 350), perhaps due to large geographic extent. Despite participating in at least one MoU administered by the CMS secretariat and being the second and fourth largest hosts of CMS species respectively, neither China nor Russia are currently members of CMS. Non-signatory countries in group A may be more amenable to joining CMS signatories as they already contain many species listed under CMS.

Group B comprises 83 countries across Europe, Africa, and Central Asia forming the center mass of the richness-diversity diagram. Group B contains the largest proportion of signatory states of any group (79.5%) and contains countries with moderate species richness and range-size values. Countries in group B on average contain fewer CMS species than countries in group A, but both groups contain species with moderate range-sizes, found in approximately 30–40% of countries worldwide (Table 1).

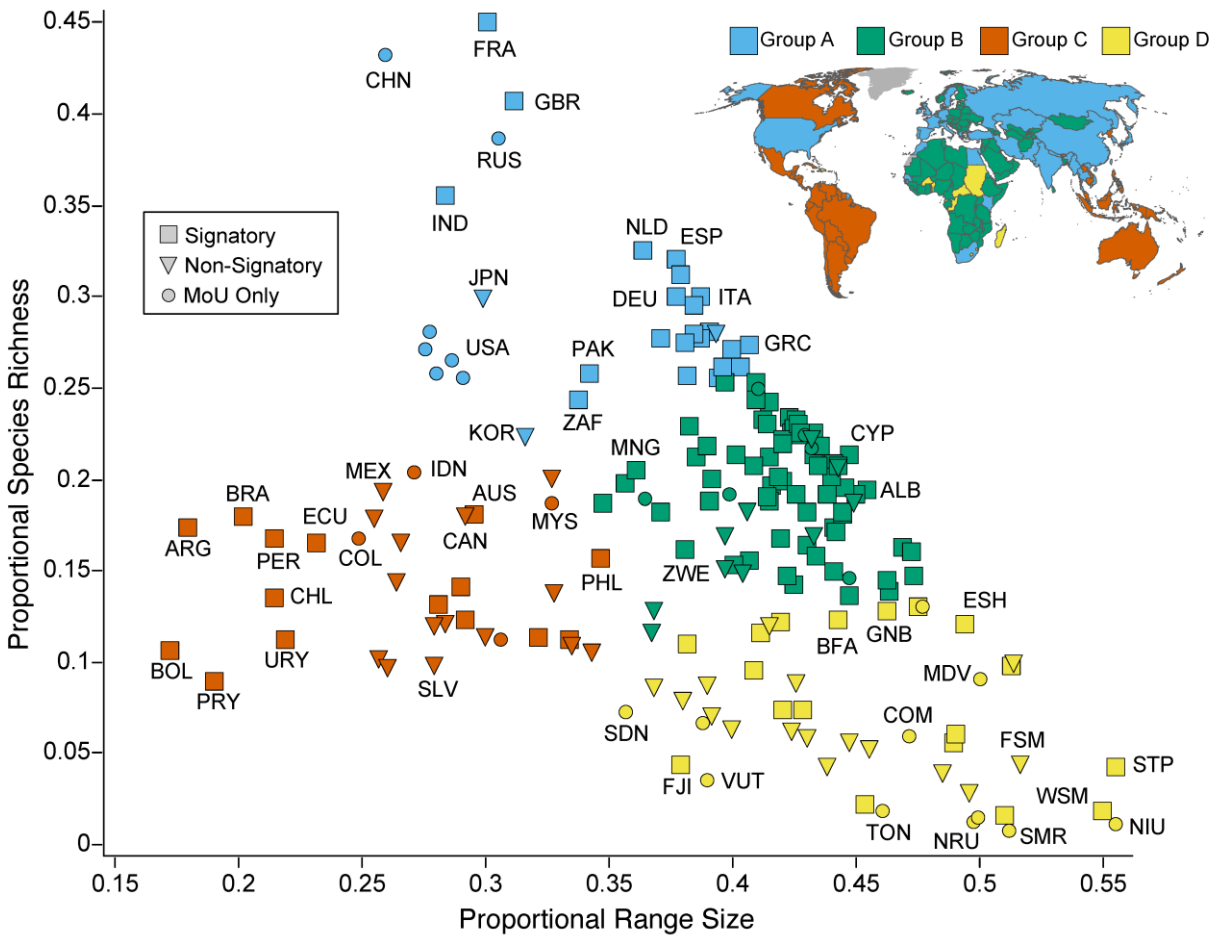

Figure 1 — Richness-diversity diagram and map of countries grouped by k-means clustering. Diagram depicts the relationship between the number of CMS species in a country and the average range-size of those species. Group A is in *light-blue*, group B is in *green*, group C is in *red*, group D is in *yellow*. Each *point* represents a sovereign country and all of its territories. Signatory states are indicated by *squares*, non-signatory states are indicated by *triangles*, and countries that have signed at least one MoU but not CMS are indicated by *circles*. Select countries are labeled on the plot with 3 letter country codes.

Group C encompasses 34 countries across North America, South America, Southeast Asia, Australia, and Oceania with CMS species that are more restricted in range-size. These species occur in relatively fewer countries (< 35%), less than 75% of all other CMS species. Many countries in group C (65.9%) are not CMS parties (notably Indonesia, Canada, and Mexico). However, because species in this group tend towards smaller range-sizes, relevant countries may be more inclined to focus on smaller, local conservation initiatives rather than a larger multilateral agreement like CMS. From a conservation perspective, each country in group C represents a large portion of the distribution of CMS species in that region such that species in this group depend on more constrained areas. Each non-signatory country in group C may significantly limit the effectiveness of the convention as a conservation tool for this group.

The 46 countries clustered in group D have the smallest average number of CMS species – approximately one quarter of the species found in group A (Table 1). Composed predominantly of island states alongside a few African and very small European states, each of the countries in group D contain < 15% of CMS species which are shared with 35–55% of other United Nations member countries. Countries in this group that are not already signatories may be difficult to recruit to CMS as, not only are there few CMS species in these countries, but the species in group D countries also tend to be fairly cosmopolitan, which reduces the impact of a single state's participation. Many countries in this group are geographically restricted in size and in immediate proximity of other small states. It is also important to note that species occurring in many countries may still occur in relatively small land-area depending on the geographic region in question.

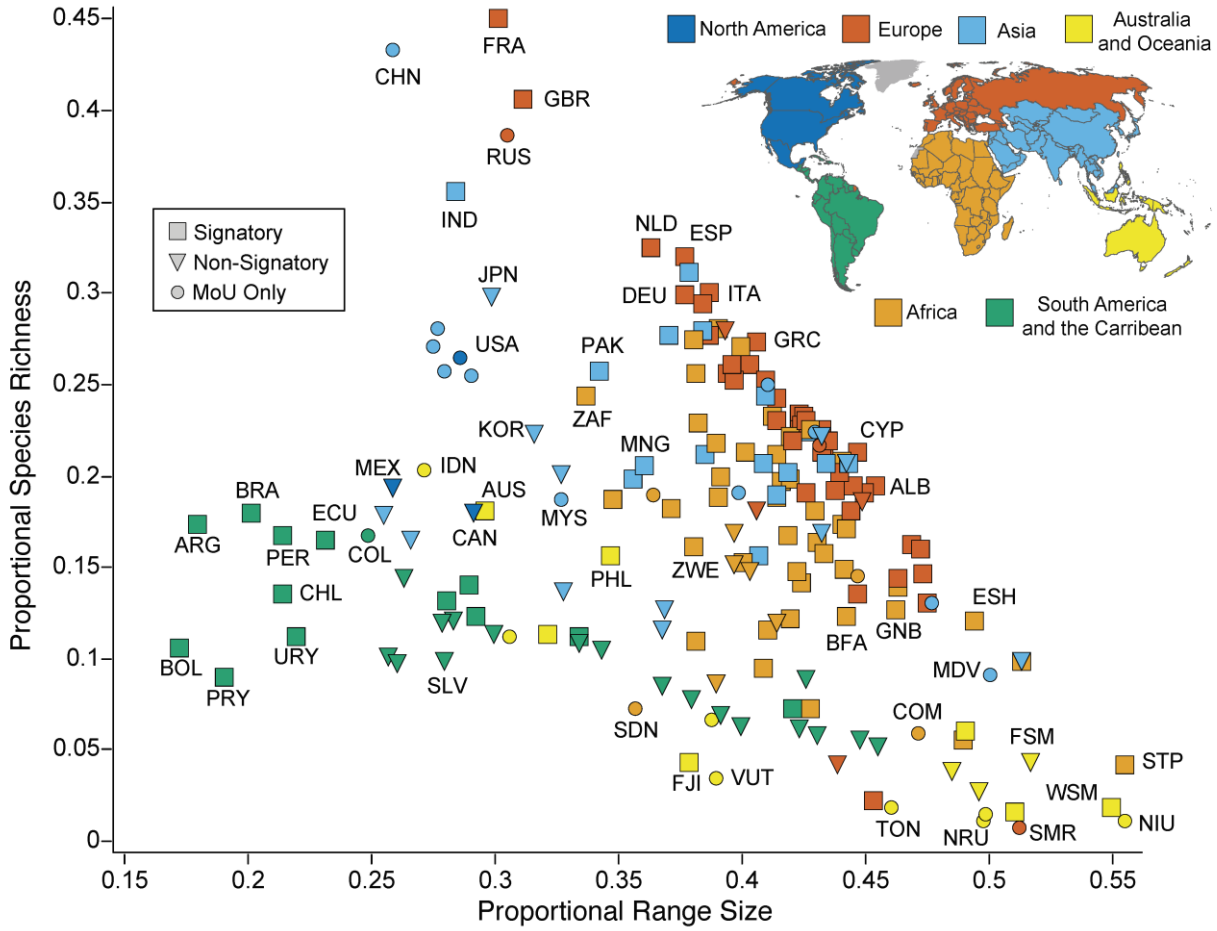

Figure 2 — Richness-diversity diagram of countries grouped by CMS geographic regions. Diagram depicts the relationship between the number of CMS species in a country and the average range-size of those species. North America is in *dark-blue*, Europe is in *red*, Asia is in *light-blue*, Australia and Oceania are in *yellow*, Africa is in *orange*, South America and the Caribbean are in *green.* Each *point* represents a sovereign country and all of its territories. Signatory states are indicated by *squares*, non-signatory states are indicated by *triangles*, and countries that have signed at least one MoU but not CMS are indicated by *circles*. Select countries are labeled on the plot with 3 letter country codes.

When looking at the range-diversity diagram with a geographic (as opposed to species-based) perspective, new patterns emerge (Figure 2). Europe, Asia, and North America contain large numbers of CMS species while South America and the Caribbean, and Australia and Oceania contain relatively fewer listed species (Table 1). Each geographic region forms visually identifiable clusters on the range-diversity diagram. Notable exceptions to this include Caribbean countries and very small European states (e.g., San Marino). Unsurprisingly, these countries have similar properties to small Oceanic states than large mainland states. Range-diversity diagrams grouped by geography alone may over-generalize countries that are in close proximity but have dissimilar species patterns.

For the 2018–2020 budgetary period, 15 states will pay the minimum contribution (<€60 year-1) while the top 4 of the contributors (Germany, France, the United Kingdom, and Italy) will pay more than €200 000 year-1 (UNEP/CMS Res 12.2, pg 5–8; Table 2). The per-species cost to becoming a signatory is at least 14% higher for the richest non-signatory states (the Unites States and Japan) than any current signatory state (Figure 3, Tables 2 and 3). The remaining largest non-signatory states, China and Russia, have comparable per-species costs to the largest signatory countries. Amongst non-signatory states, Myanmar, Thailand, Nepal, Vietnam, and Turkey stand out in particular (Figure 3, Table 2) as countries containing a large proportion of CMS species (>25%) and with relatively low participation costs (< €250 species-1 year-1).

Table 1 — Summary statistics of species richness and mean range-size of countries by group.

Grouping method	Group/region	Number of countries	Mean number of CMS species	Mean range-size of species (number of countries)	Number of signatory countries
K-means clustering	A	32	300.7	66.7	22 (68.7%)
	B	83	201.9	80.4	66 (79.5%)
	C	34	148.9	52.3	15 (44.1%)
	D	46	74.0	86.5	18 (39.1%)
Geographic region	North America	3	223.0	53.5	0 (0%)
	Europe	48	231.1	80.4	41 (85.4%)
	Asia	39	227.4	71.3	16 (41.0%)
	Australia and Oceania	19	66.2	82.2	7 (36.8%)
	Africa	54	177.2	80.0	44 (81.5%)
	South America and the Caribbean	32	114.8	32.0	13 (40.6%)

Table 2 — Expectation of financial contribution to CMS from non-signatory states containing at least 25% of CMS species to become signatories based upon proportional economic size (UNGA Res 70/416/Add.1, UNEP/CMS Res 12.2). Adjusted scale includes all signatory states.

Country	CMS species	UN contribution scale	Adjusted scale	Signatory cost (€)	Cost per species (€)
China	454	7.92%	14.25%	364 907	803.76
Russia	406	3.09%	6.10%	156 192	384.71
Japan	314	9.68%	16.87%	431 918	1375.54
Myanmar	294	0.01%	0.02%	539	1.83
Turkey	294	1.02%	2.10%	53 745	182.81
Thailand	284	0.29%	0.61%	15 603	54.94
USA	277	22.00%	31.42%	804 453	2904.17
Viet Nam	270	0.06%	0.12%	3126	11.58
Nepal	267	< 0.01%	0.01%	324	1.21

Table 3 — Estimation of financial contribution to CMS from the 10 signatory states containing the largest number of CMS species based upon proportional economic size (UNGA Res 70/416/Add.1, UNEP/CMS Res 12.2). Adjusted scale includes only signatory states.

Country	CMS species	UN contribution scale	Adjusted scale	Signatory cost (€)	Cost per species (€)
France	474	4.86%	10.24%	262 177	553.12
UK	428	4.46%	9.41%	240 810	562.64
India	374	0.74%	1.55%	39 766	106.33
Netherlands	342	1.48%	3.12%	79 964	233.81
Spain	337	2.44%	5.15%	131 817	391.15
Israel	328	0.43%	0.91%	23 202	70.74
Italy	316	3.75%	7.90%	202 231	639.97
Germany	315	6.39%	13.47%	344 732	1094.39
Portugal	310	0.39%	0.83%	21 151	68.23
Egypt	295	0.15%	0.32%	8201	27.80

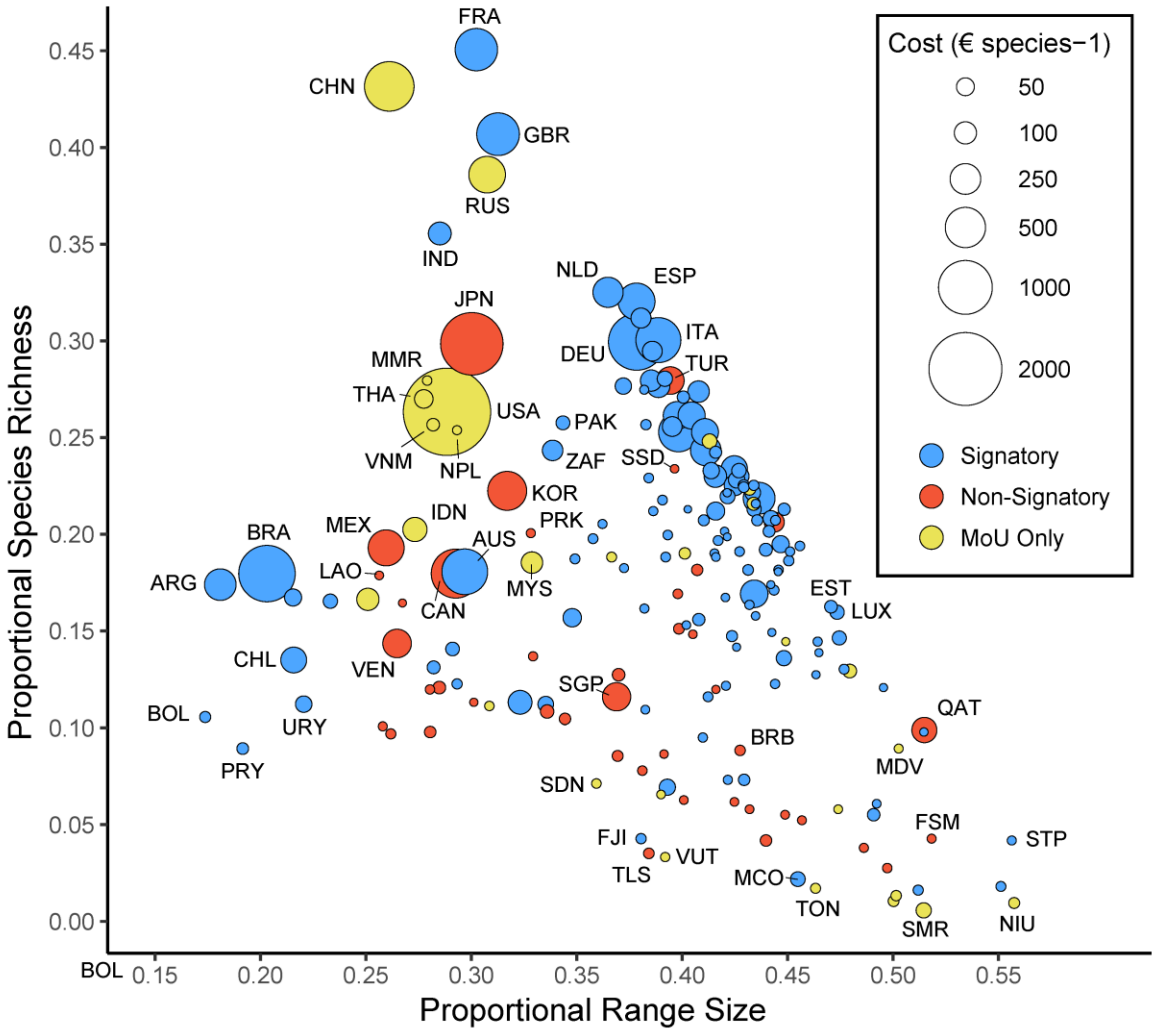

Figure 3 — Richness-diversity diagram depicting the relationship between the number of CMS species in a country and the average range-size of those species. Each *point* represents a sovereign country and all of its territories. The size of each point shows the per-species cost to be a CMS party state. Signatory states are *blue*, non-signatory states are indicated by *red*, and countries that have signed at least one MoU but not CMS are indicated by *yellow.* Select countries are labeled on the plot with 3 letter country codes.

Conclusions

While most countries in Europe, Africa, and South America are members of CMS, there are gaps in participation across Asia and North America. Countries containing a large number of CMS species, particularly those with low participation costs such as Myanmar, Thailand, Nepal, Vietnam, and Turkey may be most amenable to joining CMS. In contrast, cost may be a deterrent for non-signatory states with large economies, particularly for those countries containing few CMS species. Regardless, CMS must not ignore the importance of pursuing geographically large non-signatory countries that contain many species under the convention (e.g., Russia, China, Japan, and the United States). Of these countries, Russia and China would contribute comparable per-species cost to current signatory states with similar species compositions (e.g. France and the United Kingdom). The United States and Japan may be discouraged by disproportionately large costs necessary to become signatories. This cost burden may be alleviated with the addition of migratory species into CMS appendices with ranges in these countries.

For this study, the identity of individual species was not considered. However, it should not be assumed that all CMS species present equivalent conservation problems. CMS includes mammals, birds, reptiles, fish, and one insect with diverse ecologies, modes of movement, and migratory habits in both terrestrial and aquatic environments. Species counts are useful for broad summaries, but it is unlikely that all species are valued equally by range-states.

The only insect listed under CMS, the monarch butterfly (*Danaus plexippus*), is a prime example of the difficulties the convention faces with conservation of migratory species across non-signatory states. Monarch butterflies exhibit a wide geographic range including North America, Central and South America, Oceania and Australia, Europe, and Africa, but only North American populations of monarch butterflies are migratory (Zhan et al., 2014). Canada, the

United States, and Mexico are not parties to CMS, preferring instead to maintain independent initiatives (Oberhauser et al., 2008). While it is possible for CMS to facilitate conservation efforts of the monarch butterfly as a species, the convention has limited ability to conserve populations of monarch exhibiting migratory behavior with no North American signatory states.

Limitations in species distribution data restrict the efficacy of any conservation assessment (Seelarbokus, 2014). Distributions of migratory species are particularly difficult to catalogue given their complicated and seasonal life histories (Riede, 2004). The coarseness of available range data limited this study to a country-scale evaluation addressing only species included within CMS appendices. Future assessments of species composition patterns would benefit greatly from measures of geographic range and seasonality of movements.

The primary goal of the CMS secretariat is to facilitate cooperation and communication between member states in conservation efforts of migratory species that travel across international borders. CMS does not place stringent legal requirements upon its signatories unlike other MEAs like CITES or CBD. Rather, CMS encourages the creation of smaller agreements that may themselves contain strict requirements. This approach appeals to states opposed broad restrictions, but may hinder the efficacy of implementing localized conservation plans and protections (Baldwin, 2011). CMS must focus on filling geographic gaps in participation for the agreement to be relevant on the international scale. Large geographic gaps in participation discourage non-signatory states in North America and Asia from entering CMS on an individual basis. Non-signatory countries may contain ecological regions critical to the conservation of a migratory species such as breeding sites, migratory flyways, stopovers, or wintering areas. Moreover, as global climate change influences migration patterns (Robinson et al., 2009), CMS may become increasingly important as an MEA. Without adequate participation

from the global community, CMS is ultimately limited in its ability to facilitate conservation of migratory species.

Acknowledgements

We thank the CMS secretariat for providing data and guidance for this study. We thank our funding sources: the National Science Foundation C-CHANGE Integrative Graduate Education and Research Traineeship [grant number 0801522], the Ecology and Evolutionary Biology Department of the University of Kansas, and the Biodiversity Institute Panorama Grant. We also thank Dr. Town A. Peterson and Kate Ingenloff for manuscript editing.

References

Arita, H. T., J. A. Christen, P. Rodríguez and J. Soberón. 2008. Species diversity and distribution in presence-absence matrices: mathematical relationships and biological implications. *The American Naturalist* 172: 519-532.

Baldwin, E. A. 2011. Twenty-five years under the Convention on Migratory Species: migration conservation lessons from Europe. *Environmental Law* 41: 535-571.

Birnie, P. B., A. Boyle and C. Redgwell. 2009. *International Law and the Environment*. Oxford, United Kingdom: Oxford University Press.

Clobert, J., M. Baguette, B. T. G. and J. M. Bullock. 2012. *Dispersal ecology and evolution*. Oxford, United Kingdom: Oxford University Press.

Dodds, F., M. Howell, M. Strauss, M. O. Onestini, E. Maruma and A. Bourdy 2007. Negotiating And Implementing Multilateral Environmental Agreements (MEAs): A Manual For

NGOs. Nairobi, Kenya: UNEP Division of Environmental Law and Conventions (DELC).

Esri 2011. ArcGIS Desktop. 10 ed. Redlands, CA: Environmental Systems Research Institute.

Graves, G. R. and C. Rahbek. 2005. Source pool geometry and the assembly of continental avifaunas. *Proceedings of the National Academy of Sciences* 102: 7871-7876.

Guruswamy, L. D. 1999. The Convention on Biological Diversity: exposing the flawed foundations. *Environmental conservation* 26: 79-82.

Guruswamy, L. D. and K. L. Doran. 2007. *International Environmental Law*. St. Paul, MN: Thomson/West.

Kim, R. E. 2013. The emergent network structure of the multilateral environmental agreement system. *Global Environmental Change* 23: 980-991.

Koester, V. 2002. The five global biodiversity- related conventions: A stocktaking. *Review of European, Comparative & International Environmental Law* 11: 96-103.

Macqueen, J. 1967. Some methods for classification and analysis of multivariate observations. *Proceedings of the fifth Berkeley symposium on mathematical statistics and probability*. 1: 281-297. Oakland, CA.

Oberhauser, K., D. Cotter, D. Davis, R. Decarie, A. Behnumea, C. Galino-Leal, M. Gallina Tessaro, E. Howard, et al. 2008. North American monarch conservation plan. *Commission for Environmental Cooperation: Canada*.

R Core Team 2017. R: a language an environments for statistical computing. 3.3.3 ed. Vienna, Austria: R Foundation for Statistical Computing.

Riede, K. 2004. Global register of migratory species: from global to regional scales: final report of the R&D-Projekt 808 05 081. Federal Agency for Nature Conservation.

Robinson, R. A., H. Q. Crick, J. A. Learmonth, I. Maclean, C. D. Thomas, F. Bairlein, M. C. Forchhammer, C. M. Francis, et al. 2009. Travelling through a warming world: climate change and migratory species. *Endangered Species Research* 7: 87-99.

Seelarbokus, C. B. 2014. Assessing the effectiveness of International Environmental Agreements (IEAs). *SAGE Open* 4: 2158244014521820. doi:10.1177/2158244014521820

Soberón, J. and J. Cavner. 2015. Indices of Biodiversity Pattern Based on Presence-Absence Matrices: A GIS Implementation. *Biodiversity Informatics* 10.

Soberón, J. and G. Ceballos. 2011. Species richness and range size of the terrestrial mammals of the world: biological signal within mathematical constraints. *PLoS One* 6: e19359.

United Nations Environment Programme/Convention on the Conservation of Migratory Species, 23–28 Oct 2017. Resolution 12.2.

United Nations General Assembly, 23 December 2015. Resolution A/RES/70/416/Add.1.

Zhan, S., W. Zhang, K. Niitepold, J. Hsu, J. F. Haeger, M. P. Zalucki, S. Altizer, J. C. De Roode, et al. 2014. The genetics of monarch butterfly migration and warning colouration. *Nature* 514: 317-321.

CONCLUSION

These investigations of avian movement ecology represent novel applications of underutilized data sources and modeling methodologies. Each of these projects deliver analytical tools to address pressing questions regarding ecologically and politically important animal behaviors.

The first chapter outlined a novel model for quantifying environmental influences on route choices of migratory animals from global location sensor (GLS) data. I identified relationships between ocean surface environments and movement behaviors of *Sterna paradisaea* during seasonal migration; environmental effects on route choice and travel speeds differed between post-breeding and post-wintering migrations, indicating changes in migration strategies depending on season. The second chapter extended applications of these movement models, testing for environmental drivers of turning angles and path tortuosity of 6 pelagic seabird species in order *Procellariiformes*. Migratory trajectories of the 3 species in family *Procellariidaea* were more affected by underlying environment than home-range movements of the 3 species in family *Diodemedeidae*. These results reveal species-level preferences that may be used to identify optimal migration flyways. Further, these results suggest that GLS data can be utilized in macro-scale movement models to connect current efforts in movement ecology and distributional ecology. The third chapter evaluated natal dispersal patterns of *Streptopelia decaocto* from across North America from 1997 – 2016. Simulations revealed increased frequency of low probability dispersal events as the range of *S. decaocto* expanded from 2003 – 2008. Changes in dispersal mode during invasion across North America support the hypotheses that long-distance dispersal may be more common for colonizing populations than for resident populations. Chapter four demonstrated the overall lack of signatory states to the Convention of

Migratory Species (CMS) across Asia and North America, despite countries in these regions containing many CMS species. Differences in the financial burden, attitude towards multilateral agreements, and species coverage under the agreement, indicate that China and Russia may be more amenable to joining CMS than the United States or Japan.

Together, these projects address the implications of macro-scale animal movements, providing a suite of analytical tools that may be used to quantitatively address movement hypotheses. The novel approaches presented in these studies are not without limitations; however, they represent promising advances in movement ecology applications. As technology continues to improve, it will become possible to collect increasing amounts of high-quality tracking data for a widening variety of species. It is clear that ongoing development of analytical standards in movement ecology will be necessary to address new questions arising from these new data.

REFERENCES

Beier, P., Spencer, W., Baldwin, R. F., & McRae, B. H. (2011). Toward best practices for developing regional connectivity maps. Conserv. Biol., 25(5), 879-892.

Bennetts, R. E., Nichols, J. D., Pradel, R., Lebreton, J., & Kitchens, W. (2001). Methods for estimating dispersal probabilities and related parameters using marked animals.

Birnie, P. B., Boyle, A., & Redgwell, C. (2009). International Law and the Environment (3 ed.). Oxford, United Kingdom: Oxford University Press.

Bridge, E. S., Kelly, J. F., Contina, A., Gabrielson, R. M., MacCurdy, R. B., & Winkler, D. W. (2013). Advances in tracking small migratory birds: a technical review of light-level geolocation. J. Field Ornithol., 84(2), 121-137.

Driezen, K., Adriaensen, F., Rondinini, C., Doncaster, C. P., & Matthysen, E. (2007). Evaluating least-cost model predictions with empirical dispersal data: a case-study using radiotracking data of hedgehogs (Erinaceus europaeus). Ecol. Model., 209(2-4), 314-322.

Egevang, C., Stenhouse, I. J., Phillips, R. A., Petersen, A., Fox, J. W., & Silk, J. R. D. (2010). Tracking of Arctic Terns Sterna paradisaea reveals longest animal migration. Proc. Natl. Acad. Sci. U. S. A., 107(5), 2078-2081.

Fortin, M.-J., & Dale, M. R. T. (2005). Spatial analyisis: a guide for ecologists. Cambridge, UK: Cambridge University Press.

Holyoak, M., Casagrandi, R., Nathan, R., Revilla, E., & Spiegel, O. (2008). Trends and missing parts in the study of movement ecology. Proc. Natl. Acad. Sci. U. S. A., 105(49), 19060-19065.

Martin, T. G., Chadès, I., Arcese, P., Marra, P. P., Possingham, H. P., & Norris, D. R. (2007). Optimal conservation of migratory species. PLoS One, 2(8), e751.

Morales, J. M., Haydon, D. T., Frair, J., Holsinger, K. E., & Fryxell, J. M. (2004). Extracting more out of relocation data: building movement models as mixtures of random walks. Ecology, 85(9), 2436-2445.

Nathan, R., Getz, W. M., Revilla, E., Holyoak, M., Kadmon, R., Saltz, D., & Smouse, P. E. (2008). A movement ecology paradigm for unifying organismal movement research. Proc. Natl. Acad. Sci. U. S. A., 105(49), 19052-19059.

Nathan, R., Perry, G., Cronin, J. T., Strand, A. E., & Cain, M. L. (2003). Methods for estimating long-distance dispersal. Oikos, 103(2), 261-273.

Ovaskainen, O., de Knegt, H. J., & del Mar Delgado, M. (2016). Quantitative ecology and evolutionary biology: integrating models with data. Oxford, UK: Oxford University Press.

Pejchar, L., & Mooney, H. A. (2009). Invasive species, ecosystem services and human well-being. Trends Ecol. Evol., 24(9), 497-504.

Perrings, C., Dehnen-Schmutz, K., Touza, J., & Williamson, M. (2005). How to manage biological invasions under globalization. Trends Ecol. Evol., 20(5), 212-215.

Pimentel, D., Zuniga, R., & Morrison, D. (2005). Update on the environmental and economic costs associated with alien-invasive species in the United States. Ecol. Econ., 52(3), 273-288.

Turchin, P. (1998). Quantitative analyiss of movement. Sunderland, MA, USA: Sinnauer Associates.

Wakefield, E. D., Phillips, R. A., & Matthiopoulos, J. (2009). Quantifying habitat use and preferences of pelagic seabirds using individual movement data: a review. Mar. Ecol. Prog. Ser., 391, 165-182.